Evaluating the Effects of Grain Size and Divalent Cation Concentration on the Attenuation of Viruses and Microspheres through Crushed Silica Sand

by

Peter S. K. Knappett

A thesis
presented to the University of Waterloo
in fulfilment of the
thesis requirement for the degree of
Master of Applied Science
in
Civil Engineering

Waterloo, Ontario, Canada, 2006

AUTHOR'S DECLARATION

I hereby declare that I am the sole author of this thesis. This is a true copy of the thesis, including any required final revisions, as accepted by my examiners.

I understand that my thesis may be made electronically available to the public.

ABSTRACT

Over the last decade in North America, an increasing number of microbiological drinking water regulations have been used to manage groundwater resources that are potentially influenced by surface water. Regulations such as the Ontario Ministry of Environment Regulation 505, which requires at least a 60 day groundwater travel time between surface waters and drinking water wells, have been created with limited understanding of subsurface pathogen transport processes. Groundwater Under Direct Influence studies (GUDI or GWUDI in USA) are conducted to assess the need to treat well water at an extraction point. Currently, there is a lack of knowledge regarding factors that affect the transport of pathogens through porous media at the surface water-groundwater interface. Such information is required to supply sufficient quantities of drinking water in a cost effective and safe manner.

Factors that affect pathogen transport through porous media include: properties of the pathogen (i.e. surface charge, size, and morphology), properties of the granular media (i.e. mineralogy, size, texture, angularity) and properties of the water (i.e. pH, ionic strength and content, and natural organic matter). This study examines the effects of ionic strength, grain size and influent virus concentrations on pathogen transport in porous media. Fourteen column tests were conducted using the bacteriophage MS2 and 1.5 μm microspheres; two commonly used non-pathogenic surrogates representative of human viruses and bacteria, respectively. Two size distributions of crushed silica sand, with median grain diameters of 0.7 and 0.34 mm, and two ionic strengths of 8 and 95 mmol/L were used. A 2^2 partial factorial design was used with a minimum of two replicates of each combination of the parameters.

The results show that complete breakthrough of both viruses and microspheres occurred in medium sand at low ionic strength. It was found that increasing ionic strength by Ca^{2+} addition precluded breakthrough of MS2 in both the medium and fine sands. This represents a greater than 8 log reduction in peak effluent concentration and essentially complete attenuation.

In fine sand, with low ionic strength water, a 5 log reduction in peak MS2 concentrations was observed. In the same sand at high ionic strength, no MS2 broke through the column, corresponding to a greater than 8 log removal. Since complete attenuation occurred in both grain sizes at high ionic strength, the effect of higher ionic strength in the fine sand was indistinguishable from the effect observed from raising the ionic strength in the medium sand.

In contrast to the viruses, microsphere transport was essentially unaffected by increasing ionic strength under the conditions investigated. A 1 log reduction in peak concentration was observed in the high ionic strength water in the medium sand. In spite of this, grain size had a profound effect on the attenuation of microspheres. There was no evidence of microsphere breakthrough in any of the fine sand columns at the low or high ionic strengths, yielding a greater than 5 log reduction in microsphere concentration associated with grain size alone. The effect of varying virus concentration was also investigated. It was found that varying the concentration of viruses between 10^5 and 10^7 pfu/ml had no discernable effect on their observed transport characteristics; normalised peak breakthrough concentration, percent attenuation and retardation relative to a bromide tracer.

Based on the results from this Thesis, in a riverbank filtration environment, there is reason to expect that, at comparable water qualities and in similar porous media, multiple logarithmic reductions of viruses and bacteria would occur over the much longer (than column length) flowpaths associated with RBF. There is also reason to expect this attenuation capability to vary based on riverbank grain size and water chemistry.

Acknowledgements

This thesis is not a product of one individual. There has been a group of people who have directly supported this work and many others who have indirectly contributed by enhancing my quality of life during this period of my life.

Thanks to Sharon Daniel for her help in editing this thesis and thanks to her family for feeding me and giving me a place to stay. Thanks also, to Darren and Hannah for letting me stay with them during the final week of this writing. Thanks to Yong Yin for taking care of the binding of this thesis for me, and mailing the corrections to me in Germany.

I would like to thank my supervisor Dr. Monica B. Emelko for her enthusiasm for my research and her guidance, kindness, respect and optimism under sometimes challenging circumstances. I would like to thank Michelle Van Dyke, whose wisdom and experience in microbiology has been vital to my research moving forward. I would also thank Drs. Mario and Kristin Schirmer at the UFZ Centre for Environmental Research in Leipzig for helping me to have the opportunity to study pathogens in the water environment in Germany. I would like to thank Dr. Eric Reardon, who gave me my first dose of research in the Geochemistry laboratory in Earth Sciences at The University of Waterloo.

Thank you to Mark Sobon, Bruce Stickney, Ken Bowman for helping me out in the various labs around Civil Engineering. I appreciate the assistance of Adam Arnold in the lab. Also thanks to Shayne Giles for guiding the design and construction of the columns.

I would like to thank my roommates, Willem, Ole, Christian, Julie, Laure, Yong, Jens, Juka and Jendrick, who have always contributed to a home where we can hang out and relax a little when everything is going wrong in the lab. Also thank you to the people in my bible study group that were always ready to listen to me and encourage me. Thank you to the international students that made my experience in Waterloo far more mind expanding and rich. And thanks to the members of our awesome water resources baseball team!

Last and most important, I'm thankful for my family who have been so patient and understanding as my dreams grow and change. I'm thankful for a father that showed me that learning is not dependent upon having a degree. I'm thankful for Uncle Gary who introduced me to the exciting and quirky field of Hydrogeology. I would also like to thank Dr. Papke who saw potential in me before anyone else and convinced me he was right, he's always right…except about the colour of ozone gas, it's pale blue!

Above all I'm thankful for what Jesus Christ did on the cross, wiping away my sin and giving me another chance every day to live better for Him. I pray for peace as we move ahead together into a brave new world of unprecedented research activity and international understanding.

TABLE OF CONTENTS

LIST OF TABLES

LIST OF FIGURES

Notation

Greek Characters

α	single collector attachment efficiency
ε	porosity of porous media
δ	separation distance between the surface of the grain and the particle
η	overall single collector removal efficiency
η_o	single collector collision efficiency
η_{SG}	geometrical suffusion security
λ	die off rate constant
μ	water viscosity
μ_l	inactivation rate of suspended microorganisms
μ_s	inactivation rate of microorganisms attached to a grain surface
ρ	density of water
ρ_p	density of a particle
ρ_β	bulk density of porous media
Φ^{Born}	Born engergy
Φ^{DL}	double layer repulsion force
Φ^{vdw}	van der Waals attractive force
Φ_{min1}	primary energy minimum
Φ_{min2}	secondary energy minimum

Letters

a_c	radius of grain
A_s	Happel's constant
d_{10}	grain diameter for which ten percent of the grains are smaller
C	Concentration
C_o	Concentration of influent
D_h	hydrodynamic dispersion coefficient
D_p	particle diffusivity in water
d_c	collector (grain) diameter
d_p	particle diameter
f	volumetric flow rate
g	gravity
k	the Boltzman constant
k_{att}	attachment rate coefficient
k_{det}	detachment rate coefficient
L	length of column
n	porosity of porous media
P_{eff}	total estimated number of particles released in the effluent
P_{inf}	total number of particles injected into the column
Q	inactivation rate of microorganisms
S_{DEP}	bulk concentration of pathogens retained due to size exclusion
S_{TEMP}	physicochemical sorption
S_{kin}	concentration of particles attached to kinetic attachment sites

T	absolute temperature
t_{spike}	length of time over which the spike was added
v_o	porewater flow velocity
U	approach velocity to a grain surface (approximated by the darcy velocity)
V_c	empty volume of the column
$v_{colloid}$	measured velocity of the colloid
v_p	average particle velocity through porous media
V_s	terminal settling velocity of a particle
V_f	final volume of the water and sand together
V_{sat}	saturated volume of sand
v_{tracer}	measured velocity of conservative tracer

1. INTRODUCTION

1.1 Why Study Viruses?

Over the last 30 years several batch, column, and field studies of bio-colloid transport in groundwater have resulted in a considerable body of knowledge, theories, and empirical results. A bio-colloid is any particle of colloidal size (i.e. 1 nm to 100 μm) that is living or derived from a living thing. This definition includes protozoa, bacteria and viruses. Presently, it is known that many factors affect the subsurface transport of bio-colloids. These factors include: soil properties such as mineralogy, grain size, surface roughness and organic content; water properties such as pH, ionic strength, predation and competition from other microorganisms and; properties of the bio-colloid itself such as isoelectric point and surface charge, surface morphology and size. Thus far the research has not provided a coherent picture of how these factors concurrently affect bio-colloid transport. Accordingly, the transport of bio-colloids in porous media remains a non-predictive science, even at well characterized field sites (e.g. Flynn et al., 2004a).

Although bio-colloid transport in the subsurface is not predictive, the concurrent impacts of some of the factors affecting transport are readily understood. For example, the relative impact of the ratio of grain to bio-colloid size can affect whether or not size exclusion is significant in precluding transport. This thesis set out to understand how the natural environment impacts the transport of pathogenic bio-colloids in the subsurface.

Virus transport in the subsurface was chosen for study because despite copious amounts of data that indicate outbreaks in North America and throughout the world from viral aetiology, the transport of pathogenic viruses in groundwater is still poorly understood. Moreover, due to their small size, viruses are more likely to be transported

(relative to larger pathogens) in porous media systems where size exclusion may play a substantial role in precluding bio-colloid transport. The Ontario MOE (Ministry of the Environment) and the United States Environmental Protection Agency have set rules for groundwater supply wells in recent years, permitting wells outside of a sixty day pore water travel time from the nearest surface water source to be considered "true" groundwater wells, thereby precluding the need for treatment beyond disinfection (Ontario Regulation 505 and US EPA Surface Water Filtration Rule). Several pathogen transport studies, however, have shown that 60 days may be inadequate for adequate retention and inactivation of enteric viruses (McKay et al., 1994; Schijven et al., 2000a). In contrast, many studies have shown 7 to 12 log removal of viruses over only a few metres of sand (Schijven et al., 2001; Niemi et al., 2004; Blanford et al., 2005). As a result, regulators require improved guidance for assessing the risk of pathogen passage through the subsurface and into public water supplies. One specific example of the need for improved regulatory guidance is the current lack of regulations or guidelines regarding the treatment of riverbank filtrate. Riverbank filtration (RBF) is a low cost method of surface water treatment in which a well is drilled into the shallow aquifer adjacent to a river or lake. As the well pumps water, the aquifer is recharged from the neighbouring surface water. The various reported field and laboratory data regarding pathogen transport in the subsurface have put riverbank filtration wells under scrutiny (Kuehn and Mueller, 2000) and have yielded several regulatory frameworks (MOE and US EPA) for assessing the subsequent treatment needs for RBF well water.

Of particular concern to health authorities and regulators are pathogenic viruses (Gerba, 1996). There are five characteristics of viruses that contribute to their being a

significant cause of waterborne gastroenteritis in the world. These are: 1) their small size, which often enables them to penetrate further into an aquifer (relative to larger protozoan and bacterial pathogens) (Jin and Flury, 2002), 2) their resistance to conventional water treatment methods (e.g. Adenovirus is resistant to UV irradiation and Norwalk Virus is resistant to chlorination) (Keswick et al., 1985), 3) their low minimal infectious dose (between 1-10 viruses), 4) their ability to be aerosolized readily (in contrast to larger pathogens), which increases the likelihood of secondary (specifically airborne) spread throughout a densely populated community, and 5) their long (~30 days in some cases) asymptomatic residence time (e.g. *Hepatitis E)*, during which no symptoms are present (Jameel, 1999). For example, two large *Hep E* waterborne epidemics affected 40,000 people in India in 1954 (Grabow, 1997) and again in Kanpur, India in 1992 where 80,000 people were infected (Naik et al., 1992). The purpose of the present investigation is to provide some fundamental knowledge regarding the effects of aquifer characteristics and ground water quality on the transport of viruses in a RBF context so that better regulatory guidelines for the treatment of RBF filtrate can be developed.

1.2 Objectives

The ultimate goal of this thesis work was to provide some fundamental knowledge regarding the effects of aquifer characteristics and ground water quality on virus transport in RBF regimes. After selecting the viruses and bacterial surrogates that would be utilised toward achieving this general research goal, the following objectives for achieving that goal were developed:

1) Acquire the equipment and develop the skills and knowledge necessary for the growth, detection and storage of the bacteriophages MS2 and PhiX-174.
2) Design a column appropriate for the study of virus transport at the anticipated experimental conditions (grain size, flow rate, virus adhesion characteristics) representative of a riverbank filtration setting.
3) Evaluate the effects of grain size on virus and microsphere transport and retention using crushed silica sand of consistent roughness and mineralogy.
4) Evaluate the effects of [Ca^{2+}] induced ionic strength on virus and microsphere transport through crushed silica sand.
5) Synthesize the research outcomes to provide regulatory and/or experimental guidance for further assessing the treatment requirements for riverbank filtrate.

2. BACKGROUND

2.1 Pathogens in Ground and Surface Water: Problem Characterisation

The connection between drinking water and disease outbreaks was first confirmed by John Snow in 1854. By removing the handle of a pump in London, he was able to stop a large *Cholera* outbreak, and thus provided the first evidence of human disease associated with waterborne pathogens (Szewyk et al., 2000). Since then, the twentieth century has seen an increasing awareness of the importance of water in transmitting disease. As clinical and environmental microbiological detection methods have improved and contributed to a better understanding of the sources and variety of waterborne pathogens, previous assumptions about the safety of established drinking water practices have been swept aside. An example of this increasing awareness would be the connection made between *Cholera* outbreaks and human sewage at the turn of the century after an outbreak in Hamburg, Germany. Before the outbreak, the city's sewage was discharged upstream of the city's drinking water intake along the Elbe River. The advancement in knowledge regarding the role of waterborne pathogens and disease provided the impetus to separate waste waters from drinking water sources and to chlorinate drinking waters (Szewzyk et al., 2000). Although these practices effectively treat many traditional pathogens such as *Cholera*, the incidence of waterborne disease outbreaks still remains high (e.g. Schoenen, 2001 and Macler and Merkle, 2000) because many new previously undetectable waterborne pathogens have been recognized; moreover, they are often resistant to chlorination (Gerba, 1996).

The majority of known waterborne pathogens fall into three categories: protozoa, bacteria and viruses. The following pathogens have been recognised as significant

problems by public health officials over the last several decades: the protozoa, *Cryptospordium parvum, Giardia intestinalis* and *Giardia lamblia*; the bacteria, *Escherichia coli O157, Campylobacter jejuni, Salmella enteritidis* and *Helicobacter pylori*; and the viruses, Rotavirus, Hepatitis A, Hepatitis E, Norwalk-like Virus (NLV) and Adenovirus. The path of human infection for each of these human pathogens is varied. For example, the minimal infectious dose necessary to cause disease, varies between 1 and 100,000,000 in the group specified above, (Geldreich, 1996). The minimal infectious dose is the number of pathogens that must be ingested by individuals in a population to result in at least 50 % of the people contracting the disease. In the case of the pathogens specified above, the severity of the induced disease varies from flu like symptoms to death and the locations of infection include intestine, liver, kidneys, brain and lungs. The relationship that a micro-organism has with humans guides the setting of regulations for drinking water quality (Toze, 1999) a process analogous to setting acceptable concentrations for inorganic and organic contaminants in the environment.

Pathogens also vary in their sources and behaviour in the environment. The sources of waterborne pathogens are not just restricted to human feces; they include water fowl, wild animals and almost every kind of domesticated animal (Geldreich, 1996). This leads to point sources such as sewage treatment plants and distributed sources of waterborne pathogens, such as water fowl. Outside the host most pathogens enter a dormant stage where many normal metabolic activities are shut down, allowing them to stay infective for long periods of time. In cold water, this survival time can be longer than 90 days (Geldreich, 1996) for some of these pathogens, providing a three month window of opportunity for the pathogen to be taken up by a suitable host and

multiply itself again. Therefore, since pathogens are wide spread and persistent in surface water, it is important to understand their behaviour in a riverbank filtration setting, where natural disinfecting processes are relied upon to produced safe drinking water.

2.2 Viruses

With diameters of approximately 20 to 100 nm, waterborne viruses are the smallest of the three categories of pathogens. Since size exclusion can be an important mechanism for purifying groundwater from pathogens, viruses may penetrate further into aquifers than larger classes of microorganisms such as protozoa (Lee and Kim, 2002). Viral infections may be initiated by a very low number of viruses and are usually excreted from an infected individual in very high numbers (Gerba et al., 1996). Due to detection difficulty because of their small size and their inability to be grown in a nutrient broth (Wyn-Jones and Sellwood, 2001), the impact of viruses on public health has been the most underestimated of all the classes of waterborne pathogens and likely can account for the many outbreaks of gastro-enteritis around the world where a causative agent was not identified (Lee and Kim, 2002). Viruses are known to be the main cause of gastroenteritis in the United States (Blacklow and Greenberg, 1991). Clearly, preventing the passage of viruses into potable water supplies is critical to protecting public health. Since many waterborne viruses are ubiquitous in the environment, and have relatively low infectious doses there is a need to understand their transport in water supplies; however, the difficulty in detecting many viruses of public health significance has precluded extensive investigations of their transport in natural environments. As a result,

bacteriophages (viruses that exclusively infect specific bacterial hosts) have emerged as readily quantifiable surrogates for viruses during transport investigations.

MS2 is likely the most studied bacteriophage reported in the water treatment literature. MS2 has been studied in column experiments along with other pathogenic viruses (Redman et al., 1997) and bacteriophages (Dowd et al., 1998), in a variety of media types (You et al., 2003; Zhuang and Jin, 2003) and in field experiments along with bacterial pathogens (e.g. Schijven et al., 1999). MS2 is approximately 23 nm in diameter, which is a similar size to many known waterborne pathogenic viruses (e.g. Norwalk Like Virus, Adenovirus). It also is negatively charged at neutral pHs as are most reported pathogens. Furthermore, MS2 can be quickly grown in high concentrations and easily detected at relatively low numbers using the plaque counting method at low expense (Adams, 1959). For these reasons MS2 is frequently chosen over human viruses which are dangerous to work with and difficult to detect and grow (Jin and Flury, 2002).

2.3 Pathogen Transport

Historically it has been assumed that groundwater is generally safe from microbial contamination. More recently it has been demonstrated that groundwater quality can be impacted by surface water, rainwater, and runoff water thereby compromising water quality (Lawson et al., 1991; Goss et al., 1998; Conboy and Goss, 2000; Danon-Schaffer, 2001). Goss et al. (1998) reported that 34% of 1200 southern Ontario, rural, shallow groundwater wells contained higher than acceptable faecal coliforms. They were able to positively correlate both the age and the construction of the well to bacteria presence.

Other studies have confirmed that pathogens are able to rapidly and deeply penetrate into aquifers during heavy rainfall events (Chu et al., 2001). It is therefore not surprising that several studies have revealed bacterial contamination of upper aquifers throughout large rural areas in Canada (Goss et al., 1998; Conboy and Goss, 2000). Some of these wells are Riverbank Filtration (RBF) wells located near a river, lake or stream where lateral, saturated-phase transport occurs. Riverbank Filtration is where a drinking water production well is located near surface water, drawing a significant amount of its supply through the shallow aquifer in between the well and the lake or river. RBF has long been regarded by water treatment specialists and hydrogeologists to be an important step in drinking water treatment and capable of reducing both chemical and microbiological contaminants significantly (Kuehn and Mueller, 2000). As mentioned already, under new legislation in Ontario (MOE Regulation 505) and the United States (US EPA Surface Water Filtration Rule), such wells are considered as groundwater wells under the influence of surface water (GUDI or GWUDI) until proven otherwise.

To understand the nature of saturated phase (e.g. RBF type) transport of protozoan, bacterial or viral contamination of aquifers, the advection-dispersion equation has been modified for use in the study of pathogen transport. This equation allows a numerical modelling approach to predict the safety of valuable groundwater sources (Matthess et al., 1988; Schijven and Simunek, 2002). The one-dimensional equations that attempt to describe the transport of small biocolloids such as viruses in porous media are:

2-1

$$n\frac{\partial C}{\partial t} = nD_h \cdot \frac{\partial^2}{\partial x^2}C - nv_p \cdot \left(\frac{\partial}{\partial x}C\right) - \frac{\partial \rho_\beta S_{kin}}{\partial t} - Q$$

2-2

$$\frac{\partial \rho_\beta S_{kin}}{\partial t} = nk_{att}C - k_{\det}\rho_\beta S_{kin}$$

2-3

$$Q = n\mu_l C + \mu_s \rho_\beta S_{kin}$$

where C is the pathogen concentration in water at time t, n is porosity, D_h is the hydrodynamic dispersion coefficient, x is the distance from the influent point, v_p is the average velocity of the pathogen over distance x, ρ_b is the bulk density of the porous media, S_{kin} is the concentration of pathogens attached to kinetic adsorption sites, Q is the inactivation rate, k_{att} is the attachment rate coefficient and k_{det} is the detachment rate coefficient, and μ_s and μ_l are sorbed and liquid (or free) inactivation rates, respectively.

These equations above (2-1 to 2-3) were modified by the removal of a term for equilibrium sorption (S_{eq}) and the removal of a redundant term for attached virus inactivation in equation 2-2, which also appears as the last term in equation 2-3 ($\mu_s\rho_\beta S_{kin}$). The significance of these modifications will be discussed further below. These equations have several limitations. For example, this particular form of the equations assumes one type of kinetic physicochemical sorption site. Other models (e.g. Ryan and Elimelech, 1996, and Schijven and Hassanizadeh, 2000) acknowledge the existence of two types of kinetic sites (S_{kin1}, S_{kin2}) as well as an equilibrium sorption site (S_{eq}). This is because it is not yet known whether attachment is equilibrium or kinetically limited in a dynamically flowing colloid-porous media system, although work is currently being done to understand this better (e.g. Loveland et al., 1996). Schijven and Hassanizadeh (2000),

after a thorough review of available experimental evidence, concluded that in a flowing system (as appose to a static, batch system) attachment is almost always kinetically controlled. It is important to know this distinction since different conceptual models result from a kinetically controlled perspective of virus attachment versus equilibrium controlled. For example, if attachment to adsorption sites is equilibrium controlled then the saturation level of the adsorption sites would be controlled by equilibrium forces. If, however, attachment is kinetically controlled the sites would never reach the saturation level determined by equilibrium forces since the rate of attachment would be too slow (Ryan and Elimelech, 1996; Schijven and Hassanizadeh, 2000). As mentioned equation 2-1 only describes one dimension. Although three dimensional versions are available they are much more difficult to solve. This is because several of the terms in these equations are difficult to evaluate even under controlled one dimensional laboratory conditions. For example, few experiments have attempted to differentiate between attached and free deactivation rates of viruses (Grant et al., 1993; Rossi, 1994). Schijven and Hassanizadeh (2000) presented an analytical derivation from these equations demonstrating that (assuming a constant detachment rate, k_{det}) the negative slope of the tail of a bacteriophage breakthrough curve is directly related to the attached virus deactivation rate. Therefore, they recommended that bacteriophage transport experiments be carried out over enough time to measure the slope of the tail. Another deficiency in these transport equations (2-1 to 2-3) is that in their current form, they do not account for size exclusion. A description of this process and how researchers have recently proposed fitting it into the advection-dispersion equation (e.g. Foppen et al, 2005) will be discussed later.

2.4 Processes in Pathogen Attenuation

The migration of pathogens through porous media is controlled by advection, dispersion, physicochemical sorption to sediments, size exclusion and elimination. Advection and dispersion are physical parameters controlled by the mixing of the fluids and the size of the pathogen. Rate of dispersion is inversely related to colloid size. Physicochemical sorption, size exclusion and elimination, are the main processes responsible for the attenuation of pathogens in groundwater (Matthess and Pekdeger, 1988; Mcgechan and Lewis, 2002; Stevik et al., 2004; Taylor et al., 2004; Tufenkji et al., 2004). Physicochemical sorption is the result of several forces that result in the attraction between pathogen and grain, when the distance between the two is small (approximately 10 nm) (Ryan and Elimelech, 1996). Size exclusion is also called filtration (e.g. Matthess and Pekdeger, 1988) or straining (e.g. Mcgechan and Lewis, 2002, Stevik et al., 2004, Tufenkji et al., 2004) in the literature. Here, it describes the process of pathogen removal based on physical size, where the pathogen is too large to fit through the open cavity between grains in a packed porous media. Elimination can result from natural inactivation of the pathogen or can involve predation from another organism. While there are many factors influencing these three attenuation processes in the natural environment, they can be broken down into three categories: the properties of the geologic media, the water and the pathogen itself (Lawrence and Hendry, 1996). In particular pathogens are retained more effectively as the water content drops (Chu et al., 2001). Thus heavy rains will allow further vertical penetration of pathogens into soil as well as extensive runoff into surface waters (Schäfer et al., 1998; Chu et al., 2001;

Shadford et al., 1997). A survey of 76 parasitic outbreaks showed that almost all outbreaks were accompanied by high rainfall events (Schoenen, 2001).

Since protozoa are the largest class of the pathogens discussed in this review, size exclusion effects are expected to be more important in preventing their penetration into groundwater sources. Often groundwater outbreaks of protozoa have been observed when the water supply well was influenced by open water sources or when there was a direct conduit (through a failed well casing or a fracture) from the surface to the well screen (Donnelly and Stentifjord, 1997). In spite of these observations, protozoa have been frequently observed in groundwater during a major rain event (Medema and Schijven, 2001; Graczyk et al., 2000).

In saturated porous media, as in the case with riverbank filtration wells, some of the specific factors controlling the transport of pathogens are pore size, pH and the size and chemical makeup of the external shell of the pathogen (Lawrence and Hendry, 1996). This external chemical makeup results in a charge which is usually negative in polarity at near neutral water pHs (Schijven and Hassanizadeh, 2000). The size difference between larger and smaller pathogens produces different transport characteristics. For example, in a sand aquifer, bacteria will often be observed to travel at a higher speed than the mean groundwater velocity by following the faster, highly porous flow paths (Matthess et al., 1988; Ginn et al., 2002; Taylor et al., 2004). Viruses are shown to be retarded relative to the mean groundwater velocity (Woessner, 2001; Blanford et al., 2005). It has also long been known that bacterial presence in surface water is closely tied to rainfall events (Schaffer and Parriaux, 2002). Furthermore, extensive bacterial contamination of

aquifers has been found in several studies (Goss et al., 1998; Goody et al., 1998; Conboy and Goss, 2000).

Factors controlling the transport of viruses include clay content, pH, water content in the porous media, and the presence of metals and metal oxides on the grains (Chu et al., 2001; Scandura and Sobsey, 1997). It has been found that virus transport is most rapid when the clay content is low, when metal content is low, the pH is high (minimum 8), and water content is high (Lawrence and Hendry, 1996). In gravel aquifers travel distances of viruses over 900 m have been observed (Deborde et al., 1999).

Table 2-1 summarizes some important virus transport studies that have been performed in the field and in laboratory columns. It does not summarize all of the experimental work that has been reported regarding virus transport. Only those studies relevant to the current work are elaborated upon here.

All of the investigations summarized in Table 2-1 used medium to fine sand from various natural and synthetic sources. Most of the studies focused on the relative transport of several species of viruses (e.g. Dowd et al., 1998), different mineralogical (Zhuang and Jin, 2003; Flynn et al., 2004) or chemically modified grain surfaces (You et al., 2003) or the pH and the ionic strength of the water (Bales et al., 1991; Redman et al., 1997; Redman et al., 1999) and varying flow rates (Schijven et al., 2002; You et al., 2003). None of the reported column studies relevant to groundwater systems have investigated the effect of grain size by employing at least 2 different sizes of sand of similar mineralogy and angularity. Further, although the impact of grain size on bacterial and protozoan transport has been in investigated (i.e. Tufenkji et al., 2004) this has not been discussed in the context of viruses. It is possible that the impact of grain size on

virus transport has not been investigated because size exclusion is unlikely to be a significant process in virus attenuation in the subsurface.

Table 2-1 – Summary of Past Column Experiments with Viruses in Unconsolidated Porous Media

Viruses Used	Experimental Purpose	Porous Media	Pore Velocity (m/day)	Column Dimensions (LxD_i^*) (cm)	Total Number of Column Runs	Author
MS2 PhiX-174 PRD-1 QB PM2	observing differences in transport between 5 bacteriophages	Natural Brazos Alluvium Aquifer Sand	150	78 x 5	2	Dowd et al., 1998
MS2 PhiX-174	testing the effect of varying ionic strength on virus transport through Al-oxide coated sand	Al-oxide coated crushed Silica Sand	1.4	10 x 3.5	6	Zhang and Jin, 2003
MS2 PhiX-174 PRD-1	evaluating effects of varying flow rate and virus type on attenuation of 3 viruses	Dune Sand	1.5, 3.0	190 x 9	3	Schijven et al., 2002
MS2 PhiX-174	comparing attenuation of 2 viruses through different column lengths at different flow rates	Ottawa Sand	0.2 - 0.8	10.5, 20 x 9.2	9	Jin et al., 1997
MS2 PRD-1	evaluating effects on 2 viruses from varying Ca^{2+} and pH with hydrophobic modified silica grains	Silica Beads	3.2 - 4.9	15 x 0.9	7	Bales et al., 1991
MS2 PRD-1	evaluating effects of soil types, column lengths and pH levels on attenuation of 2 viruses	Borden, Cape Cod and Cambridge Sands	2.5	14.8, 10.6 x 2.7	8	Kinoshita et al., 1993
MS2 Norwalk Virus	Varying pH and comparing attenuation of MS2 with Norwalk	Crushed Quartz Sand	22	18 x NA	6	Redman et al., 1997
MS2	Varying flow rate, pH and ionic content (cations and anions) on the effects of virus attenuation	Mg-Al coated and uncoated sand		8 x 3.5		You et al., 2003
SJC3	evaluating ionic strength and cation charge and type in bacteriophage transport	Crushed Quartz Sand	21.6	20 x NA	13	Redman et al., 1999
H40/1	test the effect of different grain minerologies on virus transport through sands	Kappelen Aquifer, Quartz, Granite, Calcite Sands	60	20 x 2	25	Flynn et al., 2004b

* internal diameter
NA = not available

Dowd et al. (1998) performed transport experiments in 73 cm (5 cm inner diameter) columns injecting five different bacteriophages over a range of sizes and isoelectric points (MS2, PRD1, Qβ, PhiX-174, and PM2). Their purpose was to test the correlation between viral transport and their respective isoelectric points. The authors used porous material from a sandy aquifer (95% sand, 7% silt and 2% clay). Although the artificial groundwater used was near neutral pH, they did not report an ionic strength. They also used two experimental set ups, one using a conventional batch, flow through column and the other was a continuous flow through column in which the column effluent was reinjected into the influent end. This was done to simulate longer distances of travel through an aquifer.

For the batch column, Dowd et al. (1998) injected 2.1 pore volumes of virus-seeded groundwater into the influent and measured the effluent virus concentration over 10 pore volumes of flushing with bacteriophage-free water. The phages were introduced separately into the column (except MS2 and PhiX-174, which were introduced concurrently). Influent bacteriophage influent concentrations (C_o) ranged from 10^4 to 10^9 pfu/ml. The pore velocity was 150 m/day. The authors were able to negatively correlate isoelectric point to bacteriophage attenuation within two size groups. With the large diameter (~60 nm), bacteriophage PRD1 (69% attenuated with a pI of 4.2) was more attenuated than PM2 (30%, 7.3). Similarly with the small phages (~24 nm), MS2 (46%, 3.9) was more attenuated than PhiX-174 (2.5%, 6.6). An exception to this trend was Qβ (53%, 5.5), which was attenuated slightly more than MS2.

The negative correlation between isoelectric point and attenuation that was observed by Dowd et al. (1998) is the opposite of the typical positive correlation one

would expect from negatively charged viruses and media. This is because at neutral pH a low isoelectric point tends to indicate a more negatively charged virus, and therefore greater repulsion from the media. It is possible that in these experiments either the media contained significant amounts of positively charged grains (e.g. metal oxides) or that the ionic strength of the water was high enough to reverse the normal repulsive forces between virus and grain (Loveland et al., 1996). It is also possible that the different virus influent concentrations affected the outcomes, since these varied greatly. No replicate analyses were reported for the batch column experiments.

Pathogen attenuation in porous media systems can occur via several mechanisms that include physicochemical filtration, size exclusion, and die off (natural, predation, parasitism, competition etc). Pathogen attenuation and transport can be considered as conceptually inverse processes, that is, more transport often implies less attenuation. For example, as physicochemical filtration and size exclusion (i.e. straining) increase, pathogen attenuation increases while pathogen transport decreases. Pathogen transport is not affected by die off, however. Perceived pathogen transport can be affected by die off. These mechanisms are elaborated upon below.

2.4.1 Physicochemical Attachment

For small pathogens and coarse grained media, where size exclusion will not occur, the dominant process in pathogen attenuation consists of an interaction of several forces that result in process called physicochemical attachment (e.g. Schijven and Hassanizadeh, 2000) or filtration (Ryan and Elimelech, 1996; Ginn et al, 2002; Taylor et al, 2004). Yao et al. (1971) described the forces involved in the transport of colloids to

grain surfaces. Also important are those forces involved in the attachment and retention of those colloids, once sufficiently close to the grain surface (Ryan and Elimelech, 1996).

The overall physicochemical removal of colloids by stationary grains has been described by two main processes which occur in sequence. The first process necessary for attachment to occur is collision. Once a collision occurs attachment depends on the net strength and orientation (attraction or repulsion) of short range forces. These two sequential processes are described in equation 2-4 below (O'Melia, 1980, Elimelech and O'Melia, 1990):

$$\eta = \alpha\eta_o \qquad \textbf{2-4}$$

in which η is the overall single collector removal efficiency and α and η_o are the attachment and collision efficiencies respectively. Each of these parameters describe a process efficiency and are therefore between 0 and 1 (i.e. between 0 and 100%). α is a fraction of the number of times a colloid sticks to a grain relative to the total number of collisions. η_o describes the fraction of the number of colloids striking the grain over the total number of colloids passing through the pore space and η represents the number of times a colloid sticks to a grain over the total number of colloids passing by the grain (Ryan and Elimelech, 1996).

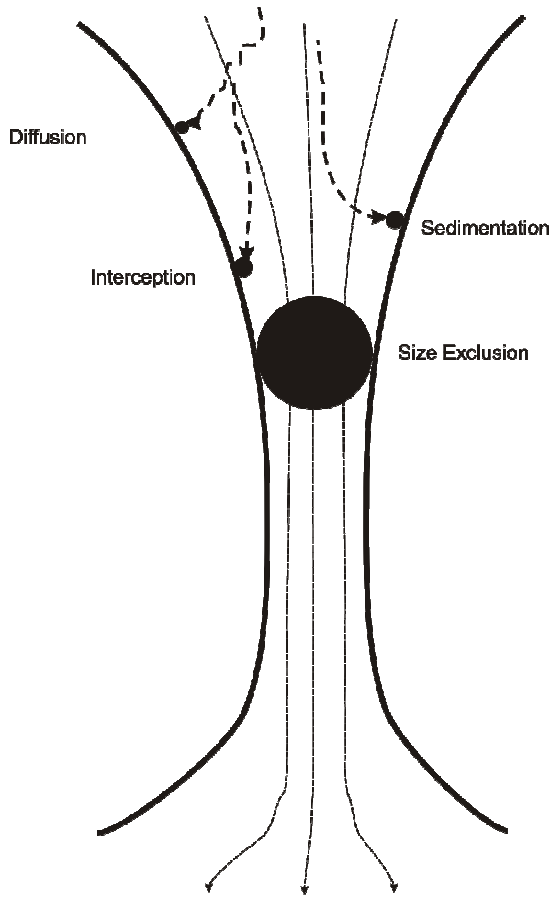

Figure 2-1 – Mechanisms that Result in Contact Between Particles and Collectors (Vinten and Nye, 1985). Fine dashed lines represent water flowpaths.

Figure 2-1 provides a visual description of the physicochemical filtration and physical mechanisms that result in contact between particles (e.g. organisms) and collectors (e.g. sand grains). The figure represents collision by diffusion, interception, sedimentation, and size exclusion. Each of these mechanisms is discussed below, although size exclusion is treated separately since it is an exclusively physical process. The long range attractive forces not represented in Figure 2-1 are van der Waals forces (Ryan and Elimelech, 1996).

2.4.1.1 Forces Affecting Pathogen Transport to Grain Surfaces (η_o)

Diffusion

Diffusion becomes more important as a transport mechanism for smaller pathogens such as viruses compared to larger ones, as can be seen in equation 2-5, which describes Brownian motion. This equation is known as Einstein's equation (Yao, 1971):

2-5

$$D_p = \frac{kT}{3\pi\mu d_p}$$

where D_p is particle diffusivity in water, k is the Boltzman constant (J/K), T is the absolute temperature (K), μ is water viscosity (g/cm/s) and d_p is the particle diameter (cm). From this equation it can be seen that there is an inverse relationship between particle diffusivity and particle diameter. Since viruses are several orders of magnitude smaller than protozoa and bacteria they will be able to diffuse more rapidly to an attachment site and in some cases may be removed more efficiently than larger pathogens. Additionally, viruses may disperse further throughout the aquifer thereby diluting the concentration of these pathogens over three dimensions. It may be important to consider that this dilution via dispersion may not be as noticeable in a short, one dimensional column, but may be a significant process acting to lower virus concentration in a three dimensional aquifer, apart from physicochemical attachment (equation 2-1).

Interception

In contrast to diffusion which has a greater effect on smaller pathogens, interception relies upon the tendency of objects to remain in motion, a property belonging

to larger colloids. The likelihood of collisions occurring due to interception can be described by the ratio below:

2-6

$$\eta_o \propto \frac{d_p}{d_c}$$

Equation 2-6 shows that the greater the ratio of the particle diameter to collector diameter the more likely collision is to occur (Ryan and Elimelech, 1996). η_o is collision efficiency d_p is particle (colloid) diameter and d_c is the collector (grain) diameter. This assumes that both particle and collector are perfectly spherical. Also assumed is that at an infinite distance from the collector $C = C_o$ (influent concentration) and that $C = 0$ at a distance $(d_p + d_c)/2$ from the centre of the spherical collector. As the particle size is increased relative to the collector size, the particle will tend to keep traveling in the same direction toward a curved grain surface rather than be subjected to the diverting forces caused by advective flux near each grain surface (Ryan and Elimelech, 1996). Due to this phenomenon part of the exterior of a larger pathogen will always approach the grain closer and sooner than any part of a small pathogen.

Sedimentation

As with the processes of diffusion and interception, sedimentation is highly dependant on the size of the pathogen. Like interception, sedimentation is proportional to pathogen size whereas diffusion is inversely proportionate to size. This means that diffusion will tend to be the dominant transport process for small pathogens and sedimentation and interception will dominate the transport of large ones. Sedimentation is the processes of downward movement of particles due to a difference in density. This process can be described by Stokes' Law in equation 2-7.

2-7

$$V_s = \frac{(\rho_p - \rho) g d_p^{\ 2}}{18\mu}$$

where V_s is the terminal settling velocity (cm/s), g is gravity (cm/s^2) and ρ_p and ρ (g/cm^3) are the densities of the particle and water respectively. Settling velocity is proportional to $d_p^{\ 2}$. This equation requires that the particle is denser than the surrounding water (i.e. it is no longer valid if V_s is negative). Stokes' Law assumes that the particles are spherical, smooth and rigid. These assumptions are not entirely valid for microorganisms, since they are rarely spherical and never smooth, because of various macromolecules extending from their surfaces. They are also not perfectly rigid, since most microorganisms are deformable to various degrees.

The above three processes contributing to collision efficiency have been integrated into one equation by Yao et al. (1971) and is applicable for a clean bead filtration where "deposition within pores has not significantly altered flow pattern or media characteristics" (Yao et al., 1971). It also should be noted that the application of this equation to a single collector assumes that collector is perfectly spherical. In addition it assumes that the collector diameter (d_c) does not change, something that in fact does occur due to the build up of colloids on grain surfaces and biofilm (or bio-fouling) formation.

2-8

$$\eta_o = \eta_D + \eta_I + \eta_G = 0.9\left(\frac{kT}{\mu d_p d_c v_o}\right)^{2/3} + 1.5\left(\frac{d_p}{d_c}\right)^2 + \frac{(\rho_p - \rho) g d_p^{\ 2}}{18\mu v_o}$$

As stated previously, η_o describes collision efficiency and must be between 0 and 1; any solutions to the above equation producing numbers outside of this range are invalid. In

equation 2-8 above, η_D, η_I, and η_G account for the processes of diffusion, interception and sedimentation respectively. It is important to note that Yao et al. (1971) introduced this equation as a conceptual model and not as an analytical equation that can be rigorously applied to make accurate predictions. This is partly because the preceding equation (2-8) assumes that the only mechanisms affecting collision efficiency are diffusion, interception and gravitation. This equation also assumes that the system is at steady state with respect to flow rate and particle concentration (dC/dt = 0). Another limitation is based on the aforementioned fact that this equation is based on a single collector. In a granular filter or groundwater media, packed grains will limit the surface area available for collision and cause more complex flow patterns around each collector. The recognition of this fact has led to the addition of an extra parameter to the above equation accounting for packed grains (Ryan and Elimelech, 1996). The most commonly used extra parameter is A_s, known as Happel's constant from the sphere-in-cell model (Happel, 1958). A review of these additional factors accounting for grain packing can be found in Ryan and Elimelech, (1996). Also available are other versions of equation 2-8 by Spielman and Friedlander (1974) and Rajagopalan and Tien (1976). Spielman and Friedlander's (1974) solution for the single collector removal efficiency (η) is only applicable to small colloids (such as viruses) where interception and sedimentation do not occur. This model also does not account for hydrodynamic interactions, such as flow fields around a grain, but rather only considers diffusion. Although Rajagopalan and Tien's (1976) equation for η_o does account for interception and sedimentation (like Yao, 1971) they also incorporate Happel's constant A_s into each of the three terms contributing

to collision. Like Spielman and Friedlander (1974), Rajagopalan and Tien (1976) do not account for hydrodynamic interactions around a grain in their term for diffusion.

Equation 2-8 was applied to the experimental conditions in this thesis to test the predictions of this conceptual model against empirical data. Figure 2-2 shows how η_o changes with colloid size. It should be noted that a minimum collision occurs at 1-3 μm. As mentioned, the collision of colloids smaller than this range is likely driven by diffusion, where larger colloids are driven by interception and sedimentation.

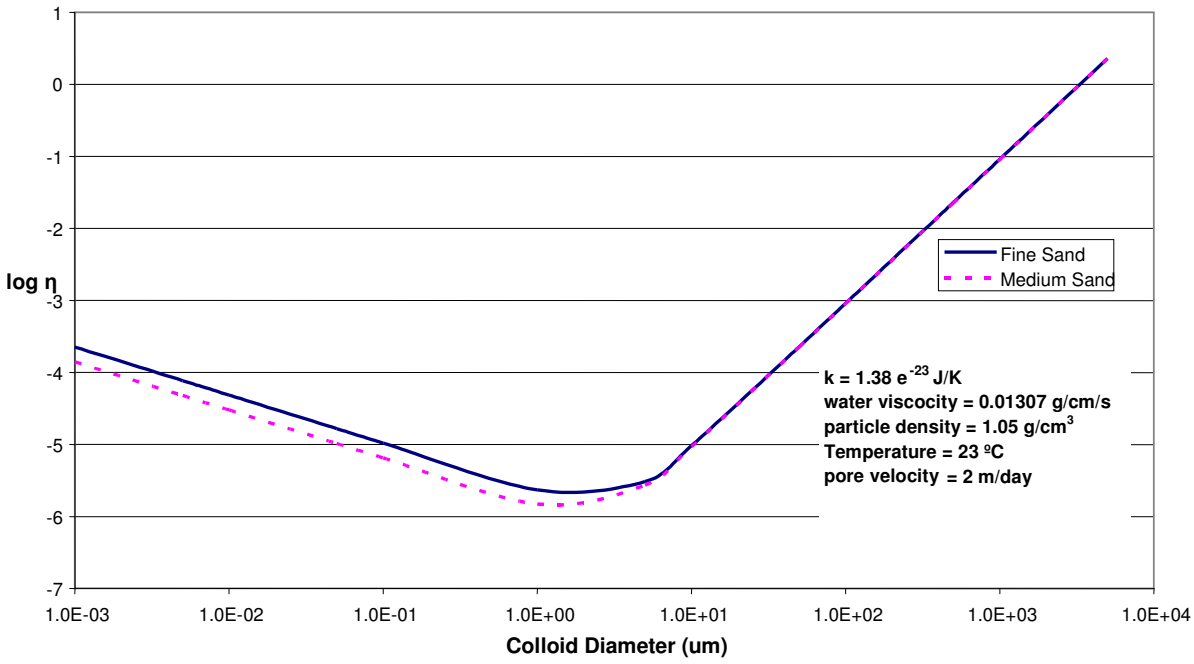

Figure 2-2 – Collision Efficiency of Different Sized Colloids in Fine and Medium Grained Sand

Figure 2-2 indicates collision efficiencies for both the fine and medium sand median grain sizes used in the present research. These predict a lower collision rate in the medium sand than the fine sand possibly suggesting less physicochemical attachment

may occur in the medium grain sand as compared to the fine sand, assuming that the attachment efficiencies (α) are equal between the two grain sizes.

2.4.1.2 Forces Affecting the Attachment and Retention of Pathogens on Grains (α)

Once a colloid collides with the surface of a grain, whether or not it remains attached to the grain is described by the attachment efficiency α. Since this is a process efficiency, as η_o, it also must lie between 0 and 1 (i.e. 0 and 100%), or between no attachment and perfect attachment every time a colloid strikes a grain surface respectively. The forces determining the attraction or repulsion between a colloid and grain at relatively close ranges are described by the Derjarguin-Landau-Verwy-Overbeek (DLVO) theory (Derjarguin and Landau, 1941, Verwey and Overbeek, 1948, Ryan and Elimelech, 1996).

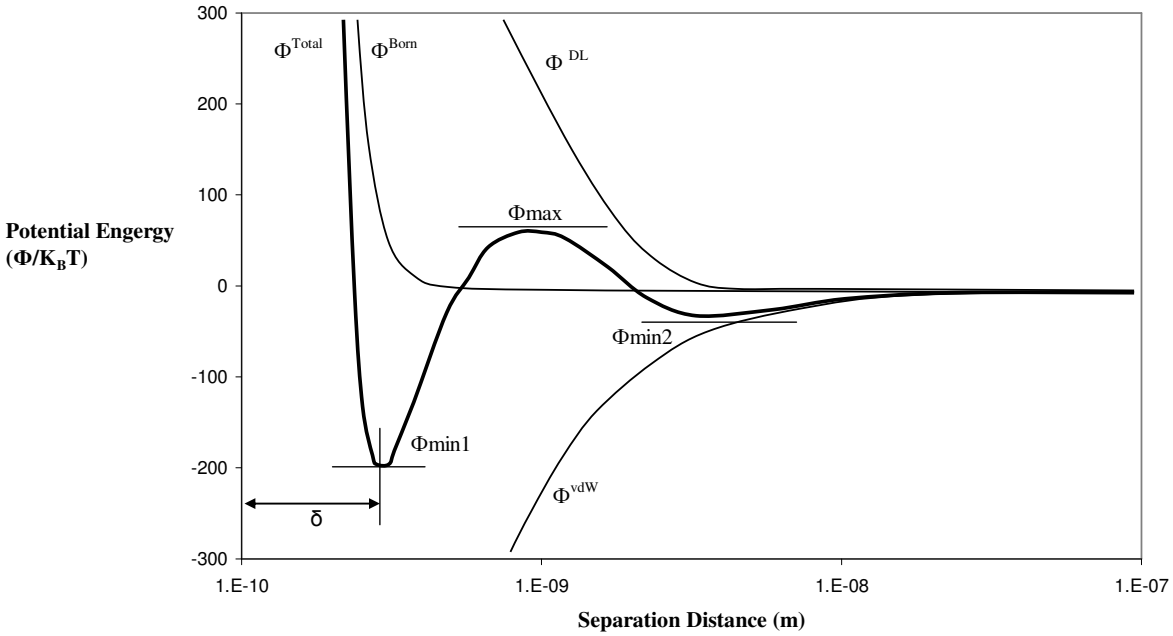

Figure 2-3 – DLVO Colloid-Grain Attraction Theory (Schijven and Hassanizadeh, 2000)

The bold line in Figure 2-3 describes the sum of the forces between a colloid and grain surface. δ is the separation distance between the surface of the grain and the colloid at the primary energy minimum (Φ_{min1}), and Φ^{Born}, Φ^{DL}, Φ^{vdw} are the Born energy, double layer repulsion and van der Waals attractive forces respectively. If the potential energy is negative, there is attraction between the colloid and grain. The above diagram is specific for the typical case in nature when both the colloid and grain carry a negative charge. These energy profiles are characterized by a shallow secondary minimum (Φ_{min2}) and a deep primary minimum (Φ_{min1}) which in turn could represent two types of attachment sites. The shallow site would be relatively further away from the grain surface and the attachment is based upon an attraction to the layer of cations around the negatively charged collector. Therefore attachment is postulated to be weak with these types of attachment sites. The primary minimum attachment site would have a stronger, more permanent hold on the colloid due to van der Waals forces. This is reflected by the depth of the primary minimum.

As the colloid approaches within a nanometer (10^{-9} m) of the grain, there is repulsion due to a double layer (dl) of ions surrounding the grain surface and a short range repulsive force called the Born energy (Ryan and Elimelech, 1996). In the case where the grain and colloid carry opposite charges there is no positive potential energy impediment to the attachment of the colloid to the grain. The DLVO energy curves in this case are characterized by a single deep minimum (Loveland et al., 1996).

Although attachment efficiency (α) can be theoretically calculated from DVLO forces alone (Swanton, 1995, Ryan and Elimelech, 1996, Schijven and Hassanizadeh,

2000), in column experiments α is usually determined empirically, once a theoretical value for η_o has been calculated, by equation 2-9 below:

2-9

$$\ln\frac{C}{C_o} = -\frac{3}{2}(1-\varepsilon)\alpha\eta_o\left(\frac{L}{d_c}\right)$$

where C is the steady state column effluent concentration, C_o is the influent, ε is the porosity, L is the effective column length and d_c is the median grain diameter (Yao et al., 1971). Equation 2-9 assumes spherical grains and a constant grain diameter in a clean filter bed. Furthermore, direct comparisons of α between experiments are limited since changes in the flow rate, and grain shape could confound any attempt to compare attachment efficiencies resulting from different grain properties or water chemistries. Therefore, although the concept of attachment efficiency, in conjunction with collision efficiency is useful to visualize physicochemical attachment, it is very difficult to know either with any certainty, since one must be theoretically calculated to know the other. Further, both the theoretical equations for collision efficiency (and that for attachment efficiencies) rely on many simplifying assumptions, some that have already been mentioned.

This semi-empirically derived attachment efficiency describes the ratio of the number of attachments that occur compared to the number of collisions. Other approaches to calculating α include the IFBL (Interaction Force Boundary Layer) approximation (Swanton, 1995) and a method that uses the relative breakthrough (RB) of a colloid relative to a conservative tracer (Pieper et al., 1997, DeBorde et al., 1999). These methods are reviewed in Ryan and Elimelech (1996). Some attachment efficiencies calculated by others work are reported in Table 2-2.

Table 2-2 – Attachment Efficiencies α for Viruses from Column Studies (6-35 cm in length) Schijven and Hassanizadeh, 2000

Virus	Media Type	pH	NaCl	α	Reference
MS2	Sand (Cape Cod)	5.7	0.1	0.007	Kinoshita et al. (1993)
		7	0.1	0.01	
		8.2	0.1	0	
	Quartz	3.5	0.01	0.12	Penrod et al. (1996)
		3.5	0.3	0.16	
		5	0.01	0.009	
		5	0.1	0.09	
		5	0.3	0.04	

The data in Table 2-2 demonstrate α is proportional to NaCl concentration (Penrod et al., 1996). In contrast, little proportionality was found between α and pH in the Kinoshita et al. (1993) study. This is in contrast to other authors that find α is highly (usually negatively) proportionate to pH (Loveland et al., 1996).

The study by Penrod et al. (1996) shows the effect of increasing ionic strength on attachment efficiency (and overall removal) using NaCl. These values were reported by Schijven and Hassanizadeh (2000). Unfortunately, it was not reported which method (RB, IFBL or semi-emperical method from equation 2-9) was used in calculating these values. The reported literature demonstrate that at similar experimental conditions (virus type, water chemistry, grain type and size), the attachment efficiency calculated for viruses often can differ over orders of magnitude, particularly when comparing laboratory and field results (Schijven and Hassanizadeh, 2000). Therefore, collision efficiency remains a conceptual model and not a predictive tool for predicting virus and pathogen transport.

2.4.1.3 The Importance of Grain Size on Pathogen Removal Efficiency

Equation 2-10 shows the single collector overall removal efficiency. It is an analytical derivation that describes the removal of small colloids by a single spherical grain resulting in the overall removal efficiency (η).

2-10

$$\eta = \frac{I}{U \cdot C_o \cdot \pi \cdot a_c^{\,2}}$$

where I is the depositon rate (s^{-1}) of colloids, U is the approach velocity (approximated by the darcy velocity), C_o is the influent concentration and a_c is the radius of the grain. The single collector removal efficiency (η) can be related to the expected concentration of the colloid at the effluent end of a column with equation 2-9. When equation 2-10 is substituted into equation 2-9 (for $\alpha\eta_o$) it is apparent that the ln of the normalized effluent colloid concentration (C/C_o) is related to the cubic inverse of the grain's radius (a_c). In other words, as the grain size decreases, the concentration of the colloid decreases exponentially (to the power of 3) faster. Although there are other forms of equation 2-10 describing η (interaction force boundary layer (IFBL) and Rajagolapan and Tien's correlation equation, reviewed in Ryan and Elimelech, 1996), they all display similar dependence on particle size. Thus, physicochemical colloid filtration theory predicts that media grain size can potentially have a substantial impact on colloid transport and attenuation porous media.

2.4.2 Size Exclusion

In contrast to physicochemical filtration, size exclusion is a strictly physical process. Long considered to be a potentially significant process in the attenuation of pathogens in fine grained aquifers (e.g. Matthess and Pekdeger, 1988), size exclusion was

considered a separate process and not included in the modified advection-dispersion (equations 2-1 to 2-3) until recently when Foppen et al. (2005) incorporated straining into this equation. They accomplished this by splitting up the deposition rate ($\partial S/\partial t$) into two terms, accounting for physicochemical sorption and straining, as demonstrated in equation 2-11 below:

2-11

$$\frac{\partial S}{\partial t} = \frac{\partial S_{DEP}}{\partial t} + \frac{\partial S_{TEMP}}{\partial t}$$

where S_{DEP} accounts for the bulk concentration of pathogens retained due to pore size exclusion and S_{TEMP} is for physicochemical sorption. This process is also known as mechanical straining and may best be explained by considering Figure 2-1.

Matthess and Pekdeger (1988) first tried to quantify the effect of size exclusion with the following two equations.

2-12

$$\eta_{SG} = \frac{d_p}{F_s \cdot d_k} \geq 1.5$$

2-13

$$d_k = 0.2 d_{10}$$

where η_{SG} is the geometrical suffusion security (an empirical term that represents a boundary condition where size exclusion will occur), d_p is the diameter of the microorganism, F_s is the empirical transit factor for suffusion (an empirical factor describing the effect of a variety of indeterminate grain properties, such as morphology, angularity or packing configuration) often assumed to be 0.12 (Foppen et al., 2005), d_k is the hydraulic equivalent diameter of pore canals and d_{10} is the grain diameter for which ten percent of the grains are smaller. As long as η_{SG} is greater than 1.5, no colloid

transport will occur (Matthess and Pekdeger, 1998; Foppen et al., 2005). F_s would be smaller for more angular and rough grains. It should also be mentioned that if pathogens are flexible, it may be possible for them to squeeze through smaller pore sizes than rigid microspheres of the same diameter. Since porous media in nature have a non uniform distribution in grain size, based upon this equation (2-12), even medium sands may be able to strain out some bacteria. Figure 2-4 shows the relative sizes of porous media and several common pathogens.

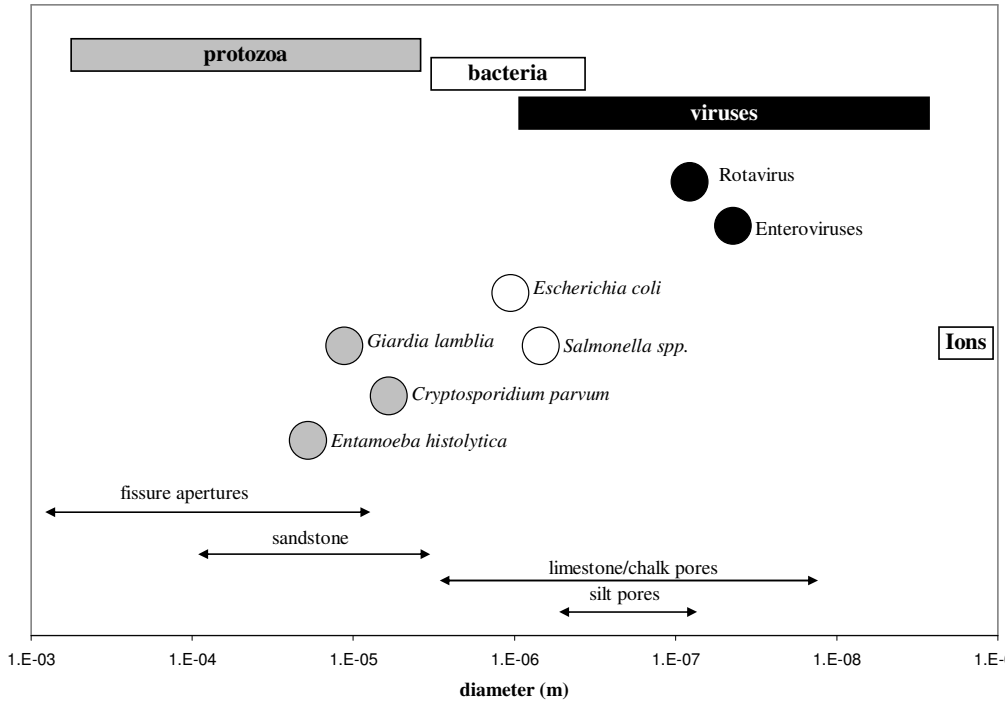

Figure 2-4 – Size comparison of common pathogens with common aquifer pores (Taylor et al., 2004)

There have been several attempts to predict the effect of size exclusion on colloid transport through different sizes of porous media. Tufenkji et al. (2004) demonstrated the importance of grain shape on the mechanical straining of *Cryptosporidium* and

microspheres. They performed a set of column experiments that demonstrated the importance of pathogen size in the range of bacteria to protozoa in very well sorted (UC = 1.24), fine grained, crushed, silica sand. The flow rate was 36 m/day with a pH of 5.7 in 0.21 mm (d_{50}) sand. Using *Cryptosporidium* (3.6 μm) and various sized microspheres (4.1, 1.9, 1.0 and 0.32 μm), they tested the effects of increasing ionic strength (1, 3.16, 10 mM KCl) on the attenuation of each of these colloids in the sand.

When Tufenkji et al. (2004) investigated *Cryptosporidium* attenuation in columns of sand they found that although there was a perceivable reduction in peak concentration of the colloids at high ionic strength (C/C_o = 0.1 in the two higher IS waters) oocysts broke through duplicate columns each at C/C_o = 0.41 when low ionic strength water was utilized. This indicated that attenuation was occurring in spite of the repulsive forces between the negatively charged pathogen and grain. Based on a purely physicochemical understanding of attenuation, one would expect that complete breakthrough would occur at such a low ionic strength, since (as discussed previously) the attachment efficiency (α) would be expected to be very low. Therefore, this attenuation was inferred to be caused by mechanical straining.

To further test their hypothesis that mechanical straining (size exclusion) was responsible for this reduction in *Cryptosporidium,* another column experiment at identical conditions to the low IS run was performed using 4.1 μm microspheres instead (similar size to *Cryptosporidium*). It was found, in duplicate runs, that similar reduction in peak concentration resulted from the use of these *Cryptosporidium*-sized microspheres (C/C_o = 0.41). Since the surface properties, charge, roughness and isoelectric point are different between these two colloids, this suggested that the attenuation was being caused by

something they had physically in common (i.e. only size) rather than something physicochemical in nature. Physicochemical attachment is affected by changes in the surface properties of the colloid (Ryan and Elimelech, 1996).

In further column experiments utilizing spherical glass beads (made of SiO_2 like the crushed silica sand used earlier) of similar size and uniformity to the (angular) crushed sand, Tufenkji et al. (2004) showed that no attenuation of either the *Cryptospordium* or the microspheres (4.1 μm) occurred, suggesting that attenuation was related to grain shape rather than grain size. This lent further credibility to the theory that a physical process rather than a physicochemical one was responsible for the attenuation. In a fourth set of experiments they passed all four sizes of microspheres (4.1, 1.9, 1.0 and 0.32 μm) through the crushed silica sand yielding complete breakthrough of all sizes except the largest one. Thus the authors concluded that mechanical straining could be a significant attenuation process with bacteria and protozoa sized pathogens in fine grained, angular sand.

Tufenkji et al. (2004) showed that in some cases (e.g. very angular, crushed silica sand) the ratio of particle diameter to median grain diameter (dp/d_{50}) need only be as high as 0.002 for significant straining to occur. Although a direct comparison to Matthess and Pekdeger's (1988) method for predicting pore size exclusion (based on the d_{10} value) is difficult, pore size exclusion at a dp/d_{50} of 0.002 certainly implies much greater retention than predicted by Matthess and Pekdeger's equation 2-12. In the larger protozoa and bacteria, pore size exclusion could be the dominant retardation factor while with viruses the most important factor is likely physicochemical sorptive forces (Matthess and Pekdeger, 1988; Schijven and Simunek, 2002).

2.4.3 Elimination

For protozoa, bacteria and viruses, as with most living things, survival time is inversely related to water temperature down to the freezing point (e.g. Schaffer, 2002). Thus the waterborne pathogens should be able to survive longer in the environment in winter and higher latitudes where water temperatures are cooler. Other factors which affect the viability of pathogens are indigenous micro-organisms, which may lead to competition, predation and parasitism, pH, chemicals and nutrient content (Matthess et al., 1988; Lawrence and Hendry, 1996; Schijven and Hassanizadeh, 2000; Jin and Flury, 2002). The equation that is most commonly used to describe natural die-off or inactivation (viruses) is (Schijven and Hassanizadeh, 2000):

$$N = N_o e^{-\lambda t} \qquad \textbf{2-14}$$

where N is the number (or concentration) of pathogens at time t. N_o is the initial concentration of pathogens and λ is a die off rate constant. λ is highly proportional to temperature, such that in warm waters this term is several orders of magnitude larger than in cold waters (4 ºC) (Schijven and Hassanizadeh, 2000). Figure 2-5 shows the typical rate of decline for viruses at different water temperatures. Also shown in this figure is the calculated die-off constant of MS2 contained in stock suspensions stored at 4 ºC in a refrigerator in the present research, calculated from equation 2-14.

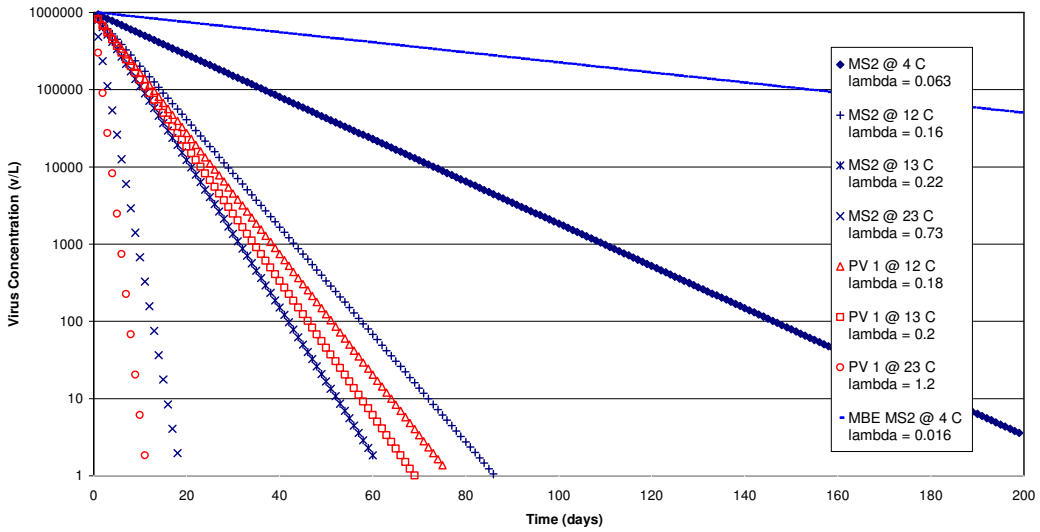

Figure 2-5 - Inactivation Rates of MS2 and Poliovirus 1 at Different Temperatures (Yates et al., 1985)

Since all pathogens are sensitive to temperature, assuming otherwise comparable conditions, warmer climates with warm surface water and groundwater temperatures will result in faster die off of harmful pathogens (Yates et al., 1985).

Groundwater and surface water have both been found to contain every type of pathogens in every populated climate and region of the world (Chu et al., 2001). In general, groundwater contains fewer organisms than surface water because of the combined attenuation processes of physicochemical attachment, size exclusion, and die-off as the water enters the aquifers vertically through the partially saturated upper soil layers or horizontally via saturated riverbanks (Harvey, 1997; Ginn et al. 2002; Taylor et al. 2004).

Computer models of pathogen transport both in surface water (Medema and Schijven, 2001; Schernewski and Jülich, 2001) and groundwater have been developed

(Matthess and Pekdeger, 1988; Schijven and Simunek, 1999; Schijven et al., 2000b; Schijven and Hassanizadeh, 2000; Chu et al., 2001; Ginn et al., 2002; Schijven and Simunek, 2002; Keller et al., 2004). Lacking in these models, however, are the quantitative details of attenuation processes and the physical, chemical and biological factors which affect these processes must be better understood. Therefore, the accuracy of these models is at best approximate in a well characterized column or field site (Schijven and Simunek, 2002; Flynn et al., 2004a). Much carefully recorded experience with colloid transport is needed to challenge and refine old conceptual and analytical models of pathogen transport.

2.5 Water Chemistry

Table 2-3 shows some typical major ion concentrations encountered in riparian groundwater settings. According to Freeze and Cherry (1979) and Appelo and Postma (1993) the only major ions missing from this table that contribute significantly to the ionic strength of a typical groundwater would be K^+, Mg^{2+} and SO_4^{2-}. The experimental ionic conditions used in the current study only included Ca^{2+}, Na^+ and Cl^-. It has been found that Ca^{2+} is more effective in attenuation than other divalent cations. Since K^+, being a monovalent cation, has less effect than divalent cations on the retention of colloid retention (Redman et al., 1998). No recent experiments have been done testing whether divalent anions affect the retention of colloids, rather traditional colloid filtration literature emphasizes the importance of cations (especially higher valent) in colloid retention (e.g. Ryan and Elimelich, 1996, Redman et al., 1998, McCarthy et al., 2002, Zhang and Jin, 2003, Xiqing et al., 2004).

Table 2-3 – Major Ion Concentrations in Natural Riparian and Groundwater Systems

Setting and Location	Reference	Ca^{2+} mg/L	Ca^{2+} mmol/L	Na^{+} mg/L	Na^{+} mmol/L	Cl^{-} mg/L	Cl^{-} mmol/L	HCO_3^{-} mg/L	HCO_3^{-} mmol/L
Base Flow Recharge to stream, Scotland	Soulsby et al., 1998	1	0.03	3	0.15	4	0.12	NR*	NR*
Riparian Glacial Outwash, Wisconsin	K. Kim, 2002	5	0.12	1	0.04	1	0.02	15	0.25
Stream Water, Japan	Ohrui and Mitchell, 1999	6	0.15	1	0.04	2	0.06	12	0.20
Stream Water, Czech	Peters et al., 1999	14	0.35	5	0.20	3	0.08	NR	NR
Shallow riparian groundwater in rainy season, California	Rains and Mount, 2002	35	0.87	17	0.74	8	0.23	275	4.51
Riparian Groundwater, France, sand and gravel alluvium with some carbonates	Negrel et al., 2003	60	1.50	20	0.87	16	0.45	244	4.00
Shallow groundwater recharged from canal water in an arid region, Nebraska	Harvey and Silbray, 2001	70	1.75	75	3.26	20	0.56	325	5.33
Shallow Karst, North China	Liu et al., 2004	85	2.12	0.14	0.01	4	0.11	250	4.10
Average US Groundwater	Appelo & Postma, 1993	50	1.25	30	1.30	15	0.42	200	3.28
	Average	**41**	**1.01**	**19**	**0.81**	**9**	**0.24**	**189**	**3.09**
	Minimum	**5**	**0.12**	**0.14**	**0.01**	**1**	**0.02**	**12**	**0.20**
	Maximum	**85**	**2.12**	**75**	**3.26**	**20**	**0.56**	**325**	**5.33**

Table 2-4 shows the range of water chemistries used in several past colloid and virus transport experiments. McCarthy et al. (2002) observed significant increases in microsphere attenuation through fractured shale by varying the [Ca^{2+}] from 0.1 to 1.0 mmol/L. Zhuang and Jin (2003) found that even small amounts of [Ca^{2+}] (0.075 mmol/L) resulted in a profound increase in the attenuation of MS2 and PhiX-174. This increase was apparent even over other solutions of comparable ionic strength, but made up of monovalent cations (Na^+ and K^+). In fact, Pillai et al. (1997) (not shown in Table 2-4) demonstrated that the attenuation of a virus in crushed silica sand was unaffected by a ten fold increase in ionic strength, using monovalent cations (1 – 10 mmol/L Na^+). Even a further ten fold increase in Na^+ (10 – 100 mmol/L) only resulted in a 1 log reduction in peak breakthrough concentration. In contrast, under the same water and soil conditions, a minor increase in Ca^{2+} (1-3 mmol/L) resulted in a 5 log reduction in peak concentration. The same effect was observed using Mg^{2+} as the divalent cation. Through the comparison and consideration of other reported results, the settings for this present work were determined to invoke a measurable effect on attenuation of pathogens at an environmentally relevant ionic strength (i.e. levels typical of shallow groundwaters).

Table 2-4 – Water Chemistry for Column-Scale Colloid and Virus Transport Experiments

Experimental Purpose	Colloid Used	Author	Na	K	Ca	Mg	Cl	NO_3	HCO_3	CO_3	SO_4	PO_4	I	pH
		Units	mmol/L	mmol/L	mmol/L	mmol/L	mmol/L	mmol/L	mmol/L	mmol/L	mmol/L	mmol/L	mmol/L	
		Charge	1	1	2	2	-1	-1	-1	-2	-2	-3		
varying ionic strength for virus transport with Al-oxide coated sand	MS2 and PhiX-174	Zhang and Jin, 2003	5 different buffers at different ionic strengths											
relating ionic strength to colloid retention	silica microspheres	Elimelech et al., 2000	0.1-10				0.1-10						0.1-10	
varying monovalent and divalent cation conc to effect transport of colloids in Shale fractures	0.1, 0.5, 1.0, 2.1 um carboxylate-modified latex microspheres	McCarthy, McKay and Bruner, 2002	5-30		0.1-1.0		0.2-30						0.3 - 30	
using coated quartz (uncoated, hematite, polymer)	S5 and S139, 1-2 um rod shaped bacteria	McCaulou, Bales and McCarthy, 1994	0.25	0.02	0.05	0.14	0.10	0.02	0.14		0.19		1.02	
PBS, low Ionic strength	PBS low IS	Zhang and Jin, 2003	1.70	0.04			1.24					0.25	2	
CBS, low ionic strength	CBS low IS	Zhang and Jin, 2003	2.00	0.04			1.24		0.80				2	
(divalent cat present)	AGW	Zhang and Jin, 2003	1.5	0.051	0.075	0.082	0.365		1.5				2	
relating saturation level to transport, AGW	Pseudomonas fluorescens P17	Jewett et al., 1999	0.9	0.1	0.2	0.6	0.3	0.1	0.6		0.7		3.9	
varying ionic strength and flow conditions in glass beads	latex microspheres	Xiqing et al., 2004	6-50				6-50						6-50	6.92
varying pH and comparing transport of MS2 w/ Norwalk in sand	MS2 and recombinant (no RNA) Norwalk	Redman and Grant et al., 1997	10				10						10	5, 7
clogging of limestone fractures, on site simulated GW >70 m deep	various indigenous biofilm secreting bacteria	Ross, et al., 2001	23.37	0.19	0.15	0.16	10.57	0.06		0.15	0.16	0.06	18.6	8.2
comparing soil types and pH levels	MS2 and PRD-1	Kinoshita, Bales, Gerba et al., 1993	100				100						100	various
Phosphate buffered saline	PBS	Zhang and Jin, 2003	140	3			103					20	163	
Carbonate buffered saline	CBS	Zhang and Jin, 2003	160	3			103		60				163	
comparing transport of viruses in sand, buffered AGW	MS2 and PhiX-174	Jin et al., 1997	140	3.42			103					20	213	7.5

2.6 Scope of Present Work

In light of the presented literature review, there is a need for better understanding of waterborne, viral pathogen transport from surface water to groundwater (Szewyk et al., 2000). The setting of regulations for set back distances and groundwater travel times of drinking water wells, such as GUDI (Ontario Regulation 505) needs to be based upon empirical knowledge and well tested theory of the transport of a range of sizes and types of human pathogens (Schijven et al., 2000a). In spite of this need to understand transport of a range of pathogen types and sizes (Jin and Flury, 2002), only a few dozen studies have been published in which virus transport has been examined in columns or at field sites (Schijven and Hassanizadeh, 2000). Of these studies, even fewer have been performed with both viruses and bacteria simultaneously (Scandura and Sobsey, 1997; Harvey et al., 1999; Schijven et al., 2000a; McCarthy et al., 2002; Pang et al., 2003).

The relative impacts of physicochemical filtration and size exclusion (and the associated role of angularity and size distribution of porous media) on virus attenuation are not well understood. To investigate these issues, many studies have utilized spherical beads (Ryan and Elimelech, 1996; Loveland et al., 1996; Schijven and Hassanizadeh, 2000; Jin and Flury, 2002). While spherical beads are useful for further developing physicochemical colloid filtration theory, since they better fit the assumptions implicit to those models (e.g. equation 2-8) (Ryan and Elimelech, 1996), they fail to realistically represent natural environments. Accordingly, column studies conducted with these synthetic media often fail to indicate the field-scale transport behaviour of viruses (Schijven and Hassanizadeh, 2000; Flynn et al., 2004a), bacteria (Harvey, 1997) or protozoa (e.g. Tufenkji et al., 2004) in natural granular media.

Examining the attenuation abilities of angular porous media at different sizes and water chemistry with different ionic strengths, of known pathogens (viruses, bacteria and protozoa) is essential for providing guidance for the development of surface water-groundwater interaction regulations such as that encountered in an RBF environment. Furthermore, concurrently investigating the predictions of physicochemical filtration theory and size exclusion, will enhance the fundamental understanding of colloid transport in porous media, with the ultimate goal being the development of improved quantitative models of bio-colloid transport in the subsurface.

3. MATERIALS AND METHODS

3.1 Research Approach

Figure 3-1 visually summarizes the tasks that were carried out to meet the experimental objectives and overall research goal of this thesis. Prior to conducting laboratory investigations of bacteriophage and microsphere removal by porous media at conditions consistent with riverbank filtration, three general catagories of tasks needed to be completed. These were: 1) microbiological tasks, 2) experimental apparatus development tasks, and 3) water chemistry selection tasks. These tasks, along with the preliminary, factorial design, and additional column experiments are summarized in Figure 3-1. The rationale for the experimental design, the specific components chosen, and the methods used will be discussed in this section.

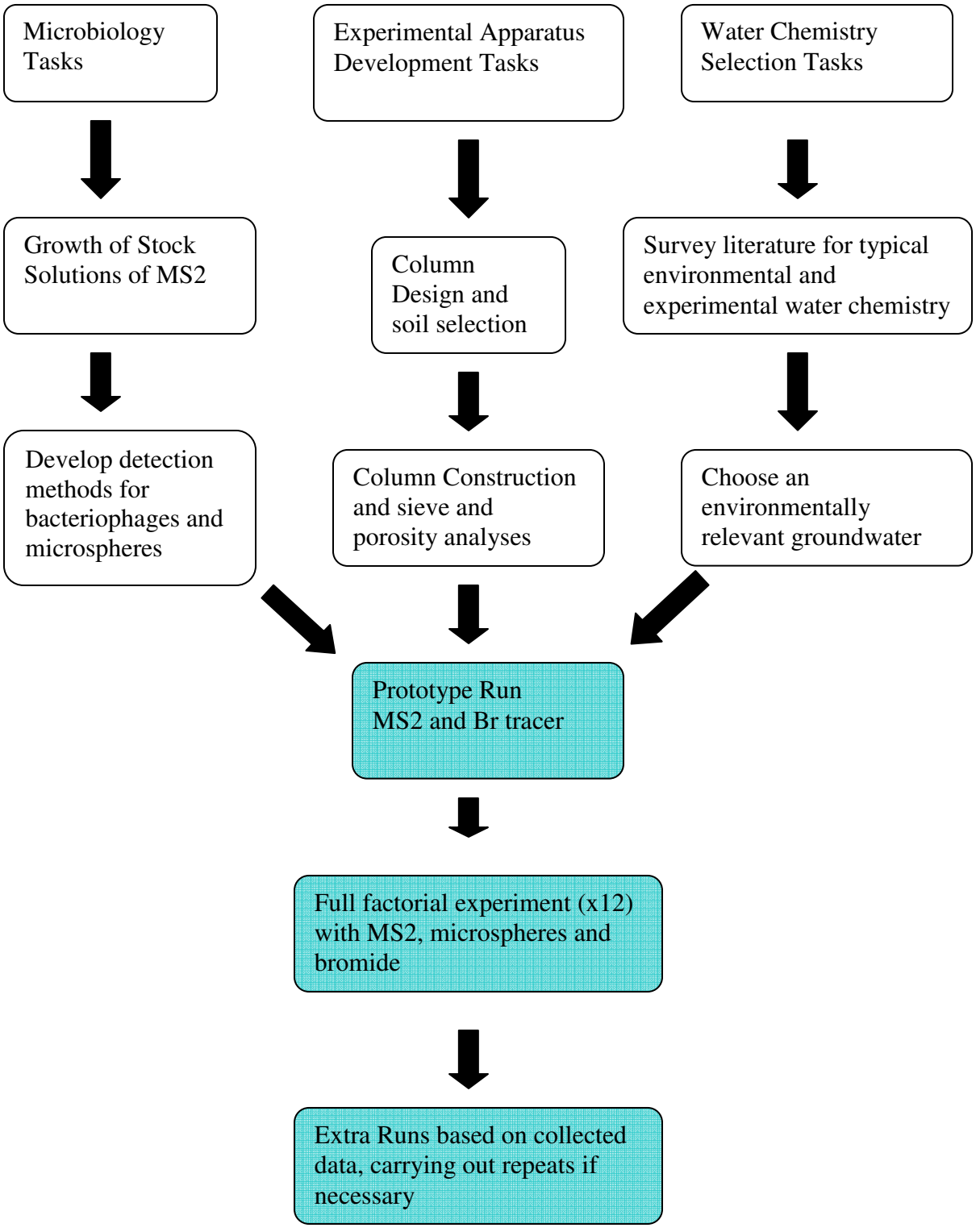

Figure 3-1 - Development Stages for Virus and Microsphere Transport Column Studies

3.2 Factorial Design

Pathogen concentration, media grain size, and water ionic strength impacts on bio-colloid attenuation were investigated utilizing a 2^2 factorial design experiment. An additional experiment was conducted (in triplicate) to confirm that the influent bacteriophage concentration did not impact the research outcomes. Each of the conditions of the factorial experiment were investigated in duplicate. The experimental conditions during each of the column studies are summarized in Table 3-1 below.

Table 3-1 – Summary of Experimental Conditions Utilized During the Column Studies

		Influent Water Chemistry				Influent Water Microbiology	
Run #	**Sand**	**$[Ca^{2+}]$ (mmol/L)**	**$[Na^{+}]$ (mmol/L)**	**$[Cl^{-}]$ (mmol/L)**	**Ionic Strength (mmol/L)**	**MS2 (pfu/mL)**	**1.5 µm Microsphere (/mL)**
1	A	Prototype run				1.E+06	
2	A	1	2	4	8	1.E+05	
3	A	1	2	4	8	1.E+07	
4	A	1	2	4	8	1.E+05	1.E+04
5	A	1	2	4	8	1.E+07	1.E+04
6	A	1	2	4	8	1.E+05	1.E+04
7	A	1	2	4	8	1.E+07	1.E+04
8	A	4.8	19.5	29.1	94.7	1.E+06	1.E+04
9	A	4.8	19.5	29.1	94.7	1.E+06	1.E+04
10	B	1	2	4	8	1.E+06	1.E+04
11	B	1	2	4	8	1.E+06	1.E+04
12	B	4.8	19.5	29.1	94.7	1.E+06	1.E+04
13	B	4.8	19.5	29.1	94.7	1.E+06	1.E+04
14	A	4.8	19.5	29.1	94.7	1.E+06	1.E+04
15	A	4.8	19.5	29.1	94.7	1.E+06	1.E+04

The impact of divalent cation concentration, Ca^{2+}, was investigated at 1.0 and 4.8 mmol/L corresponding to ionic strengths of 8 and 94.7 mmol/L. This represents a range of reasonable shallow groundwater chemistries (see Table 2-3). To isolate the impacts of grain size alone (i.e. exclusive of mineralogy, roughness, etc) on the subsurface transport

of pathogens, two different sand types (0.7 and 0.34 mm median grain size), possessing identical mineralogy and similar surface roughness were used.

3.3 Research Rationale

3.3.1 Bio-colloid Effects

MS2 was the virus selected for this research because of its similarity in size to common human viruses and pI (isoelectric point). The fact that MS2 has a similar pI (3.9) to human viruses means that it will carry the same negative charge at neutral pH, so the attachment efficiency is likely to be similar between both types of viruses. MS2 transport in natural media also has been studied extensively individually (Zhuang and Jin, 2003; Schijven et al., 2002; Jin et al., 2000; Dowd et al., 1998; Jin et al., 1997) and in conjunction with human pathogenic viruses (Meschke and Sobsey, 2003; Schijven et al., 2003; Redman et al., 1997).

The transport of bacterial-sized (1.5μm) carboxylated microspheres was also investigated. Microspheres are useful surrogates for human bacterial pathogen transport in natural (McCarthy et al., 2002) and engineered environments (Elimelech et al., 2000 and Tufenkji et al., 2004), are comparable in size to many human pathogenic bacteria, and provide a tie-point to previously reported studies that have investigated pathogen transport in porous media systems at the laboratory and field scale (Côté, 2004 and Watling, 2004). Microspheres were also included in this work to potentially demonstrate mechanistic differences between bio-colloid transport of viruses and bacteria. Since many sizes of waterborne pathogens exist, an understanding of how bio-colloid size affects subsurface transport of pathogens is critical to providing regulatory guidance for

groundwater and GUDI drinking water systems; for example, determining well set back distances (from surface water) and requisite groundwater travel times.

Table 3-5 lists the physical and chemical characteristics of some common bacteriophages and human viruses. As indicated in that table, MS2 has an isoelectric point of pH 3.9. At neutral pH, it can be inferred that MS2 has a negative charge. Relative to other bacteriophages, like PhiX-174 (with higher isoelectric points), it would be expected that MS2 would be less impeded in its movement through negatively charged silica sand, since the media grains would likely repel the like-charged virus surrogate.

It was also expected that the size difference between the viruses (30 nm) and the bacteria-sized microspheres (1500 nm) would result in differences in subsurface transport characteristics. The microspheres have a lower expected collision efficiency (Figure 2-2 and Ryan and Elimelech, 1996) relative to MS2, possibly resulting in less relative attenuation by the same porous media. The relative impact of fewer contact opportunities was concurrently investigated with the impact of media grain size, as it is possible that size exclusion plays a role in pathogen attenuation in finer sands (Foppen et al., 2004).

3.3.2 Grain Size

It is expected that decreasing the grain size of the soil will increase retention of both viruses and microspheres since the surface area of potential attachment surfaces is twice as great with the fine grained sand as the coarse one (Table 3-4). Another reason to expect the fine grained sand to better retain viruses than the medium sand is based on colloid filtration theory (Ryan and Elimelech, 1996). This has already been discussed Chapter 2.

Comparing the relative retention of microspheres by large and small media grain sizes may allow the discernment between electrostatic attachment and size exclusion pathogen attenuation mechanisms. For example, if no pathogen surrogate attachment occurs in the medium sand but considerable attenuation occurs in the fine sand, it may be concluded that size exclusion contributed to the attenuation since most of the conditions affecting physicochemical attachment (water chemistry, flow, mineralogy, grain angularity and roughness) were the same in the fine and medium sand experiments. However, due to the dependence of overall attachment efficiency (η) on media grain size as specified by the single collector model (equation 2-10), and the overall increase in media grain surface area associated with using the finer sand, the process of size exclusion is difficult to prove incontrovertibly. One of the advantages of carrying out the 2^2 factorial design experiment is that interaction or synergy between the two effects (grain size and ionic strength) can be tested. Based on colloidal filtration theory it is expected that attachment will increase with: 1) decreasing grain size (equation 2-10), because of the increase in surface area which allows more attachment, and increasing [Ca^{2+}], because of the compression of the double layer of ions which lowers the repulsive energy threshold, allowing particles to move close enough to attach to grain surfaces (Figure 2-3) (Ryan and Elimelech, 1996).

3.3.3 Soil Properties

Porosity Estimates

Media porosities were measured using the method of Brush et al. (1999). In summary, 50 ml of media were weighed and poured into a 100 ml graduated cylinder,

containing 50 ml of water. The unpacked media porosity was then estimated by the amount of water displaced by the bulk volume of the grains:

$$\varepsilon = \frac{\left(100 - V_f\right)}{V_{sat}} \qquad \textbf{3-1}$$

where V_f is the final volume of the water and sand together, ε is the unpacked porosity of the media, and V_{sat} is the saturated volume of sand. This last term accounted for the slight change in measured sand volume, calculated after the sand was poured into the water. The final volume of sand was used in the porosity calculations. The estimated porosity values are presented below in Table 3-2. The raw data for these measurements are shown in the Appendix in Table A-2.

Table 3-2 – Physical Properties Sand Types Used in Column Experiments

Code	Sand	Median Grain Diameter (mm)	Uniformity Coefficient (d_{60}/d_{10})	Porosity	Bulk Density (g/cm^3)
A	Indusmin 2010	0.7	1.9	0.43	1.43
B	Indusmin 4010	0.34	2.1	0.43	1.51

Grain Size Analyses

Sieve analyses of the two sands used in the present study were performed in triplicate (or duplicate) using approximately 800 g samples (Octagon 200 Test Sieve Shaker, Endocotts, London, England) for 20 min. Figure 3-2 shows the grain size analyses of the sands used in the present experiments. The raw data for these size distribution curves are shown in the Appendix in Table A-3 and Table A-5.

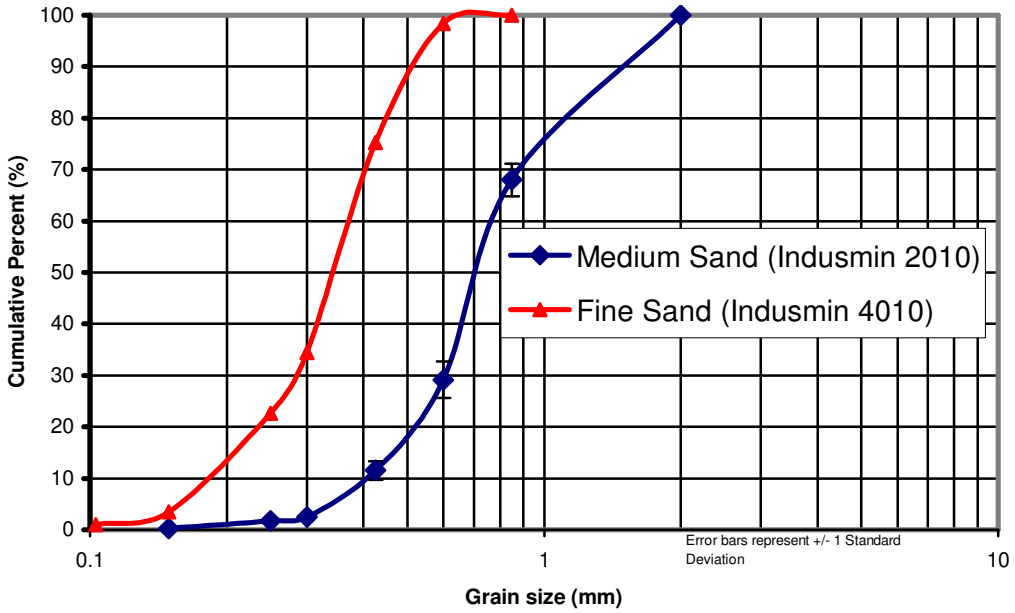

Figure 3-2 - Grain Size Curves of Sands Used Column Experiments

3.3.4 Considering Grain Properties in from a Colloid Transport Perspective

Table 3-3 summarizes the physical and mineralogical properties of these sands. The sand is crushed silica sand, over 99% pure quartz (Indusmin). In crushed sand, unlike natural unconsolidated aquifer material, the grains are very angular. Crushed sand was used to control media grain size effects while maintaining identical mineralogy and similar angularity.

In the natural environment minerals weather in an order equal to Mohr's scale of hardness (Klein and Hurlbut, 1985). In this scale quartz is near the top in hardness (a 7, where 10 is diamond), whereas feldspars (6), calcite (3) and micas (2.5) are closer to the bottom of the scale and are therefore more easily weathered. In the course of transport of mineral grains from their primary source (e.g. granite) to a deposition site, some minerals will be completely dissolved and others will be greatly reduced in size due to dissolution

over thousands of years of groundwater flow. Quartz will tend to stay intact and remain more angular than then other common minerologies. Therefore if a sand sample is taken from a riverbank site and separated according to size, it is likely that the finer, smoother grains will contain softer minerologies than the larger grains. By using artificially created (crushed) size ranges, the problem of mineralogy-biased grain roughness and size is avoided. Due to the predictions made in section 3.3.2. with regards to the importance of fine sand in attenuating colloids and reported data regarding microbial attenuation by sands containing positively charged metal-oxides (Loveland, 1996; Elimelech, 2000; You et al., 2003), it is known that a small percentage (~5 %) of fine grained mafic (frequently metal-oxide containing) media can contribute substantial increases in attenuation regardless of the size or composition of the (larger) median grain size.

Media grains of identical mineralogy and similar angularity were chosen here to isolate the effects of media grain size on pathogen attenuation in subsurface materials. Flynn et al. (2004b) found that mineralogy can have a significant effect on bacteriophage transport. Using pure feldspar, pure quartz, crushed granite, and pure calcite, they showed that the bacteriophage H40/1 was retained differently by the various media. Tufenkji et al. (2004) demonstrated that, compared to spherical silica crushed silica resulted in greater attenuation of microspheres and *Cryptosporidium*. Thus, it is important to keep mineralogy and grain shape as consistent as possible when investigating size exclusion mechanisms of pathogen attenuation by porous media.

Table 3-3– Geologic properties of sand

Code Name	Name	Median Diameter (mm)	Uniformity Coefficient (D_{60}/D_{10})	D_{10}	Hazen k (cm/s)	Minerology (% by mass) Silica (SiO2)	Iron (Fe203)	Alumina (Al2O3)	Calcia or Lime (CaO)
Sand A	Indusmin #2010	0.7	1.9	0.40	1.6E-01	99.7	0.08	0.2	0.02
Sand B	Indusmin #4010	0.34	2.1	0.18	3.2E-02	99.7	0.08	0.2	0.02

The calculated uniformity coefficient and estimated Hazen conductivity values of the sands utilized in this investigation are listed in Table 3-3. Both uniformity coefficients were low relative to those that would be expected in natural environments, indicating that the sands were very well sorted. The anticipated conductivity was calculated using the Hazen equation:

$$k = d_{10}^{2} \qquad \textbf{3-2}$$

This equation dictates that in loosely packed sand, the hydraulic conductivity is equal to the square of the grain diameter below which only 10% of the sample grains are smaller (Chapuis, 2004). It is interesting to note that equations 2-12 and 2-13 (Matthess and Pekdeger, 1988) relate pore size exclusion to the inverse of d_{10}. Therefore the finest 10% of sand impacts both conductivity and size exclusion. This relationship is logical since it is the finest grains that will fill the spaces between larger ones and therefore most greatly influence the median pore size for the entire packed column.

The media surface areas were calculated assuming that each grain was perfectly spherical, using the relationship in equation 3-3 below.

$$A = \frac{6M}{\rho_p \cdot d_p} \qquad \textbf{3-3}$$

where A is the total surface area, M is the mass of the sample, ρ_p is the particle density and d_p is the grain diameter. This equation shows that if d_p is doubled, while keeping M and ρ_p constant, then A is reduced by 50%; that is, there is a linear, inverse relationship between grain diameter and total surface area. The process of calculating theoretical surface area is outlined in Table 3-4.

Table 3-4 - Theoretical Surface Area Calculations

Name	Average Diameter (mm)	spherical surface area of average grain $4*\pi*r^2$ (mm^2)	Volume of sphere $4/3*\pi*r^3$ (mm^3)	density of quartz (g/mm^3)	mass per sphere (g)	Total Mass in Packed Column (g)	# of spheres in column	Total Surface Area (mm^2)	Total Surface Area (m^2)
Indusmin #2010	0.7	1.539	0.180	2.67E-03	4.80E-04	900	1.9E+06	2.9E+06	2.9
Indusmin #4010	0.34	0.363	0.021	2.67E-03	5.49E-05	900	1.6E+07	5.9E+06	5.9

In one packed column (with length of 20 cm and diameter of 6.35 cm, as used in the present study) of uniformly sized medium sand (0.7 mm diameter) there are 2.9 m^2 of media surface area (assuming spherical media grains). A column of the fine sand (0.34 mm diameter) would contain 5.9 m^2 of surface area. The distribution of the sand sizes and the angular, rather than spherical, shape increase the surface area of these media, however. An assessment of the true surface area of these media was beyond the scope of the present investigation.

3.3.5 Ca^{2+} Effects

Table 3-5 compares MS2 to other well studied bacteriophages and human viruses. The following discussion will focus on the expected transport characteristics of MS2, but

this table reveals the similarity between MS2 and human viruses, so it is reasonable expect that these viruses would be attenuated similarly to MS2 (Redman et al., 1997).

Table 3-5 – Physical and Chemical Characteristics of Some Common Bacteriophages and Human Viruses

	Diameter (nm)	**Genetic Material**	**Isoelectric Point**	**Source**
Bacteriophages				
MS2	20-26	ss RNA	3.9	McKay et al., 1993
PhiX-174	23	ss DNA	6.6	Dowd et al., 1998
T7	60	ds DNA		Rossi, 1994
PRD-1	62		4.2	McKay et al., 1993
Qbeta	24		5.3	Dowd et al., 1998
PM2	60		7.3	Dowd et al., 1998
Human Viruses				
Norwalk	38	ss RNA	5	Redman et al., 1997
Echo 1	27	ss RNA	5-6.4	Zerda, 1982
Coxsackie A21	27	ss RNA	4.8, 6.1 *	Murray and Parks, 1980
Poloiovirus 1	23	ss RNA	6.6	Bales et al., 1993

* for two different conformational states

In the case of MS2 transport in porous media, the effect of increasing divalent cation concentration is to block or screen the sands' negative surface charges by double layer compression and allow the MS2 to be attracted to, instead of repelled by, the sand grain (e.g. Redman et al., 1999). Therefore a decrease in MS2 transport would be expected as a result of an increase in $[Ca^{2+}]$, since the quartz media grains carry a negative surface charge. It is also possible that an increase in $[Ca^{2+}]$ can enhance transport of bio-colloids, by reversing the normal attractive forces felt between oppositely charged grain and colloid. This type of effect was observed by Zhuang and Jin (2003), who used positively charged aluminum oxide coated sand. Using negatively charged PhiX-174 and MS2 they demonstrated that virus transport increased with increasing ionic

strength. Similar effects were observed by Loveland et al. (1996), in which positively charged Fe-oxide coated sands were used. Those authors observed an increase in the detachment of the bacteriophage PRD-1 with increasing ionic strength over a range of pH. Similarly, Pillai et al., (1998) demonstrated that increasing [Ca^{2+}] from 1 to 10 mmol/L resulted in an additional 5 log reduction in peak breakthrough concentration of a wild bacteriophage, isolated from raw sewage. They also demonstrated this effect using [Mg^{2+}] over the same concentration range, resulting in a 4.5 log reduction in peak concentration of the virus.

The results of the studies summarized above are consistent with colloid filtration theory. As ionic strength increases, negatively charged viruses are surrounded by positively charged cations. These cations screen the viruses' negative charge and prevent it from approaching positively charged media grains. Furthermore, Zhuang and Jin's (2003) results showed that the effect of increasing ionic strength was much greater on MS2 than PhiX-174. At high ionic strength, MS2 behaved almost as a conservative tracer whereas at low ionic strength it barely broke through the column; only after 12 pore volumes was any MS2 detected in the column effluent. This outcome was expected because MS2 (isoelectric point 3.9) is more negatively charged at neutral pHs than PhiX-174 (6.6) and would therefore be more attracted to the positively charged Al-oxide coated grains under low ionic strength conditions.

The electrostatic forces between like and oppositely charged particles at high and low ionic strength are described in Figure 3-3. This figure indicates that at sufficiently high ionic strengths (and high enough cation charge) the normal electostatic forces between pathogens and media grains are reversed (Loveland et al., 1996).

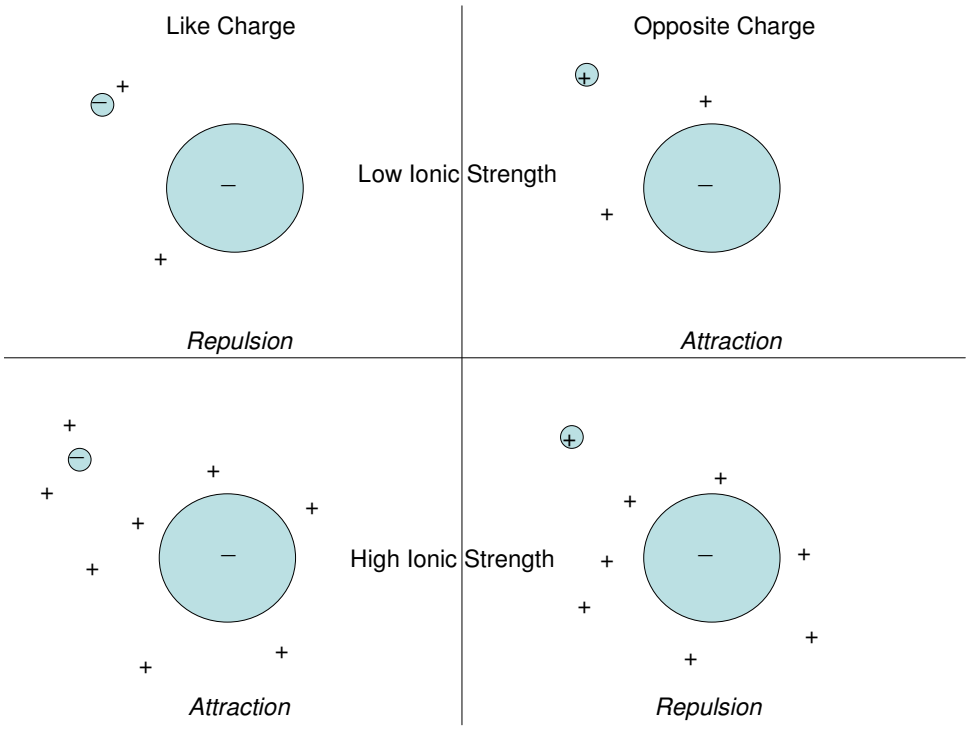

Figure 3-3 – Electrostatic Forces Between Like and Oppositely Charged Particles at High and Low Ionic Strengths

In the present study, 1.0 and 4.8 mmol/L concentrations of [Ca^{2+}] were utilized because they represent a wide range of ionic strengths that may be encountered in the natural environment (Freeze and Cherry, 1979) and are therefore more likely to have discernable impacts on pathogen attenuation (as compared to a narrower range of ionic strengths).

3.4 Microbiology

3.4.1 Bacteriophages

Measuring Growth Kinetics of *E. coli* Host Strains

Procedures for enumerating f-specific bacteriophages involve using a culture of host bacteria that are at the end of the exponential growth phase (Adams, 1959). It is at this stage in the culture's growth that the f-pili are expressed in numbers optimal for the infection of MS2. The f-pili are the site of infection for f-specific bacteriophages such as MS2. As a rule of thumb *E. coli* 15597, the host for *MS2*, are at the end of the exponential growth phase after 4 to 6 hours at 37°C. To verify this rule of thumb, a suspension of *E. coli* was grown and optical density measurements were made.

The growth kinetics of *E. coli* 15597 was characterized by measuring optical density over a period of 24 hours (wavelength 520 nm) (VERSA max tunable microplate reader, Molecular devices, USA). Optical density or the obstruction of the passage of light through an inoculated broth is directly correlated to bacterial concentration. The 96-well plate was kept at 37°C on an intermittently shaking table (1 min of continuous shaking every 15 min). 100 ml of sterile (autoclaved) nutrient broth were inoculated with 1 ml of a host bacteria culture (37 Cº) that had been grown in broth overnight (12 hours) on a continuously shaking tray. After inoculation the new suspension was swirled by hand briefly. 0.2 ml of this newly inoculated broth were added to each of 12 wells on the microplate. In addition, 12 wells were filled with sterile broth as indicators of potential contamination (negative controls). The optical density of the material in each well was measured every 15 minutes and recorded by a computer. These data yielded a growth curve indicative of the growth kinetics of the MS2 host.

Measuring Bacteriophage Concentration

The double layer agar method was used to measure bacteriophage concentration (Adams, 1959). Rossi (1994) demonstrated that in the initial contact between bacteriophage and their host bacteria, a minimal contact time (~1 min) was necessary for the optimal infection of host bacteria with bacteriophages. This finding was significant because if bacteriophages and their hosts are mixed in a dilution tube and then introduced directly into top agar then less than one minute is available for mixing before the agar solidifies. The double layer agar method used herein is outlined below.

Preparing the Stock Suspension

The stock suspension of MS2 (ATCC 15597-B1) was grown by adding 1 ml of MS2 in nutrient broth into a 200 ml culture of log phase *E. Coli* (ATCC strain 15597) that had been grown for 4-5 hours at 37 ˚C. After overnight (12 hour) incubation the *E. coli*/MS2 suspension was centrifuged at 20,000 rpm for 20 minutes. The supernatant was then filtered through a 0.2 μm filter (ZAPCAP-S Plus, Scheicher & Schuell, Dassel, Germany). The filtrate was stored at 4 ºC in sterile 250 ml glass flasks.

Measuring MS2 Concentration

The procedure for measuring MS2 concentration is presented in this section. The chemicals used in these experiments (NaCl, $CaCl_2$ and Glucose) were supplied by EMD Chemicals Inc. (Darmstadt, Germany), and the growth media (Tryptone, Bacto-yeast extract, Bacto-agar) were obtained from Becton, Dickinson & Co. (Le Pont de Claix, France).

To measure MS2 concentration, 1 ml of the MS2 liquid sample was serially diluted into each of 12 sterile test tubes containing 9 ml each of saline-calcium solution

containing 8.5 g NaCl and 0.22 g $CaCl_2$ per 1 L of Milli Q™ water. Each tube was lightly vortexed after the 1 ml sample was added. After the bacteriophage had been serially diluted, 1 ml of 4-5 hr exponential phase (for maximal population expression of the f-pilus, the site of infection for MS2) *E. coli* culture was added to each tube and lightly vortexed (5 sec). After 2 or 3 minutes, allowing for bacteriophage attachment, 1 ml of the MS2/*E. coli* suspension was pipetted into a test tube containing 5 ml of molten top agar that had been cooled so it could be held with bare hands. The MS2/*E. coli* molten agar suspension was poured over bottom agar in petri dishes and incubated at 37°C. After 12 hours, plaques appeared as clear spots in a cloudy lawn of *E. coli*.

Plaques represent areas of killed host bacteria, initiated by at least one bacteriophage in the centre of the clear spot. Once a bacterium is infected by the bacteriophage it lyses and releases bacteriophages (usually about 200) that then are able to infect neighbouring bacteria. The process continues many times until by 6-8 hours the plaques become visible to the naked eye. MS2 formed plaques approximately 3 mm in diameter.

3.4.2 Enumerating Microspheres

The general procedure for counting microspheres involved filtering (Filter assembly, Hoefer Scientific Instruments, San Fransisco, CA) a few millilitres (0.1-10 ml) of the sample through a 0.4 μm pore membrane (25 mm diameter, Polycarbonate Membrane Filters, Whatman 110607). The sample volume depended on the expected concentration of microspheres in the sample; accordingly, some samples required reprocessing so that adequate, statiscally relevant counts were obtained. The filters were mounted on microscope slides that were then sealed and stored at 4 ˚C. Microspheres

were enumerated using epifluorescence microscopy. The entire filter area was examined. The microsphere enumeration method is summarized below in point form.

- Each sample was poured into sterile stainless steel cylindrical weights on top of a 0.4 μm membrane supported by a 8 μm support filter (Nucleopore Track-Etch Membrane, Whatman Corp., Billerica, MA). The samples were filtered under mild vacuum. After filtration the membrane filter was carefully separated from the support filter using sterile tweezers and asceptic technique.
- Each filter was carefully put on a separate microscope slide over a drop of 2 % DABCO (glycerol). A cover slip was placed over the filter and then gently tapped down to spread the glycerol uniformly and to flatten out any wrinkles in the filter. Care was taken to minimize the formation of air bubbles.
- The edges of the cover slip were sealed with nail polish. The slides were labelled and stored at 4ºC.
- Microspheres were enumerated using epifluorescence microscopy at 100x magnification (Axioscop 2 Plus, Carl Zeiss, Empix, Toronto, Canada). The entire 25 mm^2 filter area was examined.

3.5 Column Design and Construction

To assess bacteriophage transport in porous media at conditions representative of riverbank filtration; columns were designed so that they would be: 1) relatively inexpensive to build, 2) suitable for measuring bacteriophage and microsphere breakthrough curves within a reasonable time frame (< 5 days), and 3) operable in a manner that adequately represented riverbank filtration conditions. Rapid assembly and

long lifetime were also desirable. Mr. Shayne Giles of the University of Waterloo helped with the column design, which was based on that of Watling (2004). That design utilized a PVC pipe with two hard plastic couplings sealed overtop of the PVC pipe at each end. Those couplings allowed caps to screw into each end of the column. There were three noteworthy problems encountered with those columns: 1) the columns were poorly sealed since the only contact between the cap and the column were the threads (no o-ring was employed); 2) the coupling kept breaking because of the fatigue and perhaps outward pressure of screwing in the caps for every column test; and 3) the caps were hard to screw in and remove, requiring a pipe wrench and often incurring damage to the column. Thus a new design was needed that could be rapidly assembled and sealed well. The column designed for the present research was called the "Rapid Assembly/Disassembly Column Design", and is shown in Figure 3-4. Two of these columns were constructed.

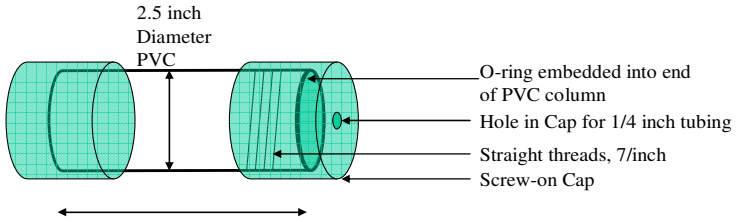

-There should be a tapered zone between the O-ring and the 1/4 inch outflow hole

-A #70 mesh will be added flush with each of the column ends

-Two ends are identical

Figure 3-4 – Rapid Assembly/Disassembly Column Design

The main differences between the column design utilized in this investigation and that of Watling (2004) were: 1) the new design utilizes an over-screw design in which the cap screws over threaded PVC pipe rather than into a threaded coupling; and 2) an o-ring was embedded into each end of the PVC column to make contact with the cap once tightened. Detailed technical drawings of the Rapid Assembly/Disassembly Column Design are provided in the Appendix (Figure A-1, Figure A-2, and Figure A-3).

3.6 Column Preparation and Operation

One end of the column was sealed and then the column was dry-packed with sand. During this process, 50 g of sand were added to the column and then the material was tamped down with a clean medal rod. This process was repeated until the column was filled. The column was carefully sealed by brushing sand off the o-ring and slowly threading the cap to avoid the disruption of the seal by soil grains between the rubber o-ring and the end of the thread cap. After packing, the column was slowly filled in an upflow mode with degassed AGW (Artificial Groundwater) from the bottom up (5 ml/min). The water was degassed using helium gas passed through a submersed, clean air diffuser, for 30 minutes before use (20 L). After saturating the column, 10 pore volumes of the prepared water of the same ionic strength (either 8 or 95 mmol/L) and composition as that in the spiked reservoirs, was pumped through each column to rinse the media of any impurities (colloids, chemicals etc).

The pore volume of a packed column was estimated based on the measured porosity of the media and the known dimensions of the column. One pore volume is equal to the volume of the column ($\pi r^2 h$, where r is the radius of the column and h is the length or height from one screen to the next), multiplied by the measured porosity for the

sand (ε). The flow rate was measured in 100 ml graduated cylinders at discrete intervals, usually every hour during a typical column experiment. To visually demonstrate this method of calculating pore volume the irregular flow data from column runs 2 and 3 are respectively presented in Appendix D. Flow was measured frequently (roughly every 20 minutes for the first 5 hours, after this the flow was measured every time a sample was taken) during this experiment. Since a leak that developed in one of the columns at 23.5 minutes (0.13 pore volumes) after the start of the experiment, the experiment was temporarily stopped.

After pre-rinsing with AGW, 2 pore volumes of spiked bacteriophage, microspheres and bromide seed suspension were pumped through the columns. Afterward, the columns were flushed with bacteriophage-free AGW for another 20 to 30 pore volumes.

The experimental apparatus is shown in Figure 3-5, which shows the reservoirs on the left hand side on magnetic stir plates. Each of the 2 L Erlenmeyer flasks held separate spike suspensions for each of the columns. The 20 L glass carboy contained the AGW used in the pre-spike rinse and post-spike flushes. The peristaltic pump (Masterflex Peristaltic Pump, Barnant Co., Barrington, IL) in the centre of Figure 3-5 drove the flow from the reservoirs to the columns, it operated on very low rpm's (20-30 rpm). The utilization of lower rpm's is important since the pulsing action of the peristaltic pump could result in temporal fluctuations in pore velocity that favour transport and detachment of colloids. Several investigations have demonstrated that colloid attachment is inversely related to pore water velocity (Jin et al., 1997; Schijven et al., 2002; McKay et al., 2002).

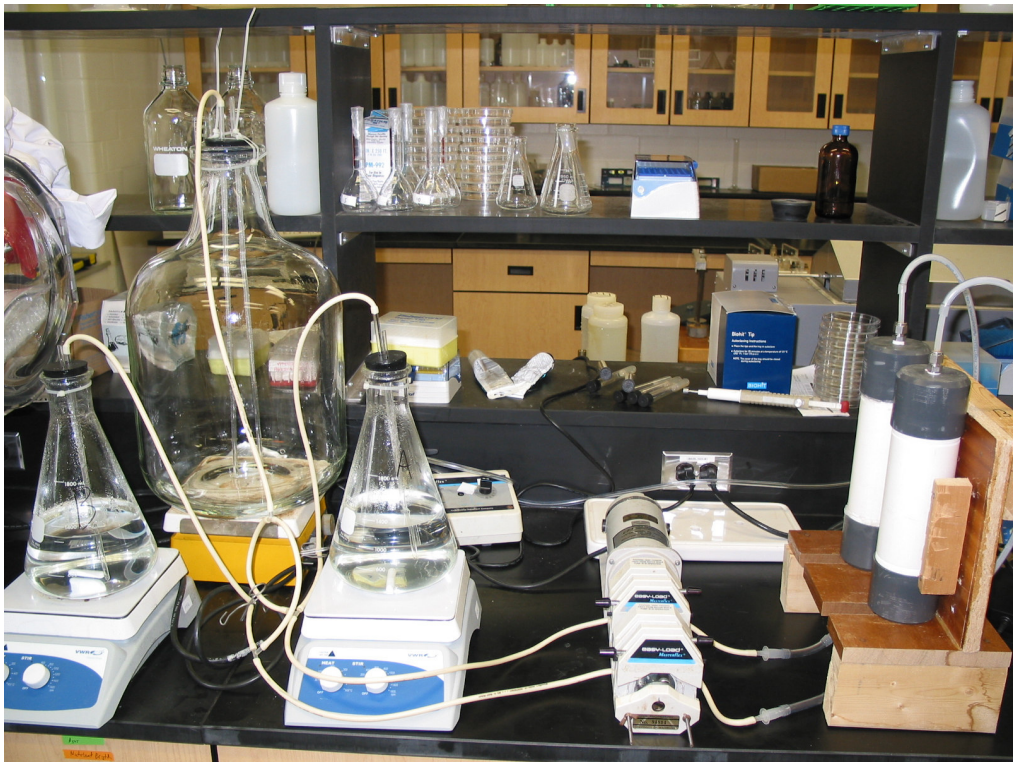

Figure 3-5 - Experimental Apparatus Utilized During Column Studies

After 2 pore volumes of spike suspension (bacteriophage, microspheres and bromide) had passed through the columns, bacteriophage-free artificial groundwater of identical chemistry to the spiked suspension (except without any NaBr) was flushed through each column for approximately another 30 pore volumes (60-72 hours). 15 ml samples were collected at least every 30 minutes until after 2 pore volumes of spiked suspension had passed through the columns. After the first two pore volumes, increasingly longer periods were used in between sampling, up to 8 hours by the end of the experiment. This sampling strategy was appropriate because changes in bacteriophage and bromide concentration during flushing were found to be very gradual. In a typical column experiment, once the first two pore volumes of spike suspension passed through the column a peak plateau was observed until the passage of

approximately 4 pore volumes, after which the effluent concentration of all spiked influent substances declined in what is referred to as the shoulder region (Schijven and Hassanizedah, 2000). In the present experiments, the shoulder region typically lasted for another 4-5 pore volumes after the peak plateau. After the shoulder region passed through the columns, the effluent concentrations of colloids (MS2 and microspheres) gradually tailed off to below their respective MDL's (Method Detection Limits). During tailing, approximately 20 samples were collected from each column and analyzed.

A typical sampling schedule is provided in Table 3-6. Single samples were collected in sterile 15 ml test tubes over intervals of approximately 6 minutes. It was important for the ionic strength and ionic content be consistent for the duration of the injection experiment since these parameters were being evaluated for the effect they had on pathogen transport. In several experiments the pH and conductivity were measured throughout the rinsing, spiking and flushing stages to ensure the provision of stable water chemistry.

Table 3-6 – Typical Sampling Schedule

Time (hr)	Pore Volumes	Event or Sample #
0	0	Pre-spike rinse with AGW
12	10	
0	0	Switch to bacteriophage/microsphere/Br spiked water
0.25	0.1	1
0.5	0.2	2
0.75	0.3	3
1	0.4	4
1.5	0.6	5
2	0.8	6
2.5	1.0	7
3	1.3	8
4	1.7	9
4.8	2.0	Switch to bacteriophage/microsphere/Br-free AGW
5	2.1	10
6	2.5	11
8	3.3	12
10	4.2	13
14	5.8	14
22	9.2	15
23	9.6	16
29	12.1	17
36	15.0	18
46	19.2	19
56	23.3	20
72	30.0	21

3.7 Measuring Bromide Concentration

Sodium bromide (NaBr) (Fischer Scientific, Fair Lawn, NJ) was used as a conservative tracer to determine the hydrologic properties of the porous media (i.e. Darcy velocity and hydrodynamic dispersion) during the column experiments. Ion chromatography (I.C.) (Dionex, Sunnyvale, CA) was used to measure the bromide concentration in the column

effluents. A 1000 mg Br/L (ppm) stock solution was utilized to prepare the bromide standards. The stock bromide solution was diluted into 1, 5, 10, 50, 100, 150 and 200 ppm standards that were analyzed in duplicate to produce a calibration curve. The bromide analysis is discussed further in the QA/QC section.

3.8 Breakthrough Curve Analysis

Peak normalised concentration, percent attenuation and retardation of the colloids relative to bromide tracer were utilized to analyze the breakthrough curves obtained during the column studies discussed herein. The specifics of these methods are discussed in the following sections.

3.8.1 Peak Normalised Concentration

The peak breakthrough concentration (C_{max}/C_o, where C_{max} is colloid concentration at the peak of the breakthrough curve and C_o is the spiked influent concentration) describes the highest colloid concentration one might expect to observe in drinking water well near a pathogen contamination source. Conceptually, given knowledge about minimum infectious dose for the particular pathogen and making some assumptions about source concentrations (C_o), of pathogens, the normalised concentration can be used to ensure the safety of well water (e.g. Schijven et al., 1999). Peak normalised breakthrough concentration also can be used to estimate the overall virus/colloid removal efficiency (η) of the virus/colloid (equation 2-9).

3.8.2 Percent Attenuation

The total number of colloids in the column effluents was calculated by integrating each breakthrough curve. The integral was approximated discretely. This process is described in equation 3-4. This estimated area under each curve is then multiplied by the

total pore space in the column resulting in an estimate of the total number of particles released in the effluent.

$$P_{eff} = \left[\sum_{n}^{i=1} \left(\frac{(c_i + c_{i-1})}{2} (v_i - v_{i-1}) \right) \right] \cdot V_c \cdot \varepsilon \quad \textbf{3-4}$$

where P_{eff} is the total estimated number of particles released in the effluent, n is the number of plotted concentration points on curve, c is concentration of each point, v is the cumulative number of pore volumes at that point, V_c is the empty volume of the column and ε is the porosity of the sand.

The total number of particles injected in the column influent was estimated the following equation 3-5.

$$P_{\text{inf}} = f \cdot t_{spike} \cdot C_o \quad \textbf{3-5}$$

in which P_{inf} is the total number of particles injected into the column, f is the flow rate (ml/hr) over the spiked time interval, t_{spike} is the length of time over which the spike was added and C_o is the influent particle concentration.

Based on equations 3-4 and 3-5, the percent attenuation was calculated using equation 3-6:

$$\%Attenuation = \left(\frac{P_{\text{inf}} - P_{eff}}{P_{\text{inf}}} \right) \cdot 100 \quad \textbf{3-6}$$

3.8.3 Relative Retardation

Relative retardation is the ratio between the tracer and colloid velocities, as described in equation 3-7:

3-7

$$R = \frac{v_{tracer}}{v_{colloid}}$$

where v_{tracer} is the measured velocity of the tracer through the media and $v_{colloid}$ is the velocity of the colloid. Assessing the velocities of each mobile substance required finding the point in time after spiking commenced when 50 % of the peak concentration (C_{50}) in the breakthrough curve was initially reached. This time was denoted t_{50}. Since the actual concentration at t_{50} was never directly measured, it was inferred by linear interpolation between the two neighbouring points; one earlier and one later than t_{50}.

3.9 Quality Assurance and Quality Control

One common challenge of working with both microorganisms and inorganic chemicals, such as bromide, is being able to quantify the uncertainty associated with each reported concentration. This uncertainty is characterised by the degree of accuracy and the amount of variability inherent in each method used for both sampling and analysis. Each method usually has a bias associated with it, a tendency to report higher or lower concentrations than actual. Microsphere recovery studies using the same method and equipment as the present study report losses of over 60% (Watling, 2004). In order to perform a recovery study an independently measured or known concentration solution must be used to assess the accuracy of the detection method in question. In the present study, no such alternative detection method or prepared suspension was available for MS2 and therefore it was impossible to assess the accuracy or bias associated with the plaque counting method. It is reasonable to say however, that the plaque forming method produces lower concentrations than actual, due to the necessity of attachment of each bacteriophage with a host bacteria and the possibility of clustering. The accuracy of the

bromide data was able to be assessed by using known standards and calibration curves for each round of measurements.

As well as accuracy, variability needed to be known for microspheres, viruses and bromide. Variability for microspheres using the same equipment and similar methods as the present study was assessed in Watling (2004). Using multiple samples from a suspension of known concentration the fluorescent microscopy counting method was found have a standard deviation within 20% of the mean. This value is also known as the coefficient of variation. Variability in measuring MS2 was assessed using triplicate plate analyses (Table B-1 and Table B-2 in the Appendix). Within the valid counting range of plaques per plate of 30 to 300 pfu (You et al., 2003) the standard deviation was always within 10% of the mean, which is indicative of excellent reproducibility. Variability in bromide analysis was estimated by the goodness of fit (R^2) of each calibration curve to the data is discussed in section 3.9.3.

There is a range of concentrations for which the reported accuracy and variability associated with each sample is valid. Below this range variability increases due to sampling and analytical processes or background noise. The concentration where this occurs is the method detection limit (MDL) and is reported below for each analysed substance. The MDL for microspheres in this experiment was set to 20 microspheres per slide (Watling, 2004). Based on Standard Methods (American Public Health Association, 1995) the MDL for MS2 was set at 1 pfu per lowest dilution. Since a zero dilution was frequently utilized (especially near the end of the breakthrough curve when concentrations were low), this resulted in an MDL of 1 pfu/ml. An upper limit of 300 pfu per plate was also set for MS2 (You et al., 2003) since above this phage density it was

found that plaques begin to overlap thereby reducing the perceived concentration of the original sample.

One of the problems associated with reporting concentration values for particles is known as non-representative sampling. Typical methods used for calculating an MDL for chemicals assume error, or deviations of observed concentrations from the true mean, to be normally distributed at low concentrations. But as described in Emelko (2001) this is not a valid assumption for discrete particles such as microspheres and viruses. This is because at low concentrations (< 20 particles per ml) the observed concentrations of a finite number of observations will be described by a Poisson distribution. Since uniform distribution of discrete particles in space cannot be assumed (i.e. see section 3.9.1 below) and a concentration less than zero cannot be reported most of the observed concentrations will centre on the true mean, while a very few samples will happen to capture an unrepresentatively large number of particles for sample size. A statistical approach for dealing with uncertainty in sampling and analysis of discrete particles at low concentrations is described and applied in Emelko (2001). Although the MDL for microspheres was derived from this method, this approach was not incorporated in the calculation of an MDL for MS2 in the present study.

3.9.1 Investigating the Evidence for Bacteriophage Clustering

Without an electron microscope, it is difficult to assess the occurrence of virus clustering (aggregation) in experiments that use plaque forming units to evaluate virus concentration. Bacteriophage clustering would be most likely to occur in the high concentration suspensions with minimal disturbance (e.g. mixing). In the present work, the stock suspensions were kept refrigerated and contained bacteriophage concentrations

of ~10^9 pfu/ml. The seed reservoirs contained lower concentrations of bacteriophages (~10^6 pfu/ml) that were mixed at low RPMs with a magnetic stir bar, a less likely environment for virus clusters than a standing solution. An increase in equilibrium forces acting to distribute the viruses equally throughout the solution would be associated with the lower concentration of viruses (Schijven and Hassanizadeh, 2000); accordingly, any bacteriophage clusters would likely disperse. The stirring action would likely further break up clusters. Finally, after passing through the columns, bacteriophage clusters could possibly disaggregate as they follow the tortuous flow paths through the porous medium. The implications of this reasoning are that one would expect that an ever greater back-calculated bacteriophage stock concentration with each dilution and/or mixing step from the original stock solution. There was no indication of bacteriophage clustering during the investigation discussed herein.

3.9.2 Controlling for Contamination in Bacteriophage Detection

Bacteriophage controls were run alongside of each set of analyses for to control for contamination. Table 3-7, lists the two different controls collected during bacteriophage analysis.

Table 3-7 - Controls Collected During Bacteriophage Detection

	Microorganisms Added			
Type	Host Bacteria	Bacteriophage	Description	Purpose
Phage control	yes	no	Exponential E coli culture in Saline solution is added to top agar	To determine phage contamination among dilutions
Saline control	no	no	Saline solution is added to top agar	To determine bacterial contamination in saline solution

No bacterial contamination was found with the saline control. The Phage control was useful because the small size of viruses sometimes permits them to be aerosolized (Greening et al., 2001), therefore there was potential for cross contamination between test tubes. No cross contamination (>15 phage controls done with MS2) was observed during this research. Although some bacterial contamination was found in a couple of the controls, this was determined to not likely effect the analysis for MS2 since it is very host specific. The Saline and Phage controls can be seen in Table B-13 and Table B-14 respectively.

3.9.3 Measuring Bromide Concentration in Column Effluent

One of the bromide calibration curves (1-200 ppm) obtained during the present investigation is presented in Figure 3-6. Least squares linear regression was used to produce this curve which yielded an excellent coefficient of determination of 99.9 %.

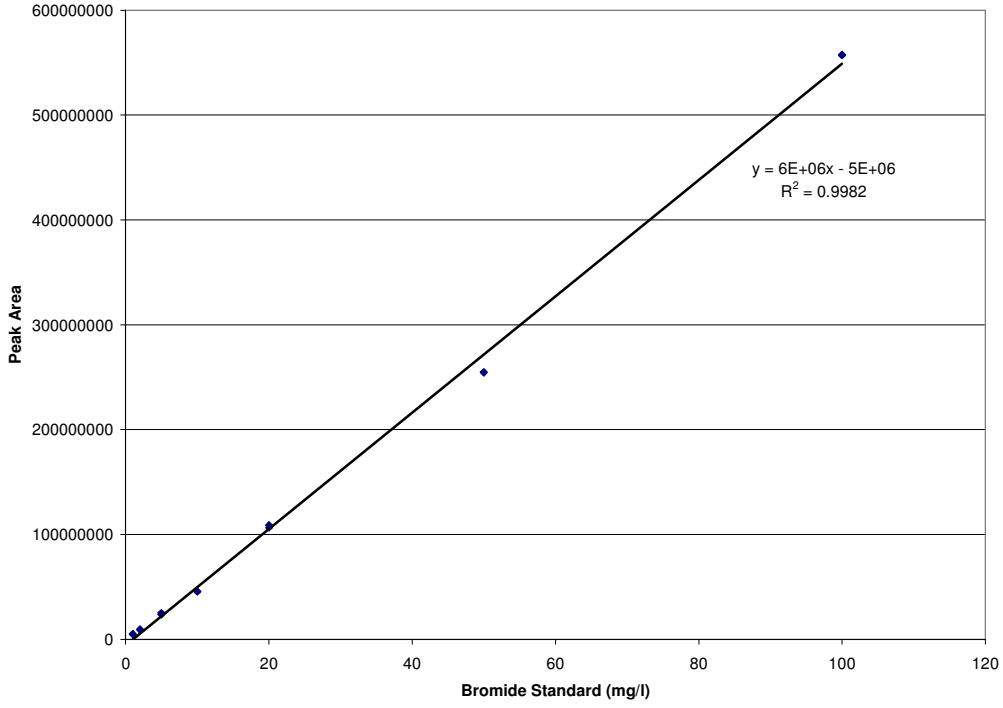

Figure 3-6 - Typical Ion Chromatography Calibration Curve for Br

The bracketed concentration zone, in between where sample standards were used, for bromide was from 1 to 100 mg/L. In addition to generating calibration curves, one injection of known concentration (Check Standard) and one blank were analysed after every 10 sample measurements. This was done to test for accuracy and contamination respectively and to indicate any analytical drift. Using the method in Standard Methods (American Public Health Association, 1995) for calculating MDL for chemicals, the standard deviation of measured concentration of seven random 10 ppm standards was calculated. These standards were pooled from across three separate ion chromatograph analyses. These seven standards should have been taken every time a bromide analysis was performed.

This standard deviation from these seven samples was multiplied by 3.14 and added to the real concentration to yield a MDL for bromide of 15 ppm. All the bromide data and I.C. calibration curves are shown in Appendix D. Each effluent sample was measured in duplicate and the average was taken in forming the breakthrough curves. R^2 values were all very high on all the calibration curves indicating both high accuracy and low variability. No blanks were shown to be contaminated since the measured bromide concentration was always below 1 ppm. The calibration curves are in the Appendix (Figure C-1, Figure C-2, Figure C-3, Figure C-4 with supporting data in Table C-1, Table C-4, Table C-11, Table C-16 respectively).

4. RESULTS AND DISCUSSION

This study examines the effects of ionic strength, media grain size, and influent virus concentration on pathogen transport in porous media. Fourteen column tests were conducted using the bacteriophage MS2 and 1.5 μm microspheres; two commonly used non-pathogenic surrogates representative of human viruses and bacteria, respectively. Two size distributions of crushed silica sand and two ionic strengths (1 and 10 mmol/L of Ca^{2+}) were used. A 2^2 factorial design was used with a minimum of two replicates of each combination of parameters. The results of these experiments are discussed below.

4.1 Microbiology

4.1.1 Measuring the Concentration of MS2 in the Stock Suspension

The figure below shows the appearance of plaque forming units (PFU) in the double layer agar technique. The plaques represent areas of killed host bacteria, initiated by at least one bacteriophage in the centre of the clear circle. MS2 (Figure 4-1) formed plaques of about 3 mm in diameter.

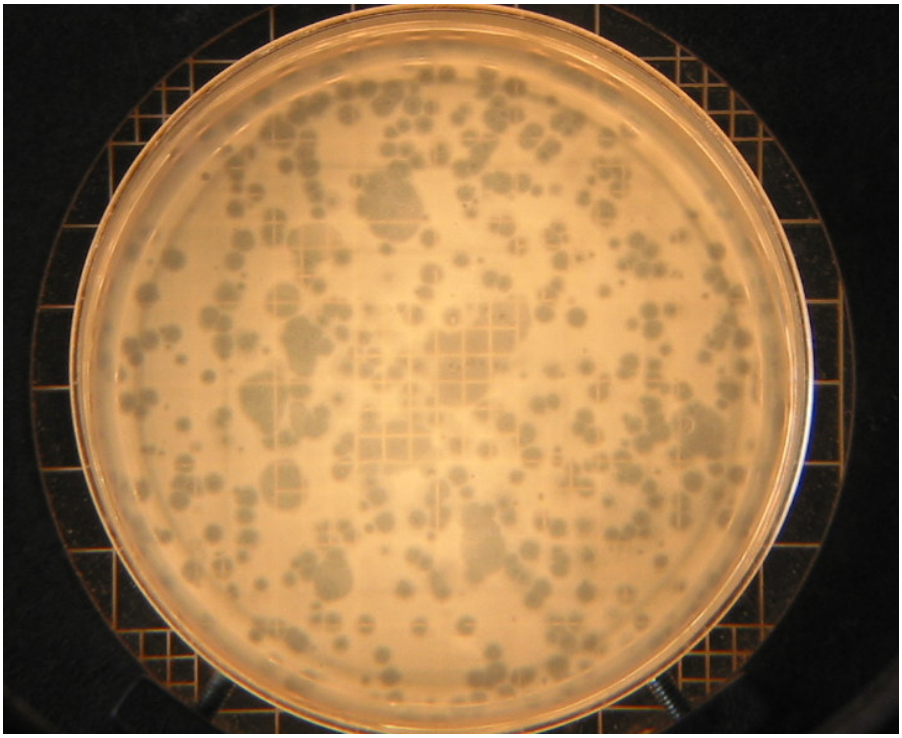

Note: The large squares on the light box are 1 cm wide.

Figure 4-1 - Plaques of MS2 in Lawn of Host Bacteria *E. coli* 15597

Table 4-1 presents the results of the first attempt to quantify the concentration of MS2 in its stock suspension. MS2 plaques were enumerated once at 18 hrs after the addition of the top agar (with MS2 and *E. coli*) to the Petri dish. At this point, plaques were clearly evident on the plates. Plaques were enumerated for a second time to assess counting variability after 40 hrs of incubation and to ensure that no more plaques appear after 18 hrs. An examination of the replicate counts obtained after 40 hours of incubation indicates quite good reproducibility of low counts, as would be expected (with coefficients of variation < 10%). When the plaque counts were high (~300 per plate) and near the upper limit of the ideal range of 30–300 pfu/plate suggested by You et al. (2003), the coefficient of variation went up to 12.6%, which is consistent with increased counting

error associated with closely clustered and occasionally overlapping plaques. The mean stock MS2 concentration was found to be 9.3×10^8 pfu/ml.

Table 4-1 - First Measurement of MS2 in Stock Suspension, October 23, 2004

Dilution from Stock Solution	Number of Bacteriophages per plate (pfu)					40 hr Average (pfu)	Standard Deviation of 40 hr Count (pfu)	Coefficient of Variation (%)	40 hr Concentration of MS2 Stock Solution (pfu/ml)
	18 hrs	40 hrs							
Counting Trial #	1	2	3	4	5				
3.81E-06	307	299	300	379	297	318.8	40.2	12.6	8.36E+07
4.77E-07	113	142	127	133	139	135.3	6.7	4.9	2.84E+08
5.96E-08	79	88	94	100		94.0	6.0	6.4	1.58E+09
7.45E-09	14	15				15.0	n/a	n/a	2.01E+09
9.31E-10	55	77	79	79		78.3	1.2	1.5	8.41E+10
Mean*									**6.48E+08**
Standard Deviation*									***8.11E+08***

* including only 10^{-7} and 10^{-8} dilutions since other dilutions lay outside of statistically valid range (30-300 pfu/plate).

Table 4-2 provides the results from the second attempt to quantify concentration of MS2 in the stock suspension. Each sample was plated in triplicate. Consistent with the previous results, the average stock MS2 concentration was 4.2×10^9 pfu/ml. The standard deviation reached 30% of the mean in the 10^{-8} dilution; however, in the 10^{-7} dilution coefficient of variation was found to be less than 4%. Subsequent analyses (presented in the Appendix in Table B-2) demonstrated that the methodology produced reproducible results. It was concluded that the MS2 enumeration method was being applied properly, as the observed results were consistent with what one would expect to observe with respect to variability and reproducibility in such plating methods (You et al., 2003).

Table 4-2 - Second Enumeration of MS2 in Stock Suspension, October 29, 2004

Dilution from Stock Solution	Number of Plaques per plate (pfu)			Average (pfu)	Standard Deviation (pfu)	Coefficient of Variation (%)	Concentration of MS2 Stock Solution (pfu/ml)	Standard Deviation Converted to pfu/ml
Plate #	**I**	**II**	**III**					
1.00E-07	252	240	256	249.3	8.3	3.3	2.5E+09	8.3E+07
1.00E-08	70	39	70	59.7	17.9	30.0	6.0E+09	1.8E+09
1.00E-09	3	5	9	5.7	3.1	53.9	5.7E+09	3.1E+09
Mean*							**4.2E+09**	

* excludes lowest dilution since the plaque densities are too low

To further ensure adequate MS2 enumeration techniques were being utilized a third enumeration experiment was conducted. The data from this experiment are summarized in Table 4-3. The triplicate data in this table indicate good reproducibility in the statistically relevant range (~14% coefficient of variation). Consistent with the previously discussed enumeration data (Table 4-1 and Table 4-2), the average stock MS2 concentration was $1.5x10^{9}$ pfu/ml.

Table 4-3 - Third Enumeration of MS2 Stock Suspension, November 19, 2004

Dilution from Stock Solution	Number of Plaques per plate (pfu)			Average (pfu)	Standard Deviation (pfu)	Coefficient of Variation (%)	Concentration of MS2 Stock Solution (pfu/ml)	Standard Deviation Converted to pfu/ml
Plate #	**I**	**II**	**III**					
9.09E-08	109	122	143	124.5	17.2	13.8	1.4E+09	1.9E+08
9.09E-09	10	14	18	14.0	4.0	28.6	1.5E+09	4.4E+08
9.09E-10	0	3	0	1.0	1.7	173.2	1.1E+09	1.9E+09
Mean *							**1.5E+09**	

* excludes lowest dilution because counts were outside of the statistically significant range. The average includes 10^{-9} dilution data because of low variability, despite counts just outside of the statistically significant range (You et al., 2003).

The MS2 concentration in the stock suspension was monitored over time because bacteriophage deactivate over time (see Yates et al., 1985 and 2.4.3 Elimination). The first 5 MS2 concentration points in Figure 4-2 (representing one stock solution)

demonstrates a rough gradual decline in MS2 over time. This decline of approximately 0.2 log per month ($\lambda = 0.016$, where λ is the die off rate constant from equation 2-14) at 4°C is somewhat lower than but still consistent with other published MS2 deactivation rates (e.g. Yates et al., 1985; Schijven and Hassanizadeh, 2000). The last four points of MS2 concentration data in Figure 4-2 represent a new stock suspension and are not included in the estimate of λ. The error bars on Figure 4-2 represent +/- one standard deviation (calculated from triplicate analyses of the same dilution tube). The raw data are provided in tables (Table 4-1 to Table 4-3) and in Appendix B.

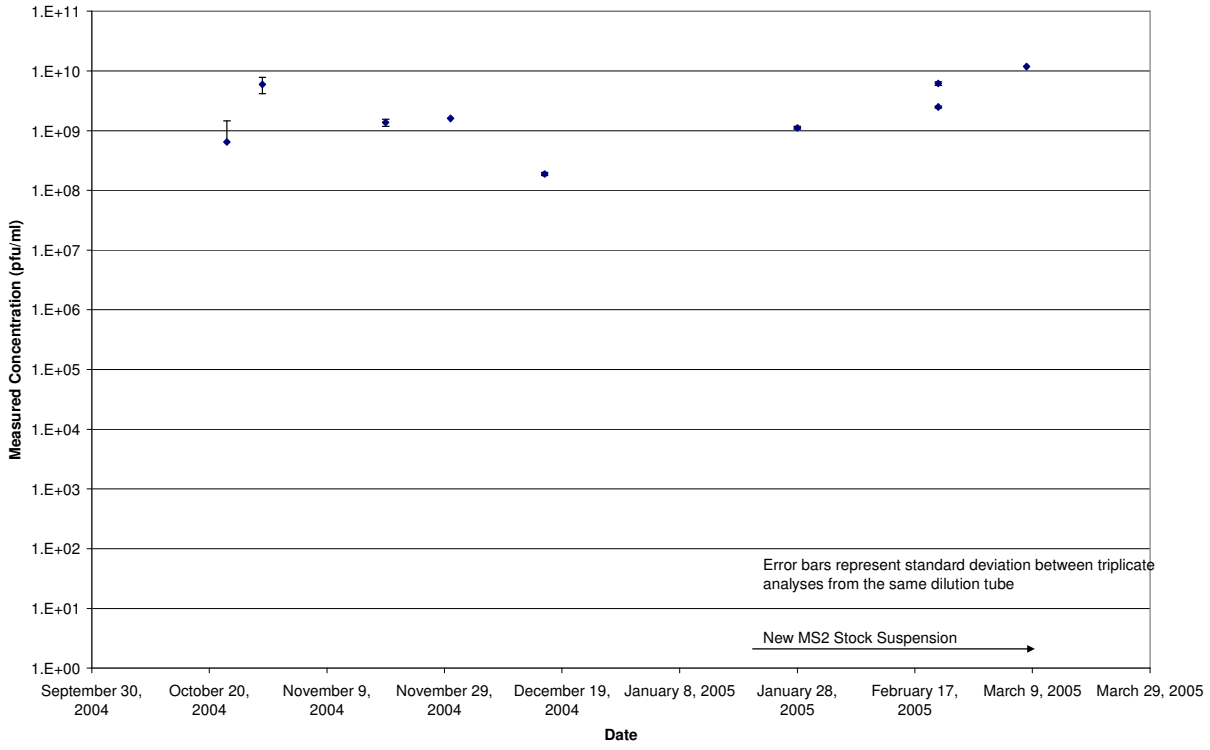

Figure 4-2 – Temporal Stability of MS2

4.1.2 Measuring Growth Kinetics of *E. coli* Host Strains

The growth kinetics of *E. coli* 15597, the host strain for MS2, was characterized by measuring optical density over a period of 24 hours. Five *E. coli* 15597 growth curves are presented in Figure 4-3. Although a sixth curve was planned, the growth data were excluded because of an unusual lag period likely associated with an error in sample preparation. As indicated in Figure 4-3, the latter portion of exponential growth was observed after approximately 180 to 300 minutes (3 to 5 hours) of growth at 37°C. This is consistent with the recommended time for an *E. coli* culture to grow at 37, prior to contact with MS2 in the molten top agar for plating (Adams, 1959).

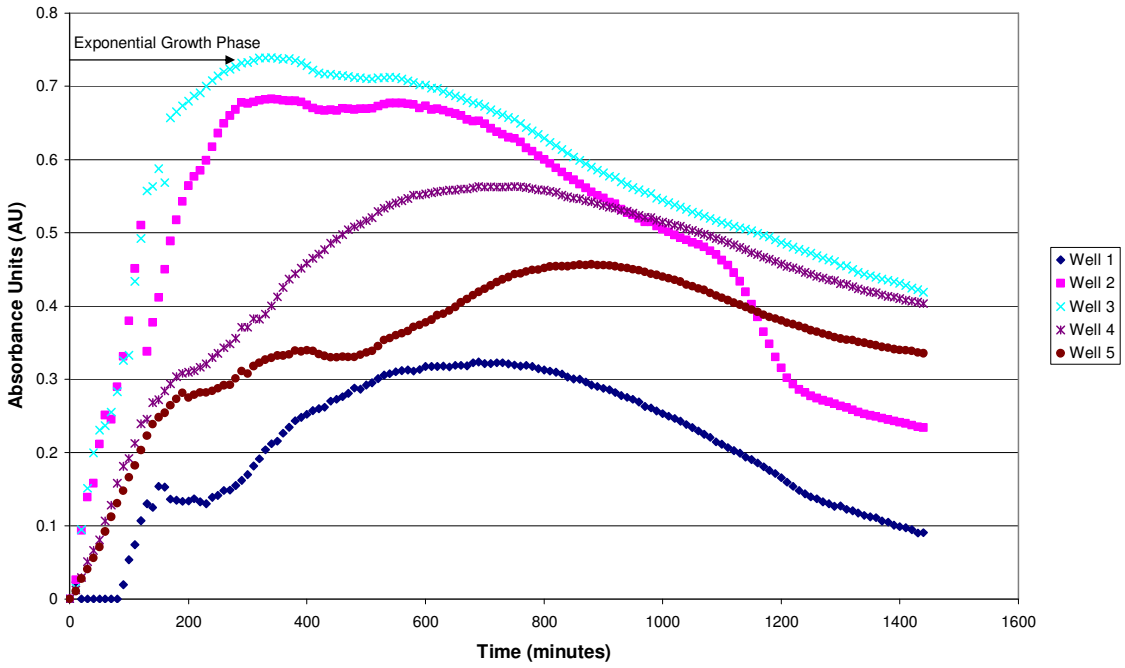

Figure 4-3 - *E. coli* 15597 Growth Curve

The five curves presented in Figure 4-3 were obtained from five different wells in the micro plate. It was somewhat surprising to note the differences in absorbance magnitude between the curves. This is in contrast to other authors that have reported

lower relative error when measuring *E. coli* growth with the spectrophotometer (e.g. Gabrielson et al., 2002). Part of the reason for this variability in the present study could be that each well was inoculated separately. It is therefore possible that differing amounts of *E. coli* culture were present in each well when incubation commenced. In spite of this difference in magnitude, the overall shape of each curve is basically the same, especially in the initial, exponential zone, noted above.

4.4 Column Tests

The breakthrough curves of MS2, bromide and microspheres from 14 column experiments are discussed in this section (the sampling schedules and flow rates, detailed analyses of MS2 and microspheres are provided in the Appendix). The column experiments were conducted two at a time. Since each column had three mobile substances injected, each figure contains up to six breakthrough curves. For each column run the first 2 pore volumes (along the abscissa) represent the period during which the spike suspension was injected. Each of the subsequent figures contains the minimal detection limits (MDLs) for MS2 and microspheres; and the solid line represents the normalised MDL for microspheres (2000 spheres/L) (Watling, 2004). The dashed line(s) represent the normalised MDL for the MS2 (1 pfu/ml) (American Public Health Association, 1995). When there are two MDLs indicated for MS2 it is because two different influent concentrations of MS2 were used. The indicators of transport (reduction in peak concentration, percent attenuation and retardation) are summarised after the breakthrough data have been presented. The measured flow rates and influent concentrations of MS2 and microspheres are also provided and discussed with the transport indicators.

Experiments 2 and 3 investigated the impact of seeded MS2 concentration on breakthrough at low ionic strength conditions in the medium sand. As the intention of these experiments was to focus on the impact of influent bacteriophage concentration on their transport in porous media, microsphere breakthrough was not evaluated. The bromide and MS2 breakthrough curves obtained during experiments 2 and 3 indicated somewhat consistent profiles of MS2 passage through the porous media. Evidence of breakthrough was observed after 1 pore volume of spiked flow had passed through the columns. Both columns released MS2 (at levels of ~250 pfu/ml) for several pore volumes after the pulse input of spike suspension.

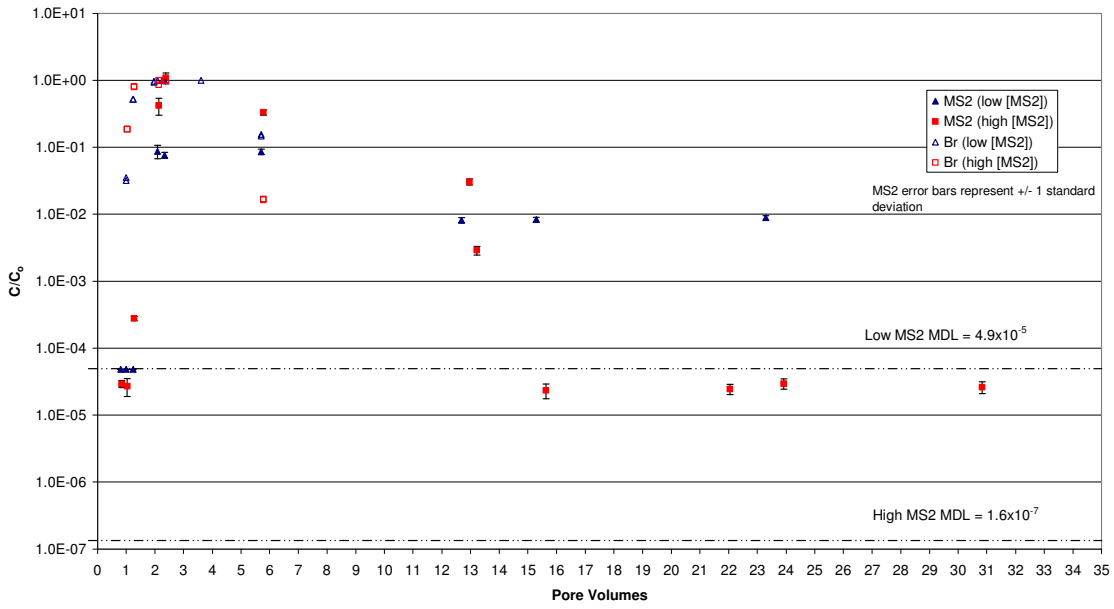

Figure 4-4 – Breakthrough Curves from Experiments 2 and 3 Investigating the Impact of Seeded MS2 Concentration on Breakthrough at Low Ionic Strength Conditions in Medium Sand.

It should be noted that each of the bromide breakthrough curve drops below the MDL (15 ppm) after 6 pore volumes. The MS2 breakthrough curves in Experiments 2 and 3 suggest that attenuation or transport through the medium sand at low ionic strength

may be impacted by seeded MS2 concentration. Although the basic shapes of the breakthrough curves are the same, the column with the lower influent MS2 concentration exhibited bacteriophage breakthrough at only 10% of the influent MS2 concentration whereas the column with the higher influent MS2 concentration exhibited breakthrough at 100% of the influent concentration. Although the data indicate a difference between the normalized peak breakthrough concentrations, it should be noted that the difference is approximately one order of magnitude, which is likely statistically insignificant given the inherent uncertainty in plating analyses (Schmidt et al., 2005).

It should be noted that during this experiment the flow was stopped 20 minutes into the spiking period due to an observed leak. Flow to the column being fed the high concentration of MS2 was stopped for 50 minutes while the other column was stopped for 90 min. This start-stop operation may also account for some of the differences in MS2 breakthrough observed during experiments 2 and 3. Static water within the porous media may provide the viruses with more opportunity to diffuse to the grain surfaces, unhindered by turbulent, dynamic flowing water (McKay et al., 2002). It is noteworthy that the two curves in Experiments 2 and 3 exhibit MS2 tailing after the initial spike passed through the columns since this was not observed in later experiments. The MS2 and bromide raw data are shown in the Appendix in Table B-2, Table C-2 and Table C-3, respectively. The flow rates for experiments 2 and 3 are also shown in Appendix D.

Experiments 4 and 5 reproduced experiments 2 and 3 to again investigate the effects of influent MS2 concentration on virus transport in porous media. In addition, microspheres were added to the influent at approximately equal concentrations to each reservoir to compare the transport of bacterial surrogates with MS2 in medium sand at

low ionic strength. The breakthrough profiles of all three injected substances demonstrate excellent similarity between the two columns; since each of the three sets of curves overly each other.

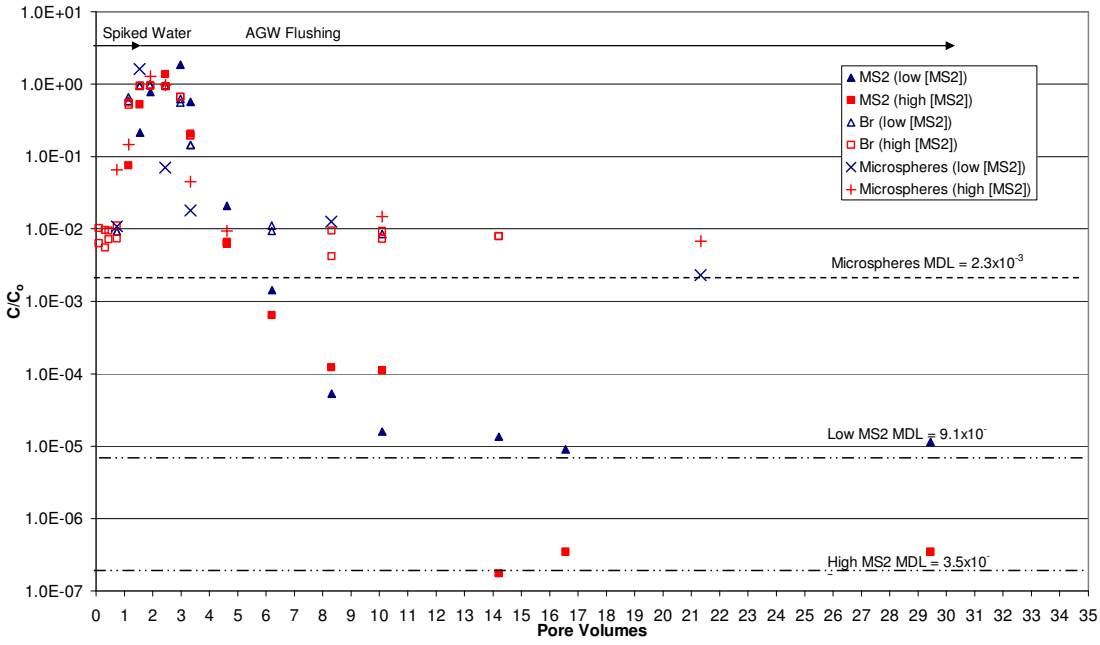

Figure 4-5 – Breakthrough Curves from Experiments 4 and 5 Investigating the Impact of Seeded MS2 Concentration on Breakthrough and Microsphere Transport at Low Ionic Strength Conditions in Medium Sand.

Figure 4-5 compares transport of the conservative bromide tracer, bacteriophages and microspheres in medium sand at low ionic strength. Unlike experiments 2 and 3 this experiment was conducted with the intended constant flow rate. Complete breakthrough in (C_{max} = 0) was observed with both MS2 and the microspheres. In contrast to this agreement in peak breakthrough, while MS2 was retarded relative to bromide (R = 0.6) the microspheres broke through slightly earlier than bromide. This may be due to the microspheres following preferential flow paths, where, because of their relatively larger size than viruses they would be excluded from smaller, more tortuous flow paths.

Breakthrough of bacteria in advance of bromide is commonly reported in the literature (Harvey et al., 1989; Woessner et al., 2001; Driese and McKay, 2004) and is often referred to as velocity biasing (Taylor et al., 2004).

Also notable from the above figure is that, in contrast with the behaviour of later microsphere experiments, the microspheres exhibit tailing similar to the bacteriophages in experiments 2 and 3. The tailing observed with the bacteriophages in experiments 2 and 3 could be partially explained by the halting of flow, creating a more favourable environment for attachment to occur, but no such event occurred in experiments 4 and 5 that could be a possible cause for the microsphere tailing. It is possible that the microspheres were attracted to something unusual (such as organics or other contamination) in the porous media that did not have as great an effect on MS2. The data from experiments 4 and 5 for MS2, microspheres and bromide are shown in the Appendix in Table B-3 and Table B-4, Table B-15, and Table C-5 and Table C-6 respectively. Table D-1 shows the flow rates and sampling schedule.

Experiments 6 and 7 were conducted with medium sand with low ionic strength. In these experiments, the bromide breakthrough curves overlapped one another and the microspheres were reasonably close in peak breakthrough and retardation. The two breakthrough curves for MS2, however, were quite different from one another and from the previous 4 column experiments that were conducted under similar conditions. The column with the high influent MS2 concentration broke through with a 3 log reduction in peak concentration. The other column effluent did not indicate any breakthrough of MS2 when the lower influent bacteriophage concentration was utilized.

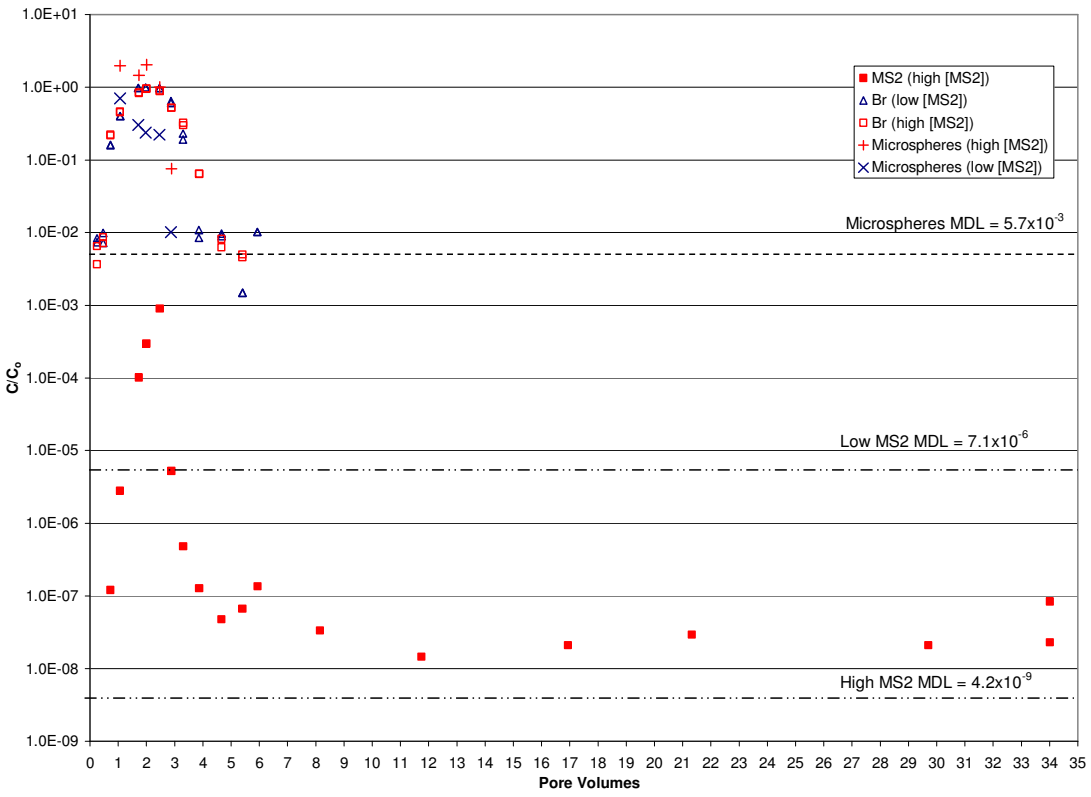

Figure 4-6 – Breakthrough Curves from Experiments 6 and 7 Investigating the Impact of Seeded MS2 Concentration on Breakthrough and Microsphere Transport at Low Ionic Strength Conditions in Medium Sand.

Overall microsphere attenuation was also different in the two columns (37 and 66% for the columns fed high and low influent MS2 concentrations respectively). These attenuations were higher than those observed during Experiments 4 and 5 under the same conditions (6 and 18% respectively). Given the variability with the microsphere detection method and the range of differences between each of the paired columns, no statistically significant differences would be expected upon comparison of the amount of attenuation observed in Experiments 4 through 7.

Consistent with experiments 4 and 5, MS2 breakthrough during Experiments 6 and 7 was retarded relative to bromide (R = 0.6) whereas the microspheres broke through earlier than bromide. These MS2 retardation results were almost identical to experiments 4 and 5. The MS2, microsphere and bromide data for experiments 6 and 7 are shown in the Appendix in Table B-5 and Table B-6, Table B-16, and Table C-7 and Table C-8 respectively. Flow rate and sampling schedule data are shown in Table D-2.

Experiments 8 and 9 were also conducted using medium sand (like Experiments 2 through 7); however, in these the ionic strength was increased to evaluate the effect of ionic strength on the transport of MS2 and microspheres in the porous medium. The MS2, microsphere and bromide data from Experiments 8 and 9 are presented Figure 4-7. Since all of the parameters (e.g. grain size, colloid, flow rates, temperature) affecting collision efficiency, η_o, (equation 2-8) remained unchanged from the previous experiments (2 through 7), it was inferred that any observed increase in overall removal of the colloids likely resulted from an increase in attachment efficiency, (α), which has been shown to be impacted by ionic strength (Kinoshita et al., 1993; Penrod et al., 1996).

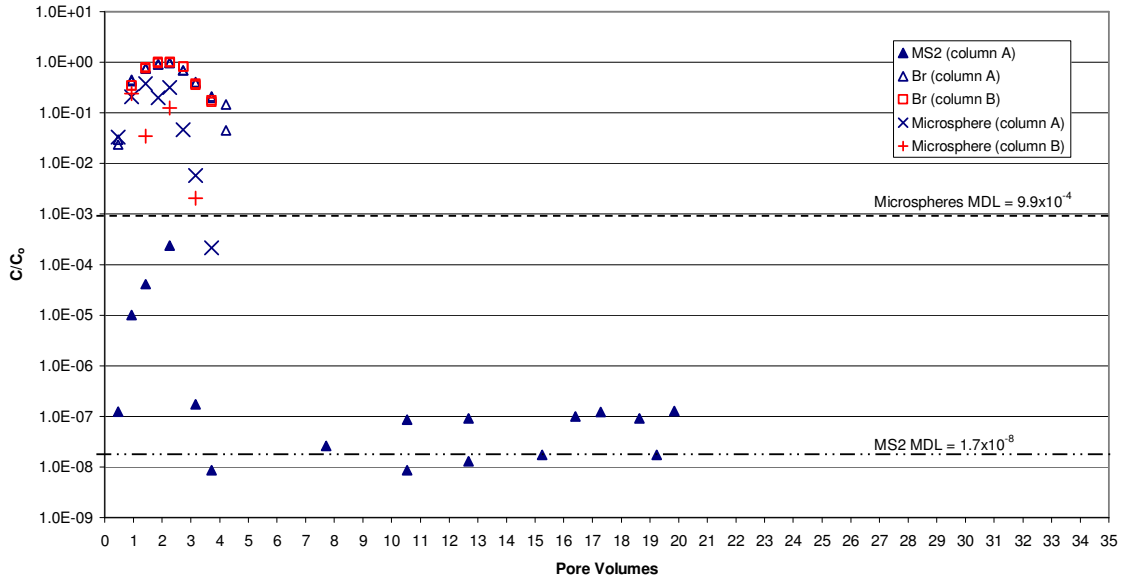

Figure 4-7 – Breakthrough Curves from Experiments 8 and 9 Investigating the Effect of Raising Ionic Strength on the Transport of MS2 and Microsphere Medium Sand.

In these experiments, a 3 log reduction in peak MS2 concentration relative to the influent (C_o) in column A was observed. Similar to column runs 6 and 7 where one column did not break through, column B yielded no MS2 in the effluent samples. These differences were observed despite almost identical flow rates (Table 4-4), temperature, soil type and water chemistry (spiked and AGW), and similar influent MS2 concentrations. The reservoir concentrations of MS2 did not decline throughout the experiments, ruling out inactivation as a cause for the apparent complete attenuation of MS2 in column B. Furthermore, no phage controls revealed MS2 contamination, ruling out contamination as the cause for apparent MS2 breakthrough in column A. The fact that the microspheres and especially bromide broke through columns A and B in similar manner suggests that the two columns were packed similarly and had similar physical flow properties. It is possible that something in column B, such as the soil (possibly

contaminated with organics) or components of the column (possibly contaminated with low levels of bleach residual from the cleaning process) acted on the sensitive bacteriophages to deactivate them. Since they are not viable, microspheres would not be susceptible to deactivation.

The MS2, microsphere and bromide data for experiments 8 and 9 are shown in the Appendix in Table B-7 and Table B-8, Table B-17, and Table C-9 and Table C-10 respectively. Table D-3 shows the flow rates and sampling schedule.

The intent of experiments 10 and 11 was to investigate the effect of decreasing grain size from a medium to fine sand on virus and bacterial surrogate transport in porous media, while maintaining low ionic strength, consistent with those utilized in experiments 2 through 7. A sharp, consistent (between the two columns) reduction in both MS2 and microspheres during Experiments 10 and 11, was observed. Comparing Experiments 2 through 7 to Experiments 10 and 11, MS2 was reduced in peak concentration by 5 log over its influent concentration, microspheres were completely attenuated due to the decrease in median grain size by approximately half (from 0.7 mm to 0.34 mm).

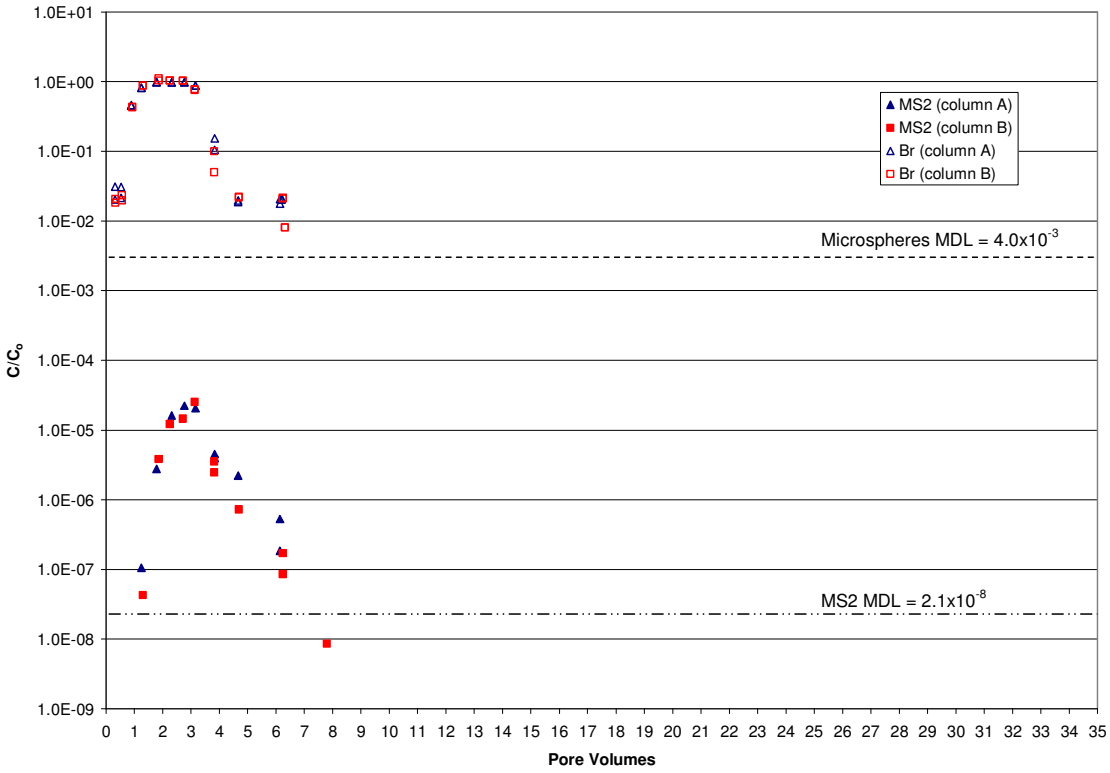

Figure 4-8 – Breakthrough Curves from Experiments 10 and 11 Investigating the Effect of Decreasing Grain Size on the Transport of MS2 and Microsphere Breakthrough at Low Ionic Strength.

Figure 4-8 demonstrates that fine sand attenuates MS2 more substantially than the medium sand (2010) (Figure 4-4 and Figure 4-5) at identical ionic strengths. Furthermore, no breakthrough of microspheres was observed during Experiments 10 and 11. It is also notable that the two MS2 breakthrough curves from Experiments 10 and 11 essentially overlapped one another, demonstrating the potential for reproducibility in column experiments conducted in the manner reported herein.

The MS2, microsphere and bromide data for experiments 10 and 11 are shown in the Appendix in Table B-9 and Table B-10, Table B-18, and Table C-12 and Table C-13 respectively. Flow rates and sampling schedule are shown in Table D-4.

Experiments 12 and 13 were performed in fine sand with high ionic strength source water. Colloid filtration theory suggests that these conditions would favour colloid attenuation. These predictions were experimentally verified in the present study and in many other studies. Both MS2 and bacterial-sized microspheres were completely attenuated during these experiments, making it only possible to estimate a minimum attenuation capacity of the column under those experimental conditions. This means that the grain size and ionic strength conditions used in this experiment were clearly able to attenuate higher concentrations of MS2 and microspheres but the maximum attenuation capacity is not known.

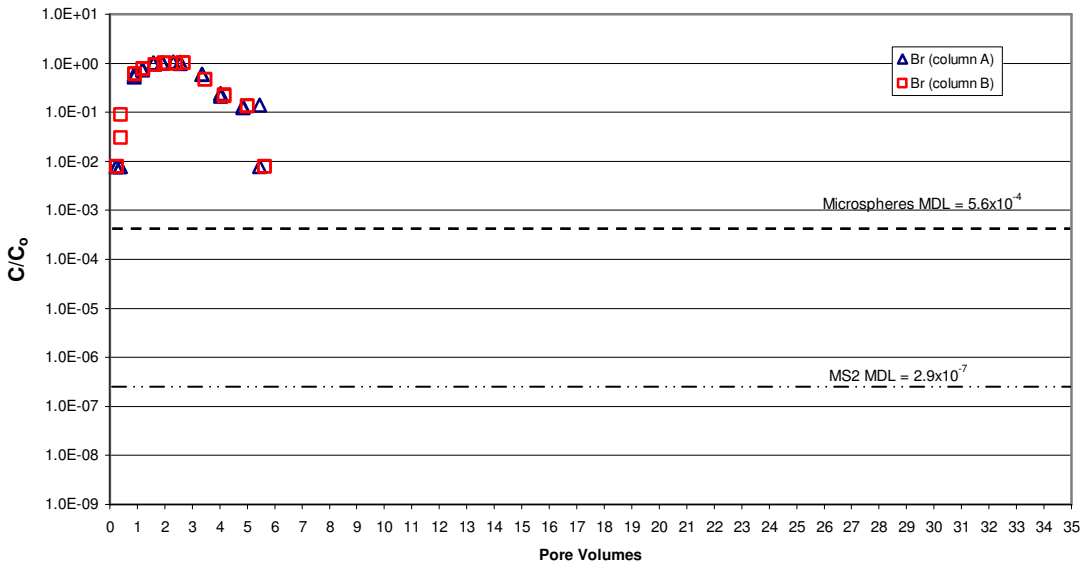

Figure 4-9 – Breakthrough Curves from Experiments 12 and 13 Investigating for Synergistic Effects on the Attenuation of MS2 and Microspheres when Grain Size was Decreased while Ionic Strength was Increased.

Despite the aforementioned fact that experiments 12 and 13 did not resolve the question which motivated their performance, the results from Experiments 12 and 13 indicated that complete attenuation of high levels of pathogen-like colloids could occur over the 20 cm of fine sand at high ionic strength (94.7 mmol/L) and calcium levels (4.8

mmol/L); conditions could reasonably be expected in an RBF setting (Table 2-3). The bromide breakthrough data indicate that the packing and hydrodynamic behaviours of these columns are similar to the other 12 column experiments performed (see Table 4-4).

It is important here to note that these experiments were conducted over a finite period of time (2 days). The degree of attenuation observed at the experimental conditions utilized herein could increase or decrease depending on experimental period. Increasing attenuation could be caused by "ripening" of the grains as colloids build up on the grains and act as additional collectors, increasing the effective size of the grains and decreasing pore spaces. This effect would tend to increase overall attenuation of colloids flowing through the media. Decreased attenuation might result from a process known as "blocking" (Ryan and Elimelech, 1996) in which the number of attachment sites is limited. Once these sites are all occupied, no more attachment occurs. If the number of attachment sites is limited it would be expected that over longer column distances significantly more attenuation would occur, however, over time decreased attenuation in a column of fixed length might be expected.

The MS2, microsphere and bromide data for experiments 12 and 13 are provided in the Appendix in Table B-11, Table B-19, and Table C-14 and Table C-15 respectively. Flow rates and sampling schedule are shown in Table D-5.

Figure 4-10 displays the results from Experiments 14 and 15. These experiments repeated Experiments 8 and 9, in which the effect ionic strength was evaluated. The MS2 and microsphere breakthrough data from Experiments 14 and 15 can be compared to those obtained during Experiments 2 through 7, to determine the effect of increased ionic strength on MS2 and microsphere transport in porous media. Similar to column B in

experiments 8 and 9, no MS2 broke through in either column in Experiments 14 and 15, while only a small (1 log) reduction in peak microsphere concentration during these experiments.

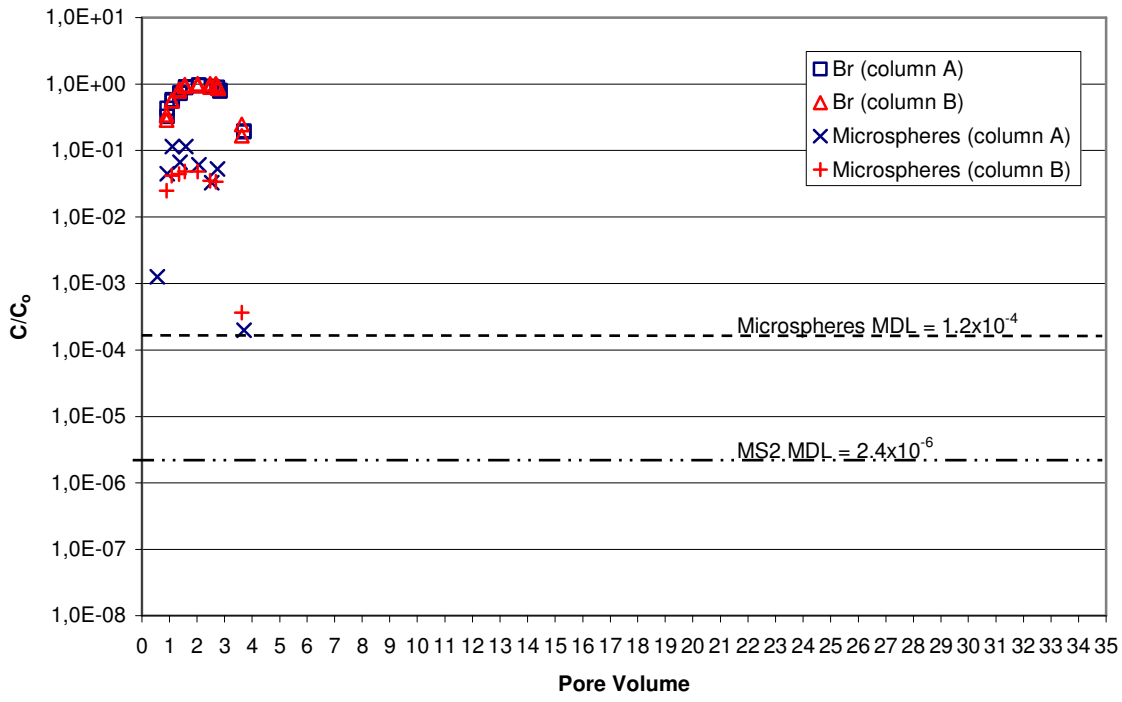

Figure 4-10 – Breakthrough Curves from Experiments 14 and 15 Investigating the Effect of Raising Ionic Strength on the Transport of MS2 and Microspheres in Medium Sand (Repeat of Experiments 8 and 9).

Comparison of Figure 4-10 and Figure 4-5 (and Figure 4-4) indicates that increasing the ionic strength reduced the peak effluent MS2 concentration by at least 5.5 logs, since no MS2 broke through either column during Experiments 14 and 15. Consistent with previous column experiments in medium sand, the microspheres broke through early relative to bromide (R=1.1). The MS2, microsphere, and bromide data for Experiments 14 and 15 are shown in the Appendix in Table B-12, Table B-20, and Table

C-17 and Table C-18 respectively. Flow rates and sampling schedule data are shown in Table D-6.

4.5 Column Test Results Summary

Table 4-4 and Table 4-5 summarize the parameter levels, flow velocities, influent concentrations of MS2, microspheres and bromide and the three main transport characteristics of interest; peak breakthrough concentration, percent attenuation and relative retardation of MS2 and microspheres in each of the 14 column experiments discussed above. The methods for calculating these values were discussed in Chapter 3.

Table 4-4 – Bacteriophage Results Summary

Column Run	Column	Ionic Strength	Sand Size	Measured Bromide Velocity using t_{50} (m/day)	Bacteriophage				
					Influent Concentration (pfu/ml)	Peak Virus Breakthrough (C/C_o)	Percent Virus Attenuated	Relative Retardation of Virus (t_{50} MS2/t_{50} Br)	Normalized MDL (C/C_o) (20 pfu/ml)
2 & 3	Low	Low	Med	1.7	2.1E+04	0.1	62.9	0.80	1.E-03
2 & 3	High	Low	Med	1.8	6.2E+06	1.1	-104.8	0.60	3.E-06
4 & 5	Low	Low	Med	2.8	1.1E+05	1.9	-25	0.53	2.E-04
4 & 5	High	Low	Med	2.9	2.8E+06	1.4	8.8	0.61	7.E-06
6 & 7	Low	Low	Med	2.7	1.4E+05	< 1 E-04	100	NA	1.E-04
6 & 7	High	Low	Med	2.7	3.4E+08	0.001	99.98	0.56	6.E-08
8 & 9	A	High	Med	2.9	1.2E+08	0.001	99.992	0.61	2.E-07
8 & 9	B	High	Med	2.7	6.3E+07	< 3E-07	100	NA	3.E-07
14 & 15	A	High	Med	3.3	3.6E+05	< 6 E-05	100	NA	6.E-05
14 & 15	B	High	Med	3.3	4.9E+05	< 4 E-05	100	NA	4.E-05
10 & 11	A	Low	Fine	3.6	3.8E+07	0.00005	99.998	0.47	5.E-07
10 & 11	B	Low	Fine	3.6	5.8E+07	0.00005	99.998	0.43	3.E-07
12 & 13	A	High	Fine	4.6	2.3E+06	< 9 E-06	100	NA	9.E-06
12 & 13	B	High	Fine	4.8	4.5E+06	< 4 E-06	100	NA	4.E-06

Table 4-5 – Microsphere Results Summary

Column Run	Column	Ionic Strength	Sand Size	Measured Bromide Velocity using t_{50} (m/day)	Microspheres				
					Influent Concentration (ms/ml)	Peak Microsphere Breakthrough (C/C_o)	Percent Microsphere Attenuated	Relative Retardation of Microspheres (t_{50} ms/t_{50} Br)	Normalized MDL (C/C_o) (20 microspheres/sample)
2 & 3	Low	Low	Med	1.7	No Microspheres Used				
2 & 3	High	Low	Med	1.8	No Microspheres Used				
4 & 5	Low	Low	Med	2.8	1.2E+03	1.61	18.4	1.06	2.E-03
4 & 5	High	Low	Med	2.9	4.8E+02	1.29	5.9	0.78	4.E-03
6 & 7	Low	Low	Med	2.7	5.9E+02	0.71	66.2	1.36	3.E-03
6 & 7	High	Low	Med	2.7	1.1E+02	1.98	37.8	1.33	2.E-02
8 & 9	A	High	Med	2.9	2.3E+03	0.38	73.6	1.22	9.E-04
8 & 9	B	High	Med	2.7	1.8E+03	0.24	87.6	1.63	1.E-03
14 & 15	A	High	Med	3.3	1.6E+04	0.11	91.7	1.11	1.E-04
14 & 15	B	High	Med	3.3	1.7E+04	0.05	95.4	1.15	1.E-04
10 & 11	A	Low	Fine	3.6	7.3E+03	< 3 E-04	100	NA	3.E-04
10 & 11	B	Low	Fine	3.6	2.6E+03	< 8 E-04	100	NA	8.E-04
12 & 13	A	High	Fine	4.6	3.1E+03	< 6 E-04	100	NA	6.E-04
12 & 13	B	High	Fine	4.8	4.1E+03	< 5 E-04	100	NA	5.E-04

4.6 Discussion

The experimental results were surprising and unexpected in a few cases, such as observing the total attenuation of MS2 in one of the column experiments in the medium sand at low ionic strength (Experiments 6 and 7), while the other experiments showed little attenuation (Experiments 2 and 3, and 4 and 5) at the same experimental conditions.

It was not surprising that increasing ionic strength had a substantial effect on MS2 attenuation in porous media. Pillai et al. (1997), under the same water and soil conditions demonstrated that a 3 times increase in Ca^{2+} (1-3 mmol/L) resulted in a 5 log reduction in MS2 peak effluent concentration. Since ionic strength (or content such as charge and ion type) is not considered in the calculation of collision efficiency (η_o) (eqation 2-8) this increase is likely a reflection of the importance of the ionic content of the double layer in increasing attachment efficiencies (α) (Ryan and Elimelech, 1996; Schijven and Hassanizadeh, 2000).

It was not necessarily expected that decreasing the median grain size by 50% would result in an additional > 5 log attenuation of microspheres since calculations only predict a slight increase in collision efficiency (η_o) (see equation 2-8 and Figure 2-2) (which is directly related to overall removal efficiency (η)) due to physicochemical filtration alone. Size exclusion estimates at this grain and microsphere size range (equations 2-12 and 2-13) do not predict that size exclusion will occur. Microspheres showed little attachment, however, even at high ionic strength in the medium sand where only physicochemical attachment would be responsible for removal (since size exclusion is highly unlikely in a medium sand). Therefore since physicochemical attachment does not appear to be important in microsphere removal in medium sand and equation 2-8 does not predict much increase in collision efficiency due to decreasing grain size, size exclusion could be a responsible process in attenuation in the fine sand.

4.6.1 Contradictory Breakthrough Curves from Paired Columns

Satisfactory explanations were not developed for all of the results obtained during the 14 column experiments. For example, it is difficult to guess what caused the apparent total attenuation in one of the columns in experiments 6 and 7. Further complicating things is that in column experiments 6 and 7, the column in which MS2 did breakthrough had lower normalized MS2 concentration than observed during the previous four column experiments (column runs 2 and 3 and 4 and 5) at identical ionic strength and porous media. An attempt to explain these results will now be made.

It is possible that MS2 deactivation affected the results observed in Experiments 6 and 7. Analysis of the MS2 reservoir throughout all experiments discourages this conclusion, however, because the influent concentration of MS2 remained essentially

constant throughout these experiments. It is possible that some residual bleach was left over in the column that failed to produce a breakthrough of MS2. This die off explanation, cannot fully account for the discrepancy in column experiments, since this could conceivably have a slight effect on virus attenuation, but nothing close to the radical more than 4 log reductions shown in experiments 6 and 7. These contradictory MS2 column experiments will be alluded to only briefly in this discussion, but should not be forgotten as they are real data.

Another anomalous result is seen when comparing experiments 8 and 9 and 14 and 15. These experiments were carried out to test the effect of raising ionic strength on virus and microsphere attenuation in medium sand. While bromide and microspheres broke through in a similar fashion in all four experiments, indicating similar physical conditions (flow rate, grain size, media packing etc), all displayed complete (> 6 log) attenuation in MS2 except for column A in experiments 8 and 9, which broke through at a 4 log peak concentration reduction (99.992 % attenuation) over influent concentration (C_o). It is possible that an error was made in measuring the masses or in the addition of $CaCl_2$ and NaCl to their respective reservoirs for columns A and B in experiments 8 and 9. Since separate reservoirs were used and small amounts of $CaCl_2$ were added (~1 g), errors in measurement or losses to the sides of the Erlenmeyer flask reservoir for column A would produce a lower [Ca^{2+}] in the spiked solution, possibly contributing to the attachment efficiency (α), yielding a higher breakthrough.

It is difficult to assess whether the variable results from the present study are typical of colloid transport experiments since unfortunately, very few researchers publish replicate column runs. Those researchers that have done multiple trials did not report

such variability in their findings as in the present investigation (e.g. Loveland et al., 1996; Pillai et al., 1997; Flynn et al., 2005).

4.6.2 Influent Bacteriophage Concentration Effects

The results showed that the concentration of the bacteriophage MS2 had little effect on its observed transport characteristics. When one compares the results from paired column experiments 2 and 3 and 4 and 5, the normalised curves are very similar in overall shape, but, in the case of experiments 2 and 3, differ in the details (such as breadth of MS2 and bromide breakthrough peaks). This difference may be likely related to the different amounts of time water flow was halted in each of the columns. Static water conditions existed for a longer amount of time in the low MS2 concentration column, potentially allowing more time for the viruses to diffuse to attachment sites. This outcome in conjunction with the results from experiments 6 and 7 weaken the conclusion that concentration does not affect transport of viruses, since in two out of three of these paired column experiments, disparate experimental outcomes were observed, potentially related to inconsistent experimental conditions. To demonstrate that influent virus concentration does not affect the transport characteristics of viruses, further experiments would need to be performed at conditions similar to those utilized during experiments 4 and 5, for which the attenuation and overall breakthrough curve shape (C/C_o and retardation) results agree with one another reasonably well.

4.6.3 Water Chemistry Effects

A general trend of increasing MS2 and microsphere attenuation with ionic strength was observed that colloid filtration theory and other researcher's experimental results support. Colloid filtration theory predicts that colloids in a like-charged

(negative) media will be attenuated more by increasing ionic strength (e.g. Loveland et al., 1996, Ryan and Elimelech, 1996, Schijven and Hassanizadeh, 2000). It is important to understand the relationship of ionic strength, specifically divalent cations, to virus and bacterial transport, given that natural or made-made fluctuations in riverbank groundwater chemistry often occur and may alter normal transport processes.

Comparison of Experiments 4 and 5 (medium sand, low IS) to experiments 14 and 15 (medium sand, high IS) indicates that increasing the calcium concentration and ionic strength in groundwater from 1 ($[Ca^{2+}]$) and 4.8 mmol/L (IS) to 5 and 94.7 mmol/L respectively, will substantially impact the transport of MS2 through sand. At low ionic strength, Experiments 4 and 5 yielded almost identical MS2 breakthrough curves with complete normalised breakthrough and little or no attenuation (8 and -25 %). Experiments 14 and 15, conducted with high ionic strength, yielded complete MS2 attenuation with at least 8 log reduction in peak normalized MS2 concentration. It should be noted that there was some variability in the observed outside of these model experimental results (2 and 3, 6 and 7 and, 8 and 9) which has already been noted above.

Redman et al. (1999) found similar results to Experiments 4 and 5, and 14 and 15. Using a filamentous bacteriophage originally isolated from sewage. When they raised the clean water influent $[Ca^{2+}]$ from 1 to 10 mmol/L in silica sand the normalised peak concentration went from 0 to 5 log (C/C_o) reduction over a 20 cm column using the similar crushed silica sand (also from Indusmin). A similar result was observed by increasing Mg^{2+} from 1 to 10 (4 log).

In contrast to the complete attenuation of bacteriophages, in the high ionic strength experiments 14 and 15, the microspheres were only 91.7 and 95.4 % attenuated

respectively. The four column runs at low ionic strength (medium sand) demonstrated 18.4, 5.9 and 66.2, 37.8 % attenuation during experiments 4 and 5, and 6 and 7 respectively. So although an increase in attenuation can be demonstrated for microspheres at the high ionic strength, given the analytical uncertainty statistical significance cannot be demonstrated.

4.6.4 Grain Size Effects

A second trend observed was the increase in attenuation with decreasing grain size. This argument is supported by colloid filtration theory. Equations 2-9 and 2-10 both show that attenuation will tend to increase with decreasing grain size. Equation 2-8 shows that collision efficiency, η_o, is inversely correlated to grain size in two of the three terms contributing to collision, diffusion and interception. Equation 2-10 indicates that overall removal efficiency (η) is inversely squared correlated to grain size. Furthermore, equation 2-9, which describes normalized reduction in peak breakthrough concentration, dictates that C/C_o is inversely logarithmic correlated to grain size. This equation also incorporates η_o, which, as mentioned above, already has two out three terms which have an inverse relationship to grain size. One would expect then, that with colloids where sedimentation was not a significant term (such as small colloids, < 1 μm, see Figure 2-2, or colloids with a density equal to water) C/C_o would then be inversely logarithmic-squared correlated to grain size (d_c). This indicates that, based on colloid filtration theory and under the colloid size (or density) conditions described above, the peak colloid concentration would be expected to greatly decrease with even a slight decrease in grain size. This statement must be qualified, however, since equation 2-9 must be taken as a whole, and there are other terms involved. For instance, if attachment efficiency, α, is

very low (as where a repulsive force acts between a colloid and a grain), then decreasing grain size may have little noticeable effect on reducing peak concentration.

Microspheres were predicted to have a low collision efficiency, relative to MS2, because of their size (Figure 2-2). Furthermore, the evident low attenuation of microspheres in the medium sand, at both low and high ionic strengths, indicates a low overall removal efficiency (η), suggesting a low attachment efficiency (α) between microsphere and grain (if attachment efficiency for microspheres was very high then one would expect a reasonably high overall removal efficiency). Therefore, since physicochemical attachment seems to not be operating, it is possible that the large attenuation of microspheres observed by decreasing grain size could be attributed to size exclusion.

Matthess and Pekdeger's (1988) model for size exclusion (equation 2-13), does not guarantee size exclusion with any confidence, with a calculated suffusion security for the present study (in fine sand) of 0.04 where a suffusion security >1.5 is required to guarantee size exclusion. It doesn't rule out the possibility of size exclusion, however. In fact Tufenkji et al. (2004) demonstrated that in some cases (e.g. very angular, crushed silica sand) the ratio of particle diameter to median grain diameter (d_p/d_{50}) need only be as high as 0.002 for size exclusion to occur. In the current study d_p/d_{50} for microspheres and fine sand was 0.004. Therefore with the microspheres, size exclusion could have contributed to the overall attenuation in the fine sand.

Under the present experimental conditions it is impossible to know whether this attenuation was caused by physicochemical attachment or size exclusion (or a combination of both). An alternative experimental design could be suggested that may

elucidate which processes are responsible for the observed attenuation. This design would involve running each experiment for the first two days as in the present study, but after two days switching the influent suspension to an eluting solution to detach any microspheres that were (physicochemical) attached to the grains, while leaving, undisturbed any microspheres blocked in pores (personal communication with Phil Schmidt, 2005).

Due to its very small size MS2 would not be expected to be retained by size exclusion in the fine sand. Nevertheless, MS2 attenuation was greatly increased by the two fold reduction in grain size, resulting in a 5 log removal in the fine sand (experiments 10 and 11), compared with little or no removal in the medium sand (experiments 2-7) at low ionic strength.

4.6.5 Detachment and Tailing in Breakthrough Curves

In some experiments greater attenuation of MS2 occurred than microspheres (experiments 6 to 9, 14 and 15). This difference in retention may be accounted for by the concept of a shadow zone (Ryan and Elimelech, 1996). The velocity of a fluid flowing passed a solid will decrease with proximity to the solid wall. Therefore, because of its lower profile, an attached virus will be exposed to lower water velocities and weaker bond-disrupting forces than attached microspheres, 100 times larger in size. The larger colloids may roll along the grain surface until they either come to rest on a part of the grain where not as great water velocities are (such as the side of the grain facing away from the oncoming flow) or these colloids could detach from the grain surface completely. Due to their lower profile, viruses would be expected to remain attached

longer than microspheres and for the same reason may also be more homogeneously distributed over the surface of a grain.

As well as being less attenuated than viruses, this potential for microsphere detachment may also explain the tailing demonstrated in experiments 4 and 5. If microspheres are slowly detached over the course of days one would expect tailing to occur. Further, if detachment occurs at a fixed rate then one would also expect the tail to be flat, which it is.

Although microsphere tailing was not demonstrated in other experiments, experiments 2 and 3 showed significant flat tailing of MS2. It is interesting that this did not occur in other experiments with MS2. As mentioned, in experiments 2 and 3, the water flow was halted, and the viruses were left in static water for about an hour. This static water may have allowed the viruses to diffuse more readily (than in flowing water) to attachment sites. Once attached, these viruses could detach over the course of days once flowing water (favouring detachment) was resumed.

Although in experiments 2 and 3, the MS2 tail was flat, Schijven and Hassanizadeh (2000) present an analytical derivation showing that (assuming a constant detachment rate) the negative slope of the tail of a bacteriophage breakthrough curve is directly related to the attached virus deactivation rate. They recommended that bacteriophage transport experiments be carried out over enough time to measure the slope of the tail. Schijven et al. (2002) (Table 2-1) demonstrated such breakthrough curves using the bacteriophages MS2, PhiX-174 and PRD1. Their breakthrough curves demonstrated obvious sloped tailing over the course of 8 to 10 days from the start of the experiment. Their experimental set up differed from the present study in a couple ways:

1) they injected a pulse over 2 days in contrast to the 4-5 hours of spiked influent in the present study; 2) they used a 2 metre long (9 cm width) column compared with the 20 cm long (5 cm width) column used in the current study. It is likely that injecting many more viruses into a much longer column would yield these observed tails over the next few days. This may be because there were more viruses added per column and detached viruses are likely to re-attach 10 times more frequently in the 2 metre column than a 20 cm column, thereby taking much longer to finally exit the column.

It should be noted that much work has gone into individually quantifying both attached and free (unattached) deactivation rates of viruses (Grant, 1993; Rossi, 1994; Schijven and Hassanizadeh, 2000; Schijven et al., 2002). In the present study, however, attached MS2 deactivation was assumed to not occur over the course of 2 days. This is supported by the fact that no free deactivation was observed in any of the 14 reservoirs.

Under appropriate experimental conditions (where sampling is continued long enough and where free deactivation rates are measured over the experimental period), natural (or eluent induced) tailing can provide much information about the processes (physicochemical attachment, size exclusion, deactivation) contributing to attenuation of pathogens in groundwater. In the context of RBF, tailing may represent a sustained threat to drinking water quality after a pathogenically contaminated river water warning is long passed (e.g. a storm or an overflowing upstream wastewater treatment plant). It is important therefore to understand not just the peak breakthrough concentrations in the effluent, but rather how long pathogens persist in the effluent after a spiked injection. It is important to realize that, as shown above in a comparison of the results in the present

study with Schijven et al. (2002), column length or soil passage distance could produce very different pathogen transport results, not reflected by shorter columns.

4.6.6 Non-constant Flow Rates

In Table 4-4 one can see that higher pore velocities were used for the fine grain sand (average 4.2 m/day) than the medium sand (2.9 m/day). The experiments were intended to be carried out at constant pore velocity. Initial porosity measurements indicated that the fine sand had a higher porosity than the medium sand. The flow rate (Q) of the columns was adjusted in order to keep the pore velocity constant. After the column experiments had been completed, repeat measurements revealed the two porosities to be roughly equal.

Colloid filtration theory predicts that virus removal (log (C/C_o)) is negatively correlated to the inverse of flow velocity to the power of two thirds (Yao et al., 1971). This derivation assumes a clean filter bed and spherical grains. Wang et al. (1981) verified this relationship in column experiments, however, utilizing poliovirus 1 and echovirus 1. Table 3-5 shows that poliovirus and echovirus are similar to MS2 in size and genetics. By substituting flow velocities of 2.9 to 4.1 m/day into this relationship, this produces a difference in normalised peak breakthrough concentration of about 0.2 log. Compared to the large attenuation rates demonstrated in these experiments, this does not represent a serious problem, but is a source of bias in the data.

4.6.7 Application of Experimental Results to RBF

While a column experiment is simplified in order to extract meaningful information about pathogen transport processes there are certain limitations in applying results from column experiments directly to a Riverbank Filtration environment. These

limitations have already been mentioned in this thesis, but are now summarized in light of the results.

From One Dimension to Three

The column was one dimensional and the media were homogeneous in content and structure. In a real riverbank aquifer there are three dimensions with considerable heterogeneity in mineralogical (and perhaps organic) content and hydraulic conductivity. This hydrogeological heterogeneity can lead to highly conductive conduits where groundwater passes easily through a Riverbank. In bedrock, fractures often provide these rapid conduits for water to flow through. This is a dramatically different environment from that used with packed sand columns in the current study. Therefore, these results from the present investigation would only be valid when applied to unconsolidated media, preferably where the variability in grain size and mineralogy is well understood.

Length

Changing from the 20 cm length used in the present study to tens or hundreds of metres would be expected to result in different transport characteristics. The results from the current study were encouraging since such a sharp reduction in viruses and bacteria-sized microspheres occurred over a short distance. Other field studies, however, at similar flow rates and in medium sand (Schijven et al., 2000 and Blanford et al. 2005) have demonstrated a sharp initial reduction over the first several metres after the injection point and then a subsequent plateau in bacteriophage concentration that continued for many metres downgradient. The authors suggest several possible reasons for this (e.g. oxidation of metals on grains in the area around injection wells forming metal-oxides which would attract colloids). Regardless, it is clear that overall colloid transport

operates differently in the field than would be predicted from column experiments in the present study since a simple extrapolation from the 20 cm length used in this experiment to 20 m would imply complete attenuation of all colloids, but this is not what has been observed in the field.

Further supporting the idea that scaling may be an issue in modelling a large scale environment is that in a similar experimental set up to the present study, by injecting a spiked influent (2 pore volumes) of several bacteriophages into 2 m columns, Schijven et al. (2002) also demonstrated tailing occurred after the initial peak had passed.

Mineralogy and Organics

Using mixtures of minerologies (calcite, quartz, feldspar) from a glacial aquifer in Switzerland, Flynn et al. (2004) demonstrated that calcite retained bacteriophages much greater than quartz or feldspar. It is also well known that metal-oxides are effective mineralogical attachment sites for negatively charged colloids, since, unlike most natural porous media, metal-oxides carry a positive charged at neutral pH (Loveland et al., 1996 and Zhuang and Jin, 2002). Thus, mimicking aquifer-scale changes in mineralogy is impossible in such homogeneous columns.

Water Quality

In an RBF environment, ionic strength and chemical content would be expected to vary somewhat randomly in a river depending on precipitation levels. A change in ionic strength could reverse the normal forces between pathogens and grains. This in turn could result in the rapid passage of, normally attenuated, pathogens from surface water to the drinking water well.

5. CONCLUSIONS AND RECOMMENDATIONS

There are several processes that affect the transport of microorganisms in groundwater, these include physicochemical attachment, size exclusion and die off. The relative contribution of each of these processes to the attenuation of pathogens is determined by the physical, chemical and biological properties of the microbe, the media and the water. This Thesis examined the effects of influent virus concentration, ionic strength, media grain size on pathogen transport in porous media. Fourteen column tests were conducted using the non-pathogenic surrogates of human viruses and bacteria MS2 and 1.5 μm microspheres respectively. Two sizes of crushed silica sand (0.7 and 0.34 mm median diameter) and two ionic strengths (1 and 10 mmol/L of Ca^{2+}) were used. A 2^2 factorial design was used to evaluate each of the parameters' effects on pathogen transport.

5.1 Conclusions

- Complete normalised breakthrough (C/C_o) in peak concentration and little (~60%) to no attenuation of viruses and microspheres was observed in low ionic strength water and medium sand.
- When virus, microsphere and bromide breakthrough was observed, viruses tended to be retarded relative to a bromide tracer while microspheres tended to breakthrough slightly earlier than bromide.
- Increasing ionic strength by increasing Ca^{2+} from 1 to 10 mmol/L increased attenuation of MS2 in both the medium and fine sands with a >6 log MS2 reduction in both media, whereas only a 1 log reduction at in peak microsphere concentration (C/C_o) in the medium sand was observed when Ca^{2+} concentration was increased.

- Decreasing the grain size resulted in a 5 log reduction in peak MS2 concentrations in low ionic strength water. In both fine and medium sand at high ionic strength no MS2 broke through the columns (>6 log removal). Thus the effect of ionic strength in fine sand was indistinguishable from the effect of ionic strength in the medium sand since complete attenuation were observed in both grain sizes at high ionic strength.
- Grain size appeared to substantially affect microsphere attenuation. No microspheres broke through any of the fine sand columns at the low or high ionic strength, yielding a minimum > 5 log reduction in peak microsphere concentration (or > 99.999 % overall attenuation). With the current experimental set up it is impossible to discern which of the processes of physicochemical attachment or size exclusion (or both) were responsible for the attenuation of microspheres in the fine sand.
- There was virtually no effect observed from varying the influent concentration of viruses (from 10^5 to 10^7 pfu/ml) on their observed transport characteristics; normalised peak breakthrough concentration, percent attenuation and retardation relative to a bromide tracer.

5.2 Recommendations

- There were several columns in which neither MS2 nor microspheres breakthrough was not observed. Whenever high ionic strength was used, the complete attenuation of MS2 was observed. When fine grain sand was used the microspheres were completely attenuated. Therefore, it is recommended that an intermediate ionic strength and grain size be chosen in a future column

experiment with MS2 and microspheres. This experiment would allow the effects of ionic strength and grain size to be quantified, since complete attenuation of MS2 and microspheres may not occur, allowing the attenuation capacity of the media to be assessed.

- Ideally protozoa, bacteria and viruses should be injected together into undisturbed columns of riverbank aquifer material or a well studied and monitored RBF aquifer. This experience could be applied to understanding of the effects of microbe size, grain size and ionic strength in an environment closer to RBF (i.e. heterogeneous mineralogy, broader grain size distribution, organics etc) as well as testing the validity of the results collected in column experiments from the present study.
- A column experiment could be performed to evaluate the relative importance of size exclusion in the attenuation of bacteria-sized microspheres in the same fine grained sand used in this experiment. This would consist of performing an experiment at low ionic strength in the fine sand. After several pore volumes have passed through after the initial spike the ionic strength could be lowered (or an eluent added) to favour detachment of microspheres from physicochemical attachment sites. The attached (physicochemical) microspheres should be released, while this alteration in water chemistry should not disturb the microspheres stuck in pores. Thus the microspheres still in the column after several pore volumes of the eluent has passed through, could be inferred to be retained by size exclusion (personal communication with Phil Schmidt, 2005).

REFERENCES

Adams, M. H., *Bacteriophages*, Interscience, 1959, pp. 450-454, New York, NY.

APHA, AWWA, WEF (American Public Health Association, American Water Works Association, and Water Environment Federation). 1995. Standard Methods for the Examination of Water and Wastewater. 19th ed. Washington, D.C.: APHA.

Alvarez, Maria E., Miguel Aguilar, Alexis Fountain, Neyda Gonzalez, Osvaldo Rascon, and David Saenz, Inactivation of MS-2 phage and poliovirus in groundwater, *Canadian Journal of Microbiology*, Vol. 46, pp. 159-165

Appelo, C. A. J., and Postma, D., Geochemistry, groundwater and pollution, A. A. Balkema, Rotterdam, The Netherlands, 1996.

Bengtsson, Göran and Lina Ekere, Predicting sorption of groundwater bacteria from size Distribution, surface area, and magnetic susceptibility of soil particles, *Water Resources Research*, Vol. 37, No. 6, pp. 1795-1812, 2001.

Blacklow, N. R., Greenberg, H. B., *New England Journal of Medicine*, Vol. 352, No. 252, 1991.

Bodley-Tickell, A. T., S. E. Kitchen and A. P. Sturdee, Occurrence of *Cryptosporidium* in agricultural surface waters during an annual farming cycle in lowland UK, *Water Research*, Vol. 36, pp. 1880-1886, 2002.

Castignolles, Nathalie, Fabienne Petit, Isabelle Mendel, Laurent Simon, Laurence Cattolico and Claudine Buffet-Janvresse, Detection of Adenovirus in the waters of the Seine River estuary by nested-PCR, *Molecular and Cellular Probes*, Vol. 12, pp. 174 – 180, 1998.

Chapron, Christopher D., Nicola A. Ballester, Justin H. Fontaine, Christine N. Frades and Aaron B. Margolin, Detection of Astroviruses, Enteroviruses, and Adenoviruses Types 40 and 41 in Surface Waters Collected and Evaluated by the Information Collection Rule and an Integrated Cell Culture-Nested PCR Procedure, *Applied and Environmental Microbiology*, Vol. 66, No. 6, 2000.

Chu, Yanjie, Yan Jin, Markus Flury and Marylynn V. Yates, Mechanisms of virus removal During transport in unsaturated porous media, *Water Resources Research*, Vol. 37, No. 2, pp. 253-263, 2001.

Ciocca, M. Clinical course and consequences of hepatitis A infection., *Vaccine*, Supplement 1, s71-74, 2000.

Conboy, M. J., M. J. Goss, Natural protection of groundwater against bacteria of fecal origin, *Journal of Contaminant Hydrology*, Vol. 43, pp. 1-24, 2000.

Cornu, Marie, Marie Laure Delignette-Muller, and Jean-Pierre Flandrois, Characterization of Unexpected Growth of Escherichia coli O157:H7 by Modeling, *Applied and Environmental Microbiology*, Vol. 65, No. 12, 1999.

Côté, Martin Marcel, A Field and Bench Scale Evaluation of Riverbank Filtration Efficacy for Removal Of *Cryptosporidium*-sized Microspheres, Dept of Civil Engineering, University of Waterloo, Waterloo, Ontario, Canada, 2004.

Coursaget, Pierre, Yves Buisson, Nathalie Enogat, Raymond Bercion, Jean-Marie Baudet, Patrick Delmaire, Dominique Prigent and Jerome Desrame, Outbreak of enterically-Transmitted hepatitis due to hepatitis A and hepatitis E viruses, *Journal of Hepatology*, Vol. 28, pp. 745-750, 1998.

Cunin, Patrick, Etienne Tedjouka, Yves Germani, Chouaibou Ncharre, Raymond Bercion, Jacques Morvan, and Paul M. V. Martin, An Epidemic of Bloody Diarrhea: *Escherichia coli* O157 Emerging in Cameroon?, *Emerging Infectious Diseases*, Vol. 5, No. 2, 1999.

Daczkowska-Kozon, Elzbieta and Jadwiga Brzostek-Nowakowska, *Campylobacter* spp. in Western Pomerania water bodies, *International Journal of Hygiene and Environmental Health*, Vol. 203, 435-443, 2001.

Danon-Schaffer, Monica N., Walkerton's Contaminated Water Supply System: A Forensic Approach to Identifying the Source, *Environmental Forensics*, Iss. 2, pp. 197-200, 2001.

Deborde, Dan C., William W. Woessner, Quinn T. Kiley and Patrick Ball, Rapid Transport of Virues in a Floodplain Aquifer, *Water Research*, Vol. 33, No. 10, pp. 2229-2238, 1999.

Derjaguin, B. V. and Landau, L., *Acta Physicochim. URSS*, Vol. 14, No. 633, 1941.

Donnelly, J. K. and E. I. Stentiford, The *Cryptosporidium* Problem in Water and Food Supplies, *Lebensm. Wiss. U. Technol*. Vol. 30, pp. 111-120, 1997.

Dowd, S. E., Pillai, S. D., Wang, S., Corapcioglu, M. Y., Delineating the Specific Influence of Virus Isoelectric Point and Size on Virus Adsorption and Transport through Sandy Soils, Applied and Environmental Microbiology, Vol. 64, No. 2, 1998.

Duim, Birgitta, Peter A. R. Vandamme, Alan Rigter, Severine Laevens, Jeroen R. Dijkstra And Jaap A. Wagenaar, Differentiation of Campylobacter species by AFLP fingerprinting, *Microbiology*, Vol. 147, pp. 2729-2737, 2001.

Effler, Paul, Margaretha Isaäcson, Lorraine Arntzen, Rosemary Heenan, Paul Canter, Timothy Barrett, Lisa Lee, Clifford Mambo, William Levine, Akbar Zaidi, and Patricia M. Griffin, Factors Contributing to the Emergence of *Escherichia coli* O157 in Africa, *Emerging Infectious Diseases*, Vol. 7, No. 5, 2001.

Elimelech, M., Nagai, M., Ko, Chun-Han, Ryan, J. N., Relative Insignificance of Mineral Grain Zeta Potential to Colloid Transport in Geochemically Heterogeneous Porous Media, *Environmental Science & Technology*, Vol. 34, No. 11, 2000.

Elimelech, M., and O'Melia, C. R*., Journal of American Water Works Association*, Vol. 80, 1988.

Emelko, M. B., Removal of *Cryptosporidium parvum* by granular media filtration, Ph.D. Dissertation, University of Waterloo, 2001.

Flynn, R., Hunkeler, D., Guerin, C., Burn, C., Rossi, P., Aragno, M., Geochemical influences on H40/1 Bacteriophage inactivation in glaciofluvial sands, *Environmental Geology*, Vol. 45, pp. 504-517, 2004a.

Flynn, R., Rossi, P., Hunkeler, D., Investigation of virus attenuation mechanisms in a fluvioglacial sand Using column experiments, *FEMS Microbiology Ecology*, Vol. 49, pp. 83-95, 2004b.

Freeze, A. and Cherry, J., Groundwater, Prentice Hall, Inc., New Jersey, USA, 1979.

Foppen, J. W. A., Mporokoso, A., Schjiven, J. F., Determining straining of *Escherichia coli* from breakthrough curves, Journal of Contaminant Hydrology, Vol. 76, pp. 191-210, 2005.

Geldreich, Edwin E., Pathogenic agents in freshwater resources, *Hydrological Processes*, Vol. 10, pp. 315-333, 1996.

Gerba, Charles P., Joan B. Rose, Charles N. Haas, and Kristina D. Crabtree, Waterborne Rotavirus: A Risk Assessment, *Wat. Res*., Vol. 30, No. 12, 1996.

Gooddy, Daren C., Paul J. A. Withers, Hamish G. Mcdonald and P. John Chilton, Behaviour And Impact of Cow Slurry Beneath a Storage Lagoon: II. Chemical Composition of Chalk Porewater After 18 Years, *Water, Air and Soil Pollution*, Vol. 107, pp. 51-72, 1998.

Goss, M. J., Barry, D. A. J., Rudolph, D. L., Contamination in Ontario farmstead domestic wells and its association with agriculture: 1. Results from drinking water wells, *Journal of Contaminant Hydrology*, Vol. 32, pp. 267-293, 1998.

Graczyk, Thaddeus K., Barry M. Evans, Clive J. Shiff, Hubert J. Karreman and Jonathan A. Patz, Environmental and Geographical Factors Contributing to Watershed Contamination with Cryptospordium parvum Oocysts, *Environmental Research Section*, Vol. 82, pp. 263-271, 2000.

Grabow, WOK, Hepatitis viruses in water: Update on risk and control, *Water SA*, Vol. 23 No. 4, October 1997.

Grant, S. B., List, E. J., Lindstrom, M. E., Kinetic analysis of virus adsorption and inactivation in batch experiments. *Water Res. Research*, Vol. 29, pp. 2067-2085, 1993.

Greening, Gail E., Michiko Mirams, and Tamas Berke, Molecular Epidemiology of 'Norwalk -Like Viruses' Associated With Gastroenteritis Outbreaks in New Zealand, *Journal of Medical Virology*, Vol. 64, pp. 58-66, 2001.

Happel, J., *AIChE* Journal, Vol. 4, No. 197, 1958.

Harvey, F. E., Sibray, S. S., Delineating Ground Water Recharge from Leaking Irrigation Canals Using Water Chemistry and Isotopes, *Ground Water*, Vol. 39, No. 3, 2001.

Harvey, R. W., George, L. H., Smith, R. L., LeBlanc, D. R., Transport of Microspheres and Indigenous Bacteria through a Sandy Aquifer: Results of Natural- and Forced-Gradient Tracer Experiments, *Environmental Science and Technology*, Vol. 23, pp. 51-56, 1989.

Hötzl, H. W. Käss and B. Reichert, Application of Microbial Tracers in Groundwater Studies, *Wat. Sci. Tech*., Vol. 24, No. 2, 1991.

Hedlund, K. O., E. Rubilar-Abreu, and L. Svensson, Epidemiology of Calicivirus Infections in Sweden, 1994-1998, *The Journal of Infectious Diseases*, Supplement 2, pp. 275-280 2000.

Huang, P. W., D. Laborde, V. R. Land, D. O. Matson, A. W. Smith, and X. Jiang, Concentration and detection of caliciviruses in water samples by reverse transcription-PCR, *Applied and Environmental Microbiology*, Vol. 66, No. 10, 2000.

Hulten, K., H. Enroth, T. Nyström and L. Engstrand, Presence of *Helicobacter* species DNA In Swedish water, *Journal of Applied Microbiology*, Vol. 85, pp. 282-286, 1998.

Hunter, P. R., Cyanobacterial toxins and human health, *Journal of Applied Microbiology Symposium Supplement*, Vol. 84, pp. 35S – 40S, 1998.

Jellison, Kristen L., Harold F. Hemond and David B. Schauer, Sources and Species of Cryptospordium Oocysts in the Wachusett Reservoir Watershed, *Applied and Environmental Microbiology*, pp. 569-575, Feb 2002.

Jameel, S., Molecular biology and pathogenesis of hepatitits E virus, Expert Reviews in Molecular Medicine, (99) 00127-1a, Cambridge University Press, 1999.

Jewett, D. G., Logan, B. E., Arnold, R. G., Bales, R. C., Transport of *Pseudomonas fluorescens* strain P17 Through quartz sand columns as a function of water content, *Journal of Contaminant Hydrology*, Vol. 36, pp. 73-89, 1999.

Jin, Y., Chu, Y., Li, Y., Virus removal and transport in saturated and unsaturated sand columns, *Journal of Contaminant Hydrology*, Vol. 43, pp. 111-128, 2000.

Jin, Y., Flury, M., Fate and Transport of Viruses in Porous Media, Advances in Agronomy, Vol. 77, pp. 39 – 103, 2002.

Jin, Y., Yates, M. V., Thompson, S. S., Jury, W. A., Sorption of Viruses during Flow through Saturated Sand Columns, *Environmental Science & Technology*, Vol. 31, No. 2, 1997.

Johnson, W. P., P. Zhang, P. M. Gardner, M. E. Fuller, and M. F. Deflaun, Evidence for Detachment of Indigenous Bacteria from Aquifer Sediment in Response to Arrival of Injected Bacteria, *Applied Environmental Microbiology*, Vol. 67, No. 10, pp. 4908- 4913, 2001.

Keller, A. A., Sirivithayapakorn, S., Chrysikopoulos, C. V., Early breakthrough of colloids and Bacteriophage MS2 in a water-saturated sand column, *Water Resources Research*, Vol. 40, pp. 1-11, 2004.

Keswick, B. H., T. K. Satterwhite, P. C. Johnson, H. L. Dupont, S. L. Secor, J. A. Bitsura, G. W. Gary, J. C. Hoff, Inactivation of Norwalk virus in drinking water by chlorine, *Applied Environmental Microbiology*, Vol. 50, No. 2, 1985.

Kim, K., Plagioclase weathering in the groundwater system of a sandy, silicate aquifer, *Hydrological Processes*, Vol. 16, pp. 1793-1806, 2002.

Kinoshita, T., Bales, R. C., Maguire, K. M., Gerba, C. P., Effect of pH on bacteriophage transport through Sandy soils, *Journal of Contaminant Hydrology*, Vol. 14, pp. 55-70, 1993.

Klein, Peter D., David Y. Graham, Alvaro Gaillour, Antone R. Opekun and E. O'Brian Smith, Water source as risk factor for *Helicobacter pylori* infection in Peruvian children*, The Lancet*, Vol. 337, 1991.

Klein, Cornelis, Hurlbut, Cornelius S. Jr., Manual of Mineralogy, John Wiley and Sons, USA, 1985.

Kücükcolak, E., B. Koopman, G. Bitton and S. Farrah, Validity of flurochrome-stained Bacteria as tracers of short-term microbial transport through porous media, *Journal Of Contaminant Hydrology*, Vol. 31, pp. 349-357, 1998.

Kuehn, W., and Mueller, U., Riverbank filtration: an overview., Journal of AWWA, Vol. 82, No. 12, 2000.

Kuhnert, Peter, Patrick Boerlin and Joachim Frey, Target genes for virulence assessment of Escherichia coli isolates from water, food and the environment, *FEMS Microbiology Reviews*, Vol. 24, pp. 107-111.

Kukkula, M., P. Arstila, M. L. Klossner, L. Maunula, C. H. Bonsdorff, P. Jaatinen, Waterborne outbreak of viral gastroenteritis, *Scandinavian Journal of Infectious Disease*, Vol. 29, No. 4, 1997.

Lawrence, J. R. and M. J. Hendry, Transport of bacteria through geologic media, *Canadian Journal of Microbiology*, Vol. 42, pp. 410-422, 1996.

Lawson, H. W., M. M. Braun, R. I. Glass, S. E. Stine, S. S. Monroe, H. K. Atrash, L. E. Lee, S. J. Englender, Waterborne outbreak of Norwalk virus gastroenteritis at a southwest US resort: role of geological formations in contamination of well water, *Lancet*, Vol. 337, No. 8751, 1991.

Lee, Seung-Hoon and Sang-Jong Kim, Detection of infectious enteroviruses and adenoviruses in tap water in urban areas in Korea, *Water Research*, Vol. 36, pp. 248 – 256, 2002.

Lind, Lena, Eva Sjögren, Kjetil Melby and Bertil Kaijser, DNA Fingerprinting and Serotyping of *Campylobacter jejuni* Isolates from Epidemic Outbreaks, *Journal of Clinical Microbiology*, pp. 892 – 896, Apr. 1996.

Liu, Z., Groves, C., Yuan, D., Meiman, J., Jiang, G., He, S., Li, Qiang, Hydrochemical variations during Flood pulses in the south-west China peak cluster karst: impacts of $CaCO_3$-H_2O-CO_2 Interactions, *Hydrological Processes*, Vol. 18, pp. 2423-2437, 2004.

Loveland, J. P., Ryan, J. N., Amy, G. L., Harvey, R. W., The reversibility of virus attachment to mineral Surfaces, *Colloids and Surfaces A: Physicochemical and Engineering Aspects*, Vol. 107, pp. 205-221, 1996.

Marshall, David G., William G. Dundon, Sarah M. Beesley and Cyril J. Smyth, *Helicobacter pylori* – a conundrum of genetic diversity, *Microbiology*, Vol. 144, 1998.

Marshall, Marilyn M., Donna Naumovitz, Ynes Ortega and Charles R. Sterling, Waterborne Protozoan Pathogens, *Clinical Microbiology Reviews*, Vol. 10, No. 1, pp. 67-85, Jan 1997.

Matthess, Georg, Asaf Pekdeger and Juergen Schroeter, Persistence and Transport of Bacteria and Viruses in Groundwater – A Conceptual Evaluation, *Journal of Contaminant Hydrology*, Vol. 2, pp. 171-188, 1988.

McKay, L. D., Harton, A. D., Wilson, G. V., Influence of Flow Rate on Transport of Bacteriophage in Shale Saprolite, *Journal of Environmental Quality*, Vol. 31, pp. 1095-1105, 2002.

McCarthy, J. F., McKay, L. D., Bruner, D. D., Influence of Ionic Strength and Cation Charge on Transport of Colloidal Particles in Fractured Shale Saprolite, *Environmental Science & Techology*, Vol. 36, No. 17, 2002.

McCaulou, D. R., Bales, R. C., McCarthy, J. F., Use of short-pulse experiments to study bacteria transport Through porous media, *Journal of Contaminant Hydrology*, Vol. 15, pp. 1-14, 1994.

Medema, G. J. and J. F. Schijven, Modelling the sewage discharge and dispersion of *Cryptospordium* and *Giardia* in surface water, *Water Resources*, Vol. 35, No. 18 2001.

Meschke, J. S. and Sobsey, M. D., Comparative reduction of Norwalk virus, poliovirus type 1, F+ RNA Coliphage MS2 and *Escherichia coli* in miniature soil columns, *Water Science and Technology*, Vol. 47, No. 3, 2003.

Molinero, M. E., I. Fernandez, M. A. Garcia-Calabuig, E. Peiro, Investigation of a Waterborne *Salmonella* ohio outbreak, *Enferm. Infecc. Microbiol. Clin*., Vol. 16 No. 5, 1998.

Monis, Paul T. and Christopher P. Saint, Development of a nested-PCR assay for the Detection of *Cryptosporidium parvum* in finished water, *Water Resources*, Vol. 35 No. 7, pp. 1641-1648, 2001.

Montgomery, D. C., Design and Analysis of Experiments Fifth Ed., John Wiley & Sons, Inc., 2001.

Muniesa, Maite, Francisco Lucena and Juan Jofre, Comparative Survival of Free Shiga Toxin 2-Encoding Phages and *Escherichia coli* Strains outside the Gut, *Applied and Environmental Microbiology*, Vol. 65, No. 12, 1999.

Naik, SR, R Aggarwal, PN Salunke, NN Mehrotra, A large waterborne viral hepatitis E Epidemic in Kanpur, India, *Bulletin of the World Health Organisation*, Vol. 70, No. 5, 1992.

Negrel, Ph., Petelet-Giraud, E., Barbier, J., Gautier, E., Surface water-groundwater interactions in an alluvial plain: Chemical and isotopic systematics, *Journal of Hydrology*, Vol. 277, pp. 248-267, 2003.

New York City Department of Environmental Protection, Waterborne Disease Risk Assessment Program 2000 Annual Report, May 2001.

Ohrui, K., Mitchell, M. J., Hydrological flow paths controlling stream chemistry in Japanese forested Watersheds, *Hydrological Processes*, Vol. 13, pp. 877-888, 1999.

O'Melia, C. R., *Environmental Science and Technology*, Vol. 14, pp. 1052, 1980.

Ono, Kazuo, Hidetaka Tsuji, Shiba Kumar Rai, Akio Yamamoto, Kuniyoshi Masuda, Takuro Endo, Hak Hotta, Takashi Kawamura, and Shoji Uga, Contamination of River Water by *Cryptosporidium parvum* Oocysts in Western Japan, *Applied and Environmental Microbiology*, Vol. 67, No. 9, 2001.

Pang, L., Close, M., Goltz, M., Sinton, L., Davies, H., Hall, C., Stanton, G., Estimation of septic tank Setback distances based on transport of *E. coli* and F-RNA phages, *Environment International*, Vol. 29, pp. 907-921, 2003.

Parashar, Umesh D., Joseph S. Bresee, Jon R. Gentsch, and Roger I. Glass, Rotavirus, *Emerging Infectious Diseases*, Vol. 4, No. 4, 1998.

Penrod, A. P., Olson, T. M., and Grant, S. B., Deposition kinetics of two viruses in packed beds of Quartz granular media, *Langmuir*, Vol. 12, pp. 5576-5587, 1996.

Peters, N. E., Cerny, J., Havel, M., Krejci, R., Temporal trends of bulk precipitation and stream water Chemistry (1977-1997) in a small forested area, Krusne hory, northern Bohemia, Czech Republic, *Hydrological Processes*, Vol. 13, pp. 2721-2741, 1999.

Pieper, A. P., Ryan, J. N., Harvey, R. W., Amy, G. L., Illangasekare, T. H., and Metge, D. W., Transport and recovery of bacteriophage PRD1 in a sand and gravel aquifer: effect of sewage-derived organic matter. *Environmental Science and Technology*, Vol. 31, pp. 1163-1170, 1997.

Pina, Sonia, Joan Jofre, Suzanne U. Emerson, Robert H. Purcell and Rosina Girones, Characterization of a Strain of Infectious Hepatitis E Virus Isolated from Sewage In an Area where Hepatitis E Is Not Endemic, *Applied and Environmental Microbiology*, Vol. 64, No. 11, pp. 4485 – 4488, 1998.

Rajagopalan, R., and Tien, C., Trajectory Analysis of Deep-Bed Filtration with the Sphere-in-cell porous Media Model, *Jour. AlChE*. Vol. 22, No. 3, 1976.

Rains, M. C., Mount, J. F., Origin of Shallow Ground Water in an Alluvial Aquifer as Determined by Isotopic and Chemical Procedures, *Ground Water*, Vol. 40, No. 5, 2002.

Redman, J. A., Grant, S. B., Olson, T. M., Adkins, J. M., Jackson, J. L., Castillo, M. S. and Yanko, W. A., Physicochemical Mechanisms Responsible for the Filtration and Mobilization of a Filamentous Bacteriophage in Quartz Sand, *Wat. Res*., Vol. 33, No. 1, 1998.

Redman, J. A., Grant, S. B., Olson, T. M., Hardy, M. E., Estes, M. K., Filtration of Recombinant Norwalk Virus Particles and Bacteriophage MS2 in Quartz Sand: Importance of Electrostatic Interactions, *Environmental Science & Technology*, Vol 31, No. 12, 1997.

Rice, E. W., R. M. Clark, and C. H. Johnson, Chlorine inactivation of Escherichia coli O157:H7, *Emerging Infectious Diseases*, Vol. 5, No. 3, 1999.

Robertson, Lucy J. and Bjorn Gjerde, Occurrence of *Cryptosporidium* oocysts and *Giardia* Cysts in raw waters in Norway, *Scandinavian Journal of Public Health*, Vol. 29, pp. 200-207, 2001.

Rochelle, Paul A., Environmental Molecular Microbiology: Protocols and Applications, Horizon Scientific Press, Wymondham, UK, 2001.

Ross, N., Villemur, R., Deschenes, L., Samson, R., Clogging of a Limestone Fracture by Stimulating Groundwater Microbes, *Water Resources*, Vol. 35, No. 8, 2001.

Goss et al., M. J., D.A.J. Barry, Rudolph, D. L., Contamination in Ontario farmstead domestic wells and its association with agriculture: 2. Results from multilevel monitoring well Installations, *Journal of Contaminant Hydrology*, Vol. 32, pp. 295-311, 1998.

Ryan, J. N. and Elimelech, M., Colloid mobilization and transport in groundwater, *Colloids and Surfaces A: Physicochemical and Engineering Aspects*, Vol. 107, pp. 1-56, 1996.

Sanchez, Jose L., Leonard N. Binn, Bruce L. Innis, Richard D. Reynolds, Terrence Lee, Felicia Mitchell-Raymundo, Stephen C. Craig, Jeffrey P. Marquez, Greg A. Sheperd, Christina S. Polyak, Johnnie Conolly, and Kimmie F. Kohlhase, Epidemic of Adenovirus-Induced respiratory illness among US military recruits: epidemiologic And immunologic risk factors in healthy, young adults, *Journal of Medical Virology*, Vol. 65, pp. 710 – 718, 2001.

Scandura, J. E. and M. D. Sobsey, Viral and Bacterial Contamination of Groundwater from On-Site Sewage Treatment Systems, *Wat. Sci. Tech*., Vol. 35, No. 11-12, 141-146, 1997.

Schaffter, Nicole, Aurele Parriaux, Pathogenic-bacterial water contamination in mountainous catchments, *Water Research*, Vol. 36, pp. 131-139, 2002.

Schäfer, Anke, Petr Ustohal, Hauke Harms, Fritz Stauffer, Themistocles Dracos and Alexander J. B. Zehnder, Transport of bacteria in unsaturated porous media, *Journal of Contaminant Hydrology*, Vol. 33, pp. 149-169, 1998.

Schernewski, Gerald, Wolf-Dieter Jülich, Risk assessment of virus infections in the Oder Estuary (southern Baltic) on the basis of spatial transport and virus decay simulations, *International Journal of Hygiene and Environmental Health*, Vol. 203, pp. 317-325, 2001.

Schijven, J. F., de Bruin, H. A. M., Hassanizadeh, S. M., de Roda Husman, A. M., Bacteriophages and Clostridium spores as indicator organisms for removal of pathogens by passage through saturated dune sand, *Water Research*, Vol. 37, pp. 2186-2194, 2003.

Schijven, J. F., Hassanizadeh, S. M., de Bruin, R. H. A. M., Two-site kinetic modeling of bacteriophages Transport through columns of saturated dune sand, *Journal of Contaminant Hydrology*, Vol. 57, pp. 259-279, 2002.

Schijven, J. F., Medema, G., Vogelaar, A. J., Hassanizadeh, S. M., Removal of microorganisms by deep Well injection*, Journal of Contaminant Hydrology*, Vol. 44, pp. 301-327, 2000a.

Schijven, J. F., Hassanizadeh, S. M., Dowd, S. E., Pillai, S. D., Modeling Virus Adsorption in Batch and Column Experiments*, Quantitative Microbiology*, Vol. 2, pp. 5-20, 2000b.

Schijven, Jack F. and Jiri Simunek, Kinetic modeling of virus transport at the field scale, *Journal of Contaminant Hydrology*, Vol. 55, pp. 113-135, 2002.

Schijven, Jack F., Wim Hoogenboezem, S. Majid Hassanizadeh, and Jos H. Peters, Modeling Removal of bacteriophages MS2 and PRD1 by dune recharge at Castricum, Netherlands, *Water Resources Research*, Vol. 35, No. 4, 1999.

Schoenen, Dirk, Requirements for the Catchment, Treatment, and Surveillance of Drinking Water To Avoid the Transmittance of Pathogenic Bacterial, Viral, and Parasitic Organisms, *Acta hydrochim. hydrobiol*., Vol. 29, No. 4, pp. 187-196, 2001.

Schwab, Kellogg J., Frederick H. Neill, Rebecca L. Frankhauser, Nicholas A. Daniels, Stehan S. Monroe, David A. Bergmire-sweat, Mary K. Estes, and Robert L. Atmar, *Applied and Environmental Microbiology*, Vol. 66, No. 1, 2000.

Shadford, C. B., D. M. Joy, H. Lee, H. R. Whiteley and S. Zelin, Evaluation and use of a Biotracer to study ground water contamination by leaching bed systems, *Journal of Contaminant Hydrology*, Vol. 28, pp. 227-246, 1997.

Soulsby, C., Chen, M., Ferrier, R. C., Helliwell, R. C., Jenkins, A., Harriman, R., Hydrgeochemistry of Shallow groundwater in an upland Scottish catchment, *Hydrological Processes*, Vol. 12, pp. 1111-1127, 1998.

Spielman, L. A., and Friedlander, S. K.*, Journal of Colloid Interface Science*., Vol. 46, No. 22, 1974.

Szewzyk, U., Szewzyk, R., Manz, W. and Schliefer, K. H., Microbiological safety of drinking water, *Annu. Rev. Microbiol*., Vol. 54, pp. 81-127, 2000.

Taylor, R., Cronin, A., Pedley, S., Barker, J., Atkinson, T., The implications of groundwater velocity variations on microbial transport and wellhead protection – review of field evidence, *FEMS Microbiology Ecology*, Vol. 49, pp. 17-26, 2004.

Thomas, C., D. J. Hill and M. Mabey, Evaluation of the effect of temperature and nutrients on the survival of Campylobacter spp. in water microcosms, *Journal of Applied Microbiology,* Vol. 86, pp. 1024 – 1032, 1999.

Tobiason, J. E., and O'Melia, C. R., Physicochemical Aspects of particle Removal in Depth Filtration *Jour. AWWA*, Vol. 80, No. 12, 1988.

Toze, Simon, PCR and the detection of microbial pathogens in water and wastewater, *Wat. Res*., Vol. 33, No. 17, pp. 3545-3556, 1999.

Tufenkji, N., Miller, G. F., Ryan, J. N., Harvey, R. W., Elimelech, M., Transport of *Cryptosporidium* Oocysts in Porous Media: Role of Straining and Physicochemical Filtration, *Environmental Science and Technology*, Vol. 38, No. 22, 2004.

Velazquez, M and Joellen M. Feirtag, *Helicobacter pylori*: characteristics, pathogenicity, detection methods and mode of transmission implicating foods and water, *International Journal of Food Microbiology*, Vol. 53, pp. 95-104, 1999.

Verwey, E. J. W., and Overbeek, J. Th. G., Theory of the Stability of Lyophobic Colloids, Elservier, Amsterdam, 1948.

Waage, Astrid S., Traute Vardund, Vidar Lund and Georg Kapperud, Detection of Small Numbers of Campylobacter jejuni and Campylobacter coli Cells in Environmental Water, Sewage, and Food Samples by a Seminested PCR Assay*, Applied and Environmental Microbiology*, Vol. 65, pp. 1636 – 1643, 1999.

Wang, D. S., Gerba, C. P., and Lance, J. C., Effect of soil permeability on virus removal through soil. *Applied and Environmental Microbiology*, Vol. 42, pp. 83-88, 1981.

Wassenaar, Trudy M. and Diane G. Newell, Genotyping of *Campylobacter spp*., *Applied And Environmental Microbiology,* Vol. 66, No. 1, 2000.

Woessner, W. W., Ball, P. N., DeBorde, D. C., Troy, T. L., Viral Transport in a Sand and Gravel Aquifer Under Field Pumping Conditions, *Ground Water*, Vol. 39, No. 6, 2001.

Xiqing, L., Scheibe, T. D., Johnson, W. P., Apparent Decreases in Colloid Deposition Rate Coefficients With Distance of Transport under Unfavorable Deposition Conditions: A General Phenomenon, *Environmental Science & Technology*, Vol. 38, No. 21, 2004.

Yao, K. M, Habibian, M. T., and O'Melia, C.R., Water and wastewater filtration: concepts and applications *Environmental Science & Technology*, Vol. 5, pp. 1105-1112, 1971.

You, Y., Vance, G. F., Sparks, D. L., Zhuang, J., Jin, Y., Sorption of MS2 Bacteriophage to Layered Double Hydroxides: Effects of Reaction Time, pH, and Competing Anions, *Journal of Environmental Quality*, Vol. 32, pp. 2046-2053, 2003.

Zhaung, J., Jin, Y., Virus Retention and Transport as Influenced by Different Forms of Soil Organic Matter, *Journal of Environmental Quality*, Vol. 32, pp. 812-823, 2003.

Zhou, Yumei, Jirapon Supawadee, Chantana Khamwan, Supin Tonsin, Supatra Peerakome, Bosu Kim, Kunio Kaneshi, Yuichi Ueda, Shigekazu Nakaya, Kaoru Akatani, Niwat Maneekarn, and Hiroshi Ushijima, Characterization of Human Rotavirus Serotype G9 Isolated in Japan and Thailand from 1995 to 1997, *Journal of Medical Virology*, Vol. 65, pp. 619 – 628, 2001.

Personal Communications

Philip Schmidt, University of Waterloo, 2005.

APPENDIX

A. EXPERIMENTAL DESIGN CONSIDERATIONS

Detailed Column Designs

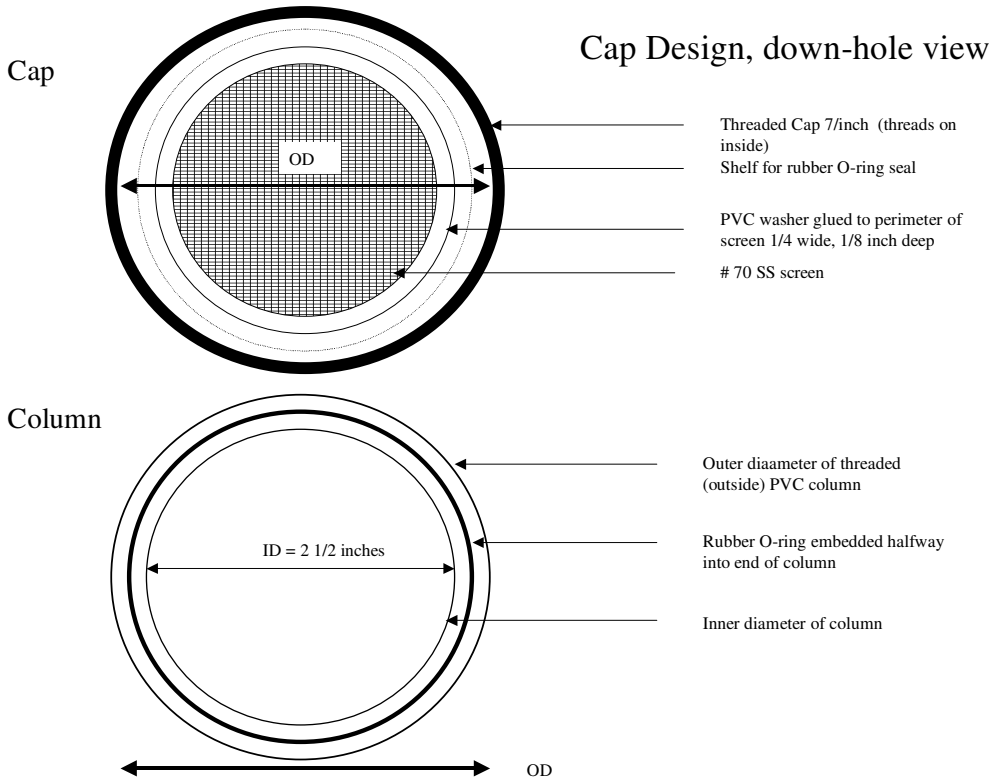

Figure A-1 - Cap Design, down-hole view

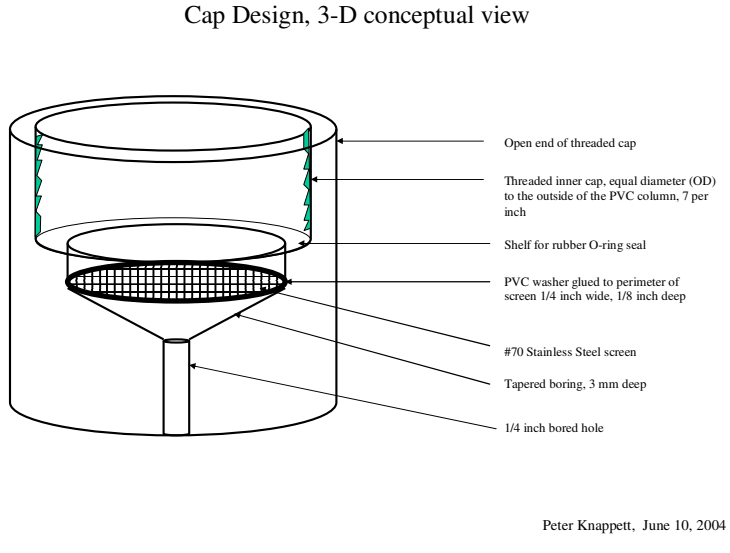

Figure A-2 - Cap Design, 3-D conceptual view

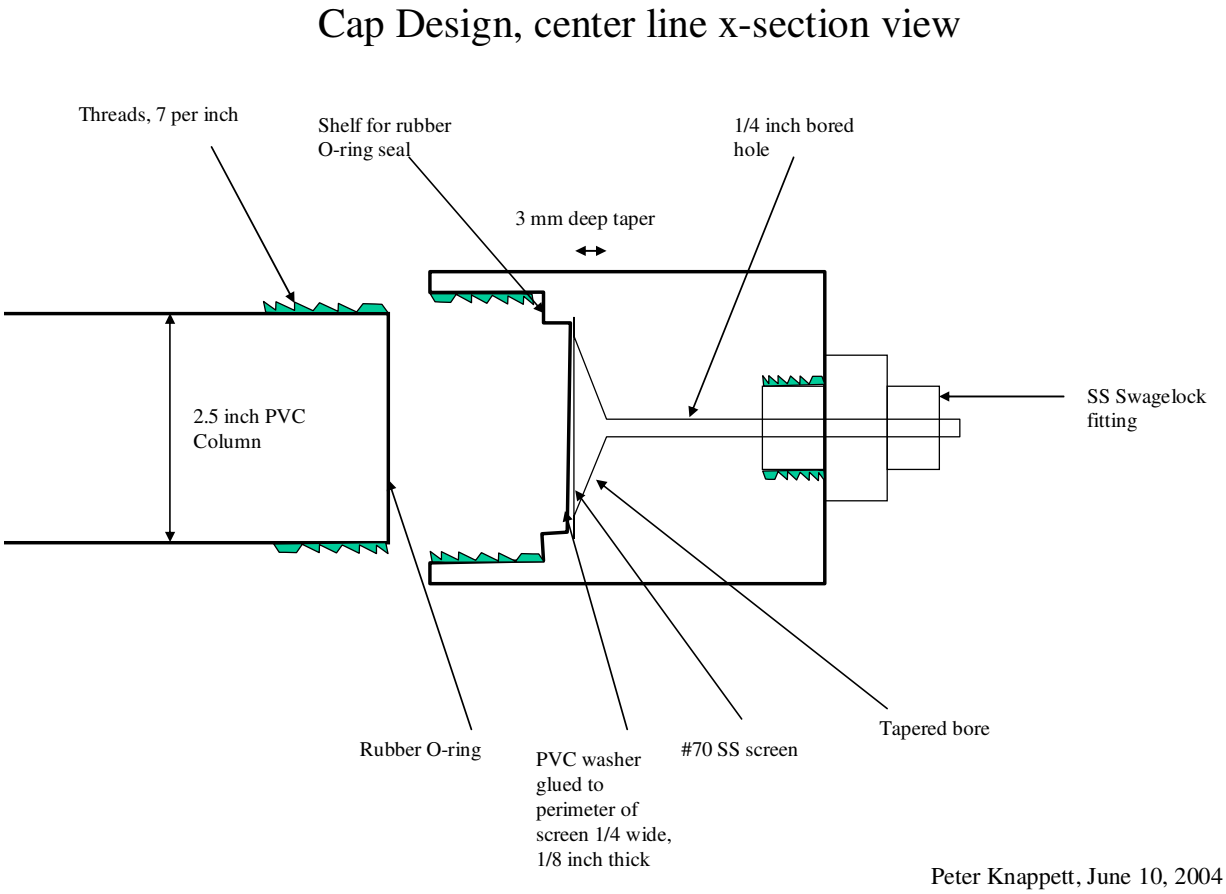

Figure A-3 - Cap Design, center line x-section view

Target Operating Conditions

Table A-1 shows the physical properties of the packed column. As well, the conductivity and pH were monitored at the influent and effluent end in order to ensure that the flushing is complete and to monitoring the ionic strength and pH of the water throughout the experiment.

Table A-1– Target Operating Conditions of Columns

Column Dimensions	
radius (cm)	3.175
length (cm)	20
volume (cm^3)	633
Grain Properties	
porosity	0.43
pore volume (cm^3)	272
Darcy Velocity (ind)	
cm/day	200
Flow Rate (dep)	
ml/hr	175

Soil Properties Measurements

Table A-2 shows the different porosity measurements made on each of the sands. Indusmin 2010 was the medium sand and Indusmin 4010 was the fine sand used for the present investigation.

Table A-2 - Porosity and Bulk Density Measurements on Silica Sands

Date	Indusmin Sand Type	V_f	Volume of water	V_{sat}	porosity	bulk density p (g/cm^3)
25-11-2004	2010	75.3	50	51.3	0.494	1.36
21-2-2005	2010 (MBE)*	79	50		0.42	1.45
21-2-2005	2010 (MBE)	79.5	50		0.41	1.50
7-6-2005	2010 (MBE)	78	50	50	0.44	1.37
7-6-2005	2010 (MBE)	77.5	50	52.5	0.45	1.42
				average (MBE)	*0.430*	*1.433*
21-2-2005	4010	78	50		0.44	1.49
7-6-2005	4010	79	50		0.42	1.51
7-6-2005	4010	79	50	53	0.42	1.53
7-6-2005	4010	78.5	50	53	0.43	
				average	*0.428*	*1.510*

* Different bag of sand than the first measurement

Table A-3 - Sieve Analysis Data for Medium Sand (Indusmin 2010)

Trial 1					
Screen #	**Aperture (mm)**	**Mass Retained by each screen (g)**	**Cumulative mass retained (g)**	**mass passing through screen (g)**	**percent of sample passing through screen**
10	2	0	0	510.5	100
20	0.85	182.08	182.08	328.42	64.3
30	0.6	199.83	381.91	128.59	25.2
40	0.425	78.53	460.44	50.06	9.8
50	0.3	39.5	499.94	10.56	2.1
60	0.25	3.53	503.47	7.03	1.4
100	0.149	5.82	509.29	1.21	0.2
pan		1.21	510.5	0	0

Trial 2					
Screen #	**Aperture (mm)**	**Mass Retained by each screen (g)**	**Cumulative mass retained (g)**	**mass passing through screen (g)**	**percent of sample passing through screen**
10	2	0	0	820.09	100.0
20	0.85	246.9	246.9	573.19	69.9
30	0.6	325.28	572.18	247.91	30.2
40	0.425	154.67	726.85	93.24	11.4
50	0.3	73.95	800.8	19.29	2.4
60	0.25	5.79	806.59	13.5	1.6
100	0.149	11.17	817.76	2.33	0.3
pan		2.33	820.09	0	0

Trial 3					
Screen #	**Aperture (mm)**	**Mass Retained by each screen (g)**	**Cumulative mass retained (g)**	**mass passing through screen (g)**	**percent of sample passing through screen**
10	2	0	0	813.85	100.0
20	0.85	246.54	246.54	567.31	69.7
30	0.6	306.89	553.43	260.42	32.0
40	0.425	151.42	704.85	109	13.4
50	0.3	84.22	789.07	24.78	3.0
60	0.25	8.19	797.26	16.59	2.0
100	0.149	13.51	810.77	3.08	0.4
pan		3.08	813.85	0	0

Table A-4 - Sieve Analysis Summary for Medium Sand

Screen #	Aperture (mm)	Average percent of sample passing through screen	Standard Deviation
10	2	100.0	0.0
20	0.85	68.0	3.2
30	0.6	29.1	3.5
40	0.425	11.5	1.8
50	0.3	2.5	0.5
60	0.25	1.7	0.3
100	0.149	0.3	0.1

Table A-5 - Sieve Analysis Data for Fine Sand (Indusmin 4010)

		Trial 1			
Screen #	Aperture (mm)	Mass Retained by each screen (g)	Cumulative mass retained (g)	mass passing through screen (g)	percent of sample passing through screen
20	0.85	0	0	277.68	100.0
30	0.6	4.52	4.52	273.16	98.4
40	0.425	64	68.52	209.16	75.3
50	0.3	115.43	183.95	93.73	33.8
60	0.25	33.77	217.72	59.96	21.6
100	0.149	50.91	268.63	9.05	3.3
140	0.103	6.6	275.23	2.45	0.9
pan		2.45	277.68	0	0.0

		Trial 2			
Screen #	Aperture (mm)	Mass Retained by each screen (g)	Cumulative mass retained (g)	mass passing through screen (g)	percent of sample passing through screen
20	0.85	0	0	727.81	100.0
30	0.6	11	11	716.81	98.5
40	0.425	169.52	180.52	547.29	75.2
50	0.3	292	472.52	255.29	35.1
60	0.25	82.48	555	172.81	23.7
100	0.149	145.83	700.83	26.98	3.7
140	0.103	19.33	720.16	7.65	1.1
pan		7.65	727.81	0	0.0

Table A-6 - Sieve Analysis Summary for Fine Sand

Screen #	Aperture (mm)	Average percent of sample passing through screen
20	0.85	100.0
30	0.6	98.4
40	0.425	75.3
50	0.3	34.4
60	0.25	22.7
100	0.149	3.5
140	0.103	1.0

B. MICROBIOLOGY

Bacteriophages

MS2 Stock suspension data are presented in Table B-1. Two stock suspensions were made December 15, 2004 and January 27, 2005.

Table B-1 – Plaque Counting Concentration Measurements on MS2 Stock Suspension

December 16, 2004

Dilution from Stock Solution	Number of Plaques per plate			Average	Standard Deviation	Concentration of MS2 Stock Solution (pfu/ml)	Standard Deviation Converted to pfu/ml
Plate #	I	II	III				
5.13E-08	9	10	10	9.7	0.6	1.88E+08	1.13E+07

January 28, 2005

Dilution from Stock Solution	Number of Plaques per plate			Average	Standard Deviation	Concentration of MS2 Stock Solution (pfu/ml)	Standard Deviation Converted to pfu/ml
Dilution\Plate #	I	II	III				
5.64E-07	607	656	190	631.5	34.6	1.12E+09	6.14E+07

This is back calculated stock concentration from reservoir measurements

February 21, 2005

Dilution from Stock Solution	Reservoir Sample Name	Number of Plaques per plate			Average	Standard Deviation	Concentration of MS2 Stock Solution (pfu/ml)	Standard Deviation Converted to pfu/ml
Dilution\Plate #		I	II	III				
6.83E-08	R H	441	386	434	420.3	29.9	6.15E+09	4.38E+08
6.83E-08	R L	172	163	176	170.3	6.7	2.49E+09	9.75E+07

March 8, 2005

Dilution from Stock Solution	Number of Plaques per plate			Average	Concentration of MS2 Stock Solution (pfu/ml)
Dilution\Plate #	I	II	III		
5.13E-08	607			607.0	1.18E+10

Bacteriophage Measurements for Column Experiments

Table B-2 – Column Effluent MS2 Data from Experiments 2 and 3

MS2 High Resolution Data - Low Concentration **Volume of Column (cm^3) =** **598**

From Start of MS2 **Plate count** **Volume of water in packed column (ml) =** **257**

Sample #	Time (hr)	Pore Volumes	I	II	III	tube #	dilution	MS2 (pfu/ml)	Standard Deviation	Normalized MS2 Conc (C/C_o)	Normalized Standard Deviation (SD/C_o)	# MS2 Released in Effluent
3	2	1	0		0	0	1.0E+00	1.0E+00	0.0E+00	4.9E-05	0.0E+00	5.05E+01
5	3	1	0	0	0	0	1.0E+00	1.0E+00	0.0E+00	4.9E-05	0.0E+00	6.11E+01
6	3	1	0	0	0	1	9.1E-02	1.0E+00	0.0E+00	4.9E-05	0.0E+00	1.99E+05
8	4	2		137	190	1	9.1E-02	1.8E+03	4.1E+02	8.7E-02	2.0E-02	1.04E+05
9	5	2	160	133	137	1	9.1E-02	1.6E+03	1.6E+02	7.6E-02	7.8E-03	1.45E+06
10	7	6	160	147	177	1	9.1E-02	1.8E+03	1.7E+02	8.6E-02	8.0E-03	1.74E+06
11	10	13	184	152	166	0	1.0E+00	1.7E+02	1.6E+01	8.1E-03	7.8E-04	1.14E+05
13	21	15	163	162	190	0	1.0E+00	1.7E+02	1.6E+01	8.3E-03	7.7E-04	3.65E+05
15	27	23	168	194	188	0	1.0E+00	1.8E+02	1.4E+01	8.9E-03	6.6E-04	
										Total in Effluent		3.98E+06
Influent		0	172	163	176	2	8.3E-03	2.1E+04	8.1E+02	**Total in Influent**		1.1E+07
										Percent Recovery		**37.1**

MS2 High Resolution Data - High Concentration

From Start of MS2 **Plate count**

Sample #	Time (hr)	Pore Volumes	I	II	III	tube #	dilution	MS2 (pfu/ml)	Standard Deviation	Normalized MS2 Conc (C/C_o)	Normalized Standard Deviation (SD/C_o)	# MS2 Released in Effluent
4	2	1	206	166	169	0	1.0E+00	1.8E+02	2.2E+01	2.9E-05	3.6E-06	8.73E+03
6	3	1	192	109	195	0	1.0E+00	1.7E+02	4.9E+01	2.7E-05	7.9E-06	5.72E+04
7	3	1	162	142	162	1	9.1E-02	1.7E+03	1.3E+02	2.8E-04	2.1E-05	2.88E+08
8	4	2	152	144	235	4	6.8E-05	2.6E+06	7.4E+05	4.2E-01	1.2E-01	2.96E+08
9	5	2	558	404	417	4	6.8E-05	6.7E+06	1.3E+06	1.1E+00	2.0E-01	3.83E+09
10	7	6	141	126	150	4	6.8E-05	2.0E+06	1.8E+05	3.3E-01	2.9E-02	2.05E+09
11	10	13	140	127	156	3	7.5E-04	1.9E+05	1.9E+04	3.0E-02	3.1E-03	6.59E+06
12	11	13	157	162	122	2	8.3E-03	1.8E+04	2.6E+03	2.9E-03	4.3E-04	5.57E+06
13	21	16	169	103	160	0	1.0E+00	1.4E+02	3.6E+01	2.3E-05	5.8E-06	2.43E+05
14	25	22	160	121	172	0	1.0E+00	1.5E+02	2.7E+01	2.5E-05	4.3E-06	8.04E+04
15	27	24	217	170	157	0	1.0E+00	1.8E+02	3.2E+01	2.9E-05	5.1E-06	3.04E+05
16	34	31	197	134	152	0	1.0E+00	1.6E+02	3.2E+01	2.6E-05	5.3E-06	
										Total in Effluent		6.48E+09
Influent		0	441	386	434	4	6.8E-05	6.2E+06	4.4E+05	**Total in Influent**		3.2E+09
Influent*			421			4	6.8E-05	6.2E+06		**Percent Recovery**		**204.8**

* mixing host with MS2 in dilution solution as aposed to in the top agar tube

Table B-3 – Column Effluent MS2 Data from Experiments 4 & 5, Low [MS2]

MS2 High Resolution Data - Low Concentration				Volume of Column (ml) =				598
From Start		Plate count		Volume of water in packed column (ml) =				245
Sample #	**Pore Volumes**	**I**	**II**	**dilution**	**MS2 (pfu/ml)**	**MS2 averaged by sample # (pfu/ml)**	**Normalized MS2 (C/C_o)**	**# MS2 Released in Effluent**
4	0.7							
5	1.2	90	48	1.0E+00	6.9E+01			
6	1.6	237	199	1.0E-02	2.2E+04			
6	1.6	24	27	1.0E-03	2.6E+04	2.4E+04	2.1E-01	2.5E+06
7	1.9	4	13	1.0E-04	8.5E+04			
7	1.9	81	60	1.0E-03	7.1E+04			
7	1.9	12	8	1.0E-04	1.0E+05	8.5E+04	7.7E-01	5.1E+06
9	3.0	21		1.0E-04	2.1E+05			
9	3.0	1	3	1.0E-05	2.0E+05			
9	3.0	200	171	1.0E-03	1.9E+05			
9	3.0	17	19	1.0E-04	1.8E+05			
9	3.0	2	3	1.0E-05	2.5E+05	2.1E+05	1.9E+00	4.0E+07
10	3.3	8	7	1.0E-04	7.5E+04			
10	3.3	0	0	1.0E-05	0.0E+00			
10	3.3	92	107	1.0E-03	1.0E+05			
10	3.3	9	6	1.0E-04	7.5E+04	6.2E+04	5.7E-01	1.2E+07
11	4.6	0	1	1.0E-04	5.0E+03			
11	4.6	95	104	1.0E-01	1.0E+03			
11	4.6	22	12	1.0E-02	1.7E+03			
11	4.6	1	2	1.0E-03	1.5E+03	2.3E+03	2.1E-02	1.1E+07
12	6.2	0	0	1.0E-04	0.0E+00			
12	6.2	0	0	1.0E-05	0.0E+00			
12	6.2	217	110	1.0E+00	1.6E+02			
12	6.2	18	14	1.0E-01	1.6E+02			
12	6.2	3	0	1.0E-02	1.5E+02	1.6E+02	1.4E-03	5.0E+05
13	8.3	8	15	1.0E+00	1.2E+01			
13	8.3	1	0	1.0E-01	5.0E+00			
13	8.3	0	0	1.0E-02	1.0E+00	5.8E+00	5.3E-05	4.4E+04
14	10.1	2	3	1.0E+00	2.5E+00			
14	10.1	0	0	1.0E-01	1.0E+00	1.8E+00	1.6E-05	
15	14.2	0	0	1.0E+00	1.0E+00	1.5E+00	1.4E-05	
16	16.6	0	0	1.0E+00	1.0E+00	1.0E+00	9.1E-06	
18	29.4	3	1	1.0E+00	2.0E+00			
18	29.4	1	0	1.0E+00	5.0E-01	1.3E+00	1.1E-05	
Influent 1		86	95	1.0E-03	9.1E+04	**Total MS2 in Effluent**		7.08E+07
Influent 1 (trial 2)		117	110	1.0E-03	1.1E+05	**Total MS2 in Influent**		5.7E+07
Influent 2		121	132	1.0E-03	1.3E+05	**Percent MS2 Recovery**		**125.0**
			Average		**1.1E+05**			
			Standard Deviation		**1.8E+04**			

Table B-4 – Column Effluent MS2 Data from Experiments 4 & 5, High [MS2]

MS2 High Resolution Data - High Concentration				Volume of Column (ml) =				598
From Start		Plate count		Volume of water in packed column (ml) =				245
Sample #	**Pore Volumes**	**I**	**II**	**dilution**	**MS2 (pfu/ml)**	**MS2 averaged by sample # (pfu/ml)**	**Normalized MS2 (C/C_o)**	**# MS2 Released in Effluent**
4	0.7							
5	1.1	18	25	1.00E-04	2.2E+05	2.2E+05	7.5E-02	1.1E+07
6	1.5	155	144	1.0E-04	1.5E+06	1.5E+06	5.2E-01	8.7E+07
8	2.4	361	419	1.0E-04	3.9E+06	3.9E+06	1.4E+00	6.3E+08
10	3.3	564	610	1.0E-03	5.9E+05	5.9E+05	2.1E-01	5.1E+08
11	4.6	120	136	1.0E-02	1.3E+04			
11	4.6	15	21	1.0E-03	1.8E+04	1.5E+04	6.3E-03	1.0E+08
12	6.2	333	352	0.1	3.4E+03			
12	6.2	175	168	1.0E-01	1.7E+03			
12	6.2	20	17	1.0E-02	1.9E+03	2.3E+03	6.5E-04	3.6E+06
13	8.3	624	660	1	6.4E+02			
13	8.3	123	106	0.1	1.1E+03			
13	8.3	51	34	1.0E-01	4.3E+02			
13	8.3	5	2	1.0E-02	3.5E+02	6.4E+02	1.2E-04	
14	10.1	335	300	1	3.2E+02	3.2E+02	1.1E-04	1.3E+06
15	14.2	0		1	1.0E+00			
15	14.2	1	0	1.0E+00	5.0E-01	7.5E-01	1.8E-07	
16	16.6	0	0	1	1.0E+00	1.0E+00	3.5E-07	
18	29.4	1		1	1.0E+00			
18	29.4	1	1	1.0E+00	1.0E+00	1.0E+00	3.5E-07	
						Total MS2 in Effluent		1.35E+09
Influent 1		236	303	1.0E-04	2.7E+06	**Total MS2 in Influent**		1.5E+09
		23	25	1.0E-05	2.4E+06	**Percent MS2 Recovery**		**92.0**
Influent 1 (trial 2)		269	311	1.0E-04	2.9E+06			
		38	30	1.0E-05	3.4E+06			
			Average		**2.8E+06**			
			Standard Deviation		**4.2E+05**			

Table B-5 – Column Effluent MS2 Data from Experiments 6 & 7, Low [MS2] Column

MS2 High Resolution Data - Low Concentration				**Volume of Column (ml) =**			**598**
From Start		**Plate count**		**Volume of water in packed column (ml) =**			***245***
Sample #	**Pore Volumes**	**I**	**II**	**dilution**	**MS2 (pfu/ml)**	**Normalized MS2 (C/C_o)**	**# MS2 Released in Effluent**
3	0.7	0	0	1.E-01			
4	1.1	0	0	1.E+00			
5	1.7	0	0	1.E-01			
5 (trial 2)	1.7	0	0	1.E+00			
6	2.0	0	0	1.E+00			
7	2.5	0	0	1.E-01			
7	2.5	1	0	1.E-03			
7 (trial 2)	2.5	0	0	1.E+00			
8	2.9	0	0	1.E+00			
9	3.3	0	0	1.E-02			
9 (trial 2)	3.3	0	0	1.E+00			
11	4.7	0	0	1.E+00			
14	8.1	0	0	1.E+00			
16	11.6	0	0	1.E+00			
19	29.5	0	0	1.E+00			
Influent	0.1	11	17	1.E-04	**1.4E+05**		
					Total MS2 in Effluent		0.00E+00
					Total MS2 in Influent		0.0E+00
					Percent MS2 Recovery		

Table B-6 – Column Effluent MS2 Data from Experiments 6 & 7, High [MS2] Column

MS2 High Resolution Data - High Concentration				Volume of Column (ml) =			598
From Start		Plate count		volume of water in packed column (ml) =			245
Sample #	**Pore Volumes**	**I**	**II**	**dilution**	**MS2 (pfu/ml)**	**Normalized MS2 (C/C_o)**	**# MS2 Released in Effluent**
3	0.7	25	33	1.0E+00	2.9E+01	1.2E-07	3.1E+04
4	1.1	60	74	1.0E-01	6.7E+02	2.8E-06	2.1E+06
5	1.7	274	213	1.0E-02	2.4E+04	1.0E-04	3.3E+06
6	2.0	66	76	1.0E-03	7.1E+04	3.0E-04	1.8E+07
7	2.5	200	231	1.0E-03	2.2E+05	9.0E-04	1.1E+07
8	2.9	14	11	1.0E-02	1.3E+03	5.2E-06	7.4E+04
9	3.3	7	16	1.0E-01	1.2E+02	4.8E-07	1.1E+04
10	3.9	14	47	1.0E+00	3.1E+01	1.3E-07	4.3E+03
11	4.7	13	10	1.0E+00	1.2E+01	4.8E-08	2.6E+03
12	5.4	20	12	1.0E+00	1.6E+01	6.7E-08	3.4E+03
13	6.0	26	39	1.0E+00	3.3E+01	1.4E-07	1.2E+04
14	8.2	7	9	1.0E+00	8.0E+00	3.3E-08	5.3E+03
16	11.8	5	2	1.0E+00	3.5E+00	1.5E-08	
17	16.9	1	0	1.0E-01	5.0E+00	2.1E-08	
18	21.3	7	7	1.0E+00	7.0E+00	2.9E-08	
19	29.7	1	0	1.0E-01	5.0E+00	2.1E-08	
20	34.0	1	3	1.0E-01	2.0E+01	8.3E-08	
20 (trial 2)	34.0	11	0	1.0E+00	5.5E+00	2.3E-08	
Influent 1		270	410	1.0E-06	3.4E+08		
Influent 1 (trial 2)		26	14	1.0E-07	2.0E+08		
Influent 3		18	18	1.0E-07	1.8E+08		
			Average		**2.4E+08**		
			Standard Deviation		**8.7E+07**		
					Total MS2 in Effluent		3.44E+07
					Total MS2 in Influent		1.7E+11
					Percent MS2 Recovery		**0.020**

Table B-7 – Column Effluent MS2 Data from Experiments 8 & 9, Column A

MS2 High Resolution Data - A				Volume of Column (ml) =			598
	From Start	Plate count		Volume of water in packed column (ml) =			245
Sample #	Pore Volumes	I	II	dilution	MS2 (pfu/ml)	Normalized MS2 (C/C_o)	# MS2 Released in Effluent
1	0.2						
2	0.3						
3	0.5	2	3	1.E-01	2.5E+01		
3 (trial 2)	0.5	5	2	1.E+00	3.5E+00	1.2E-07	
4	0.9	128	104	1.E-01	1.2E+03	1.0E-05	7.0E+04
5	1.4	689	801	1.E-01	7.5E+03		5.3E+05
5	1.4	8	6	1.E-03	7.0E+03		
5 (trial 2)	1.4	240	242	1.E-01	2.4E+03		
5 (trial 2)	1.4	21	25	1.E-02	2.3E+03	4.2E-05	2.1E+05
6	1.9						
7	2.3	598	415	1.E-02	5.1E+04		
7	2.3	4	3	1.E-04	3.5E+04		
7 (trial 2)	2.3	120	132	1.E-02	1.3E+04		
7 (trial 2)	2.3	9	11	1.E-03	1.0E+04	2.4E-04	1.3E+06
9	3.2	2	2	1.E-01	2.0E+01	1.7E-07	
10	3.7	0	2	1.E+00	1.0E+00	8.7E-09	1.5E+03
11	4.2						
12	5.9						
13	7.7	1	5	1.E+00	3.0E+00	2.6E-08	
14	10.5	0	2	1.E-01	1.0E+01	8.7E-08	
14	10.5	1	1	1.E+00	1.0E+00	8.7E-09	0.0E+00
15	12.7	15	6	1.E+00	1.1E+01	9.1E-08	3.1E+03
15 (trial 2)	12.7	1	2	1.E+00	1.5E+00	1.3E-08	
16	15.2						
17	15.2	3	1	1.E+00	2.0E+00	1.7E-08	
18	16.4	12	11	1.E+00	1.2E+01	1.0E-07	2.0E+03
19	17.3	18	10	1.E+00	1.4E+01	1.2E-07	2.9E+03
20	18.6	18	3	1.E+00	1.1E+01	9.1E-08	4.2E+03
21	19.2	2	2	1.E+00	2.0E+00	1.7E-08	9.7E+02
22	19.8	11	18	1.E+00	1.5E+01	1.3E-07	1.3E+03
Influent 1		13	10	1.E-07	1.2E+08		
Influent 1 (trial 2)		51	59	1.E-06	5.5E+07		
		5	10	1.E-07	7.5E+07		
					Total MS2 in Effluent		2.16E+06
					Total MS2 in Influent		2.8E+10
					Percent MS2 Recovery		**0.008**
							99.9924

Table B-8 – Column Effluent MS2 Data from Experiments 8 & 9, Column B

MS2 High Resolution Data - B				Volume of Column (ml) =			598
	From Start	Plate count		Volume of water in packed column (ml) =			245
Sample #	**Pore Volumes**	**I**	**II**	**dilution**	**MS2 (pfu/ml)**	**Normalized MS2 (C/C_o)**	**# MS2 Released in Effluent**
3	0.47	0	0	1.0E+00			
4	0.94	0	1	1.0E-01			
5	1.42	0	0	1.0E-01			
5	1.42	0	0	1.0E-02			
7	2.28	0	0	1.0E-02			
7	2.28	0	0	1.0E-03			
8	2.74	0	0	1.0E-01			
8	2.74	0	0	1.0E-02			
9	3.17	0	0	1.0E-01			
10	3.73	0	0	1.0E+00			
12	5.96	2	0	1.0E+00			
13	7.81	0	0	1.0E+00			
14	10.79	0	2	1.0E+00			
15	12.85	0	0	1.0E+00			
16	15.29	0	0	1.0E+00			
17	15.35	0	0	1.0E+00			
18	16.50	0	0	1.0E+00			
19	17.40	0	0	1.0E+00			
20	18.74	0	0	1.0E+00			
Influent 1		68	58	1.0E-06	6.3E+07		
					Total MS2 in Effluent		0.00E+00
					Total MS2 in Influent		2.9E+11
					Percent MS2 Recovery		**0.0**

Table B-9 – Column Effluent MS2 Data from Experiments 10 & 11, Column A

MS2 High Resolution Data - A				Volume of Column (ml) =			598
From Start		Plate count		Volume of water in packed column (ml) =			245
Sample #	**Pore Volumes**	**I**	**II**	**dilution**	**MS2 (pfu/ml)**	**Normalized MS2 (C/C_o)**	**# MS2 Released in Effluent**
3	0.9	0	0	1.E-01	0.0E+00	0.0E+00	
4	1.2	5	3	1.E+00	4.0E+00	1.1E-07	1.8E+02
5	1.8	13	8	1.E-01	1.1E+02	2.8E-06	7.6E+03
6	2.3	55	68	1.E-01	6.2E+02	1.6E-05	4.9E+04
7	2.8	71	98	1.E-01	8.5E+02	2.2E-05	8.4E+04
8	3.2	72	84	1.E-01	7.8E+02	2.1E-05	8.4E+04
9	3.8	154	191	1.E+00	1.7E+02	4.5E-06	8.2E+04
9	3.8	5	25	1.E-01	1.5E+02	4.0E-06	
10	4.7	57	112	1.E+00	8.5E+01	2.2E-06	2.5E+04
11	6.1	4	10	1.E+00	7.0E+00	1.8E-07	1.7E+04
11	6.1	2	2	1.E-01	2.0E+01	5.3E-07	
12	6.2	0	0	1.E+00	0.0E+00	0.0E+00	
13	7.6	0	0	1.E+00	0.0E+00	0.0E+00	
17	12.1	0	0	1.E+00	0.0E+00	0.0E+00	
20	18.4	0	0	1.E+00	0.0E+00	0.0E+00	
Influent 1	0.1	301	458	1.E-05	**3.8E+07**		
		9	6	1.E-07	**7.5E+07**		
					Total MS2 in Effluent		**3.48E+05**
					Total MS2 in Influent		**2.6E+10**
					Percent MS2 Recovery		**0.0013**

Table B-10 – Column Effluent MS2 Data from Experiments 10 & 11, Column B

MS2 High Resolution Data - B				Volume of Column (ml) =			598
From Start		Plate count		Volume of water in packed column (ml) =			245
Sample #	**Pore Volumes**	**I**	**II**	**dilution**	**MS2 (pfu/ml)**	**Normalized MS2 (C/C_o)**	**# MS2 Released in Effluent**
3	0.9	0	0	1.0E-01	0.0E+00	0.00E+00	
4	1.3	3	2	1.0E+00	2.5E+00	4.28E-08	1.2E+02
5	1.9	20	25	1.0E-01	2.3E+02	3.85E-06	1.6E+04
6	2.2	82	60	1.0E-01	7.1E+02	1.22E-05	4.7E+04
7	2.7	74	96	1.0E-01	8.5E+02	1.46E-05	9.4E+04
8	3.1	125	169	1.0E-01	1.5E+03	2.52E-05	1.2E+05
9	3.8	144		1.0E+00	1.4E+02	2.47E-06	
9	3.8	13	28	1.0E-01	2.1E+02	3.51E-06	1.5E+05
10	4.7	53	31	1.0E+00	4.2E+01	7.19E-07	2.8E+04
11	6.2	9	11	1.0E+00	1.0E+01	1.71E-07	1.0E+04
11	6.2	0	1	1.0E-01	5.0E+00	8.56E-08	
12	6.3	0	0	1.0E+00	0.0E+00	0.00E+00	
13	7.8	1	0	1.0E+00	5.0E-01	8.56E-09	
17	12.5	0	0	1.0E+00	0.0E+00	0.00E+00	
20	19.1	0	0	1.0E+00	0.0E+00	0.00E+00	
Influent 1	525	545	623	1.0E-05	**5.8E+07**		
		6	3	1.0E-07	**4.5E+07**		
					Total MS2 in Effluent		4.67E+05
					Total MS2 in Influent		3.5E+10
					Percent MS2 Recovery		**0.0014**

Table B-11 – Column Influent MS2 Data from Experiments 12 & 13

MS2 Data - Column A				Volume of Column (ml) =		598
	From Start	Plate count		Water in column (ml) =		245
Sample #	Pore Volumes	I	II	dilution	MS2 (pfu/ml)	
3	NA*	0	0	1.E+00	ND	
3	NA	0	0	1.E-01	ND	
5	NA	0	0	1.E+00	ND	
5	NA	0	0	1.E-01	ND	
7	NA	0	0	1.E+00	ND	
7	NA	0	0	1.E-01	ND	
9	NA	0	0	1.E+00	ND	
9	NA	0	0	1.E-01	ND	
10	NA	0	0	1.E+00	ND	
11	NA	0	0	1.E+00	ND	
13	NA	0	0	1.E+00	ND	
16	NA	0	0	1.E+00	ND	
19	NA	0	0	1.E+00	ND	
21	NA	0	0	1.E+00	ND	
23	NA	0	0	1.E+00	ND	
Influent 1		224	232	1.E-05	**2.3E+07**	
		42	35	1.E-06	**3.9E+07**	
				Total MS2 in Influent		**1.6E+10**

* Not Applicable

MS2 Data - Column B				Volume of Column (ml) =		598
	From Start	Plate count		Water in column (ml) =		245
Sample #	Pore Volumes	I	II	dilution	MS2 (pfu/ml)	
3	NA	1	0	1.E+00	ND	
3	NA	0	0	1.E-01	ND	
5	NA	2	1	1.E+00	ND	
5	NA	0	0	1.E-01	ND	
7	NA	1	1	1.E+00	ND	
7	NA	0	0	1.E-01	ND	
9	NA	0	0	1.E+00	ND	
9	NA	0	1	1.E-01	ND	
10	NA	0	0	1.E+00	ND	
11	NA	0	0	1.E+00	ND	
13	NA	0	0	1.E+00	ND	
16	NA	0	0	1.E+00	ND	
19	NA	0	0	1.E+00	ND	
21	NA	0	0	1.E+00	ND	
23	NA	0	0	1.E+00	ND	
Inflent 1		469	440	1.E-05	**4.5E+07**	
		44	48	1.E-06	**4.6E+07**	
				Total MS2 in Influent		**3.2E+10**

Table B-12 – Column Influent MS2 Data from Experiments 14 & 15

MS2 Data - Column A				Volume of Column (ml) =		598
	From Start	Plate count		Water in column (ml) =		245
Sample #	Pore Volumes	I	II	dilution	MS2 (pfu/ml)	
3	NA	0	0	1.E+00	ND	
5	NA	0	1	1.E-01	ND	
5	NA	0	0	1.E-03	ND	
8	NA	0	0	1.E-01	ND	
8	NA	0	0	1.E-03	ND	
11	NA	0	0	1.E-01	ND	
15	NA	0	0	1.E+00	ND	
19	NA	0	0	1.E+00	ND	
	(extra plate)					
Influent 1	40	30	37	1.E-04	**3.6E+05**	
		1	0	1.E-06	**5.0E+05**	
				Total MS2 in Influent		**2.5E+08**

MS2 Data - Column B				Volume of Column (ml) =		598
	From Start	Plate count		Water in column (ml) =		245
Sample #	Pore Volumes	I	II	dilution	MS2 (pfu/ml)	
3	NA	0	0	1.E+00	ND	
5	NA	0	0	1.E-01	ND	
5	NA	0	0	1.E-03	ND	
8	NA	0	0	1.E-01	ND	
8	NA	0	0	1.E-03	ND	
11	NA	0	0	1.E-01	ND	
15	NA	0	0	1.E+00	ND	
19	NA	0	0	1.E+00	ND	
Inflent 1		49	48	1.E-05	**4.9E+06**	
				Total MS2 in Influent		**3.4E+09**

Table B-13 – Saline Controls for Bacteria Contamination

Detection Round	Date	Number of Colonies	Notes
Stock	18.10.2004	23	
Stock	21.10.2004	ND	NBp
Stock	23.10.2004	20	
Stock	28.10.2005	40	
Experiment 1	2.12.2004	ND	
Experiments 4 & 5	7.4.2005	ND	
Experiments 4 & 5	7.4.2005	ND	

* No bacteriophages were detected in this round of analyses

Table B-14 – Bacteriophage Controls

Detection Round	Date	Number of Plaques	Notes
Stock	28.10.2004	ND	
Stock	18.11.2004	ND	
Experiment 1 (Prototype Run)	1.12.2004	ND	
Stock	28.1.2005	ND	
Experiments 2 & 3	24.2.2005	ND	NBp
Experiments 4 & 5	28.3.2005	ND	
Experiments 4 & 5	28.3.2005	ND	NBp
Experiments 4 & 5	5.4.2005	ND	NBp
Experiments 4 & 5	11.4.2005	ND	
Experiments 4 & 5	11.4.2005	ND	
Experiments 4 & 5	21.4.2005	ND	NB
Experiments 4 & 5	22.4.2005	1	
Experiments 6 & 7	19.5.2005	ND	
Experiments 8 & 9	19.5.2005	ND	
Experiments 6 & 7	20.5.2005	ND	
Experiments 8 & 9	2.6.2005	ND	
Experiments 10 & 11, 12 & 13	7.6.2005	ND	
Experiments 14 & 15	14.6.2005	ND	

** No bacterial lawns were grown in this round of analyses

Microsphere Measurements for Column Experiments

The measured concentrations in the effluent and reservoir samples were presented similar to MS2 and calculations on total microspheres released and in the influent were also identical to those used for MS2. Unlike MS2 duplicate analyses were not performed because the entire effluent volume sample was frequently consumed in one analysis.

Table B-15 – Column Effluent Microsphere Data from Column Experiments 4 & 5

Low MS2 Column				**Volume of Column (ml) = Microspheres**		**598**
Sample #	**Cumulative Pore Vol**	**Volume (ml)**	**Count**	**Concentration (msp/ml)**	**Normalised (C/C_o)**	**# released in effluent**
4	0.7	12.1	163	13	0.01	
6	1.5	0.1	199	1990	1.61	2.1E+05
8	2.4	1	87	87	0.07	2.4E+05
10	3.3	5	111	22	0.02	1.2E+04
13	8.3	9.9	154	16	0.01	2.4E+04
17	21.3	12.2	35	3	0.00	3.1E+04
Influent 1		0.1	23	230		
Influent 1 (trial 2)		1	1235	**1235**		
				Total Microspheres in Effluent		**5.2E+05**
				Total Microspheres in Influent		**6.4E+05**
				Percent Recovery		**18.4**

High MS2 Column				**Volume of Column (ml) = Microspheres**		**598**
Sample #	**Cumulative Pore Vol**	**Volume (ml)**	**Count**	**Concentration (msp/ml)**	**Normalised (C/C_o)**	**# released in effluent**
3	0.4	12	ND	0		
4	0.7	12.6	398	32	0.07	1.2E+03
5	1.2	1	71	71	0.15	5.5E+03
6	1.6	7.8	TM*			
7	1.9	0.1	62	620	1.29	6.8E+04
8	2.5	12.8	6000	469	0.97	7.5E+04
9	3.0	8.8	TM			
10	3.3	13.2	286	22	0.04	5.6E+04
11	4.6	11.8	53	4	0.01	4.3E+03
14	10.1	6	43	7	0.01	8.2E+03
17	21.3	11.6	38	3	0.01	1.5E+04
Influent 1		0.05	2	40		
Influent 1 (trial 2)		1	482	**482**		
Influent 3		12.2	TM			
				Total Microspheres in Effluent		**2.3E+05**
* Too Many				**Total Microspheres in Influent**		**2.5E+05**
				Percent Recovery		**5.9**

Table B-16 - Column Effluent Microsphere Data from Column Experiments 6 & 7

Low MS2 Column				Volume of Column (ml) = Microspheres		598
Sample #	**Cumulative Pore Vol**	**Volume (ml)**	**Count**	**Concentration (msp/ml)**	**Normalised (C/C_o)**	**# released in effluent**
3	0.73	not taken		0		
4	1.08	10	4174	417	0.71	1.9E+04
5	1.72	1	180	180	0.30	4.9E+04
6	1.98	1	141	141	0.24	1.1E+04
7	2.47	1	131	131	0.22	1.7E+04
8	2.88	1	6	6	0.01	7.3E+03
9	3.30	1	ND	0	0.00	
10	3.87	1	ND	0	0.00	
Influent		1	592	**592**	1.00	
				Total Microspheres in Effluent		**1.0E+05**
				Total Microspheres in Influent		**3.0E+05**
				Percent Recovery		**33.8**

High MS2 Column				Volume of Column (ml) = Microspheres		598
Sample #	**Cumulative Pore Vol**	**Volume (ml)**	**Count**	**Concentration (msp/ml)**	**Normalised (C/C_o)**	**# released in effluent**
3	0.73	not taken		0		
4	1.08	10	2076	208	1.98	9238
5	1.74	1	154	154	1.47	30553
6	2.00	1	215	215	2.05	12739
7	2.48	1	106	106	1.01	19635
8	2.89	1	8	8	0.08	5977
9	3.31	1	ND	0	0.00	
10	3.87	1	ND	0	0.00	
Influent		1	105	**105**	1.00	
				Total Microspheres in Effluent		**7.8E+04**
				Total Microspheres in Influent		**1.3E+05**
				Percent Recovery		**62.2**

Table B-17 – Column Effluent Microsphere Data from Column Experiments 8 & 9

Column A				Volume of Column (ml) =	Microspheres	598
Sample #	**Cumulative Pore Vol**	**Volume (ml)**	**Count**	**Concentration (msp/ml)**	**Normalised (C/C_o)**	**# released in effluent**
3	0.47	5	386	77	0.03	
4	0.94	2	962	481	0.21	3.4E+04
5	1.42	1	875	875	0.38	8.4E+04
6	1.86	1	468	468	0.20	7.5E+04
7	2.27	1	741	741	0.32	6.3E+04
8	2.73	1	108	108	0.05	5.1E+04
9	3.16	2	27	14	0.01	6.7E+03
10	3.72	10	5	1	0.00	
Influent		0	231	**2310**		
				Total Microspheres in Effluent		**3.1E+05**
				Total Microspheres in Influent		**1.2E+06**
				Percent Recovery		**26.4**

Column B				Volume of Column (ml) =	Microspheres	598
Sample #	**Cumulative Pore Vol**	**Volume (ml)**	**Count**	**Concentration (msp/ml)**	**Normalised (C/C_o)**	**# released in effluent**
3	0.47	5	0	0	0.00	
4	0.94	2	846	423	0.24	2.5E+04
5	1.42	1	61	61	0.03	3.0E+04
7	2.27	1	221	221	0.13	3.1E+04
9	3.16	10	36	4	0.00	2.6E+04
Influent		0	175	**1750**		
				Total Microspheres in Effluent		**1.1E+05**
				Total Microspheres in Influent		**9.0E+05**
				Percent Recovery		**12.4**

Table B-18 – Column Effluent Microsphere Data from Column Experiments 10 & 11

				Volume of Column (ml) =		598
Column A					**Microspheres**	
Sample #	**Cumulative Pore Vol**	**Volume (ml)**	**Count**	**Concentration (msp/ml)**	**Normalised (C/C_o)**	**# released in effluent**
5	1.79	10	ND	0		
6	2.32	10	ND	0		
7	2.76	10	ND	0		
8	3.16	10	ND	0		
9	3.83	10	ND	0		
10	4.66	10	ND	0		
Influent				**733**	1.00	
				Total Microspheres in Effluent		**0.0E+00**
				Total Microspheres in Influent		**5.1E+05**
				Percent Recovery		**0.0**

				Volume of Column (ml) =		598
Column B					**Microspheres**	
Sample #	**Cumulative Pore Vol**	**Volume**	**Count**	**Concentration (ms/ml)**	**Normalised (C/C_o)**	**# released in effluent**
5	1.86	10	2	0		
6	2.25	10	ND	0		
7	2.72	10	ND	0		
8	3.14	10	ND	0		
9	3.82	10	1	0		
10	4.69	10	1	0		
Influent				**256**	1.00	
				Total Microspheres in Effluent		**0.0E+00**
				Total Microspheres in Influent		**1.5E+05**
				Percent Recovery		**0.0**

Table B-19 – Column Effluent Microsphere Data from Column Experiments 12 & 13

				Volume of Column (ml) =		598
Column A					**Microspheres**	
Sample #	**Cumulative Pore Vol**	**Volume (ml)**	**Count**	**Concentration (msp/ml)**	**Normalised (C/C_o)**	**# released in effluent**
4	1.18	10	ND	0		
6	1.90	10	1	0		
Influent			310	**3100**		
				Total Microspheres in Effluent		**0.0E+00**
				Total Microspheres in Influent		**1.8E+06**
				Percent Recovery		**0.0**

				Volume of Column (ml) =		598
Column B					**Microspheres**	
Sample #	**Cumulative Pore Vol**	**Volume**	**Count**	**Concentration (ms/ml)**	**Normalised (C/C_o)**	**# released in effluent**
4	1.11	10	ND	0		
6	1.98	10	2	0		
Influent			405	**4050**		
				Total Microspheres in Effluent		**0.0E+00**
				Total Microspheres in Influent		**2.5E+06**
				Percent Recovery		**0.0**

Table B-20 – Column Effluent Microsphere Data from Column Experiments 14 & 15

				Volume of Column (ml) =		598
Column A					**Microspheres**	
Sample #	**Cumulative Pore Vol**	**Volume (ml)**	**Count**	**Concentration (msp/ml)**	**Normalised (C/C_o)**	**# released in effluent**
2	0.56	10	199	20	0.00	
3	0.92	2	1399	700	0.04	3.3E+04
4	1.11	1	1793	1793	0.11	6.1E+04
5	1.39	1	1046	1046	0.07	1.0E+05
6	1.59	1	1802	1802	0.11	7.6E+04
7	2.07	1	960	960	0.06	1.7E+05
8	2.54	1	518	518	0.03	8.9E+04
9	2.75	1	830	830	0.05	3.6E+04
11	3.71	10	31	3	0.00	1.0E+05
Influent			1609	**15725**	1.00	
Influent (trial 2)			1536	**Total Microspheres in Effluent**		**6.7E+05**
				Total Microspheres in Influent		**8.1E+06**
				Percent Recovery		**8.3**

				Volume of Column (ml) =		598
Column B					**Microspheres**	
Sample #	**Cumulative Pore Vol**	**Volume**	**Count**	**Concentration (ms/ml)**	**Normalised (C/C_o)**	**# released in effluent**
3	0.90	2	820	410	0.02	
4	1.08	1	693	693	0.04	2.6E+04
5	1.35	1	729	729	0.04	5.0E+04
6	1.56	1	799	799	0.05	4.0E+04
7	2.02	1	800	800	0.05	9.6E+04
8	2.48	1	583	583	0.04	8.2E+04
9	2.69	1	559	559	0.03	3.0E+04
11	3.63	1	6	6	0.00	6.9E+04
Influent			1656	**16560**	1.00	
				Total Microspheres in Effluent		**3.9E+05**
				Total Microspheres in Influent		**8.5E+06**
				Percent Recovery		**4.6**

C. ION CHROMATOGRAPHY ANALYSES OF BROMIDE

The analysis of bromide was carried out using Ion Chromatography as described in Standard Methods (American Public Health Association, 1995). The results are plotted in Chapter 4, the supporting data and calibration curves are shown in this section. Each series of analyses required the preparation of calibration standards, check standards and blanks to accompany the effluent samples. Blanks and check standards were taken every ten injections to control for temporal drift in the Ion Chromatograph. Duplicate injections were made yielding two bromide concentration values for each effluent sample. In some rare cases, only one bromide concentration is reported for an effluent sample. This is because sometimes only one value was reported by the Ion Chromatograph, possibly because something went wrong with the second injection. Although at least the first 12 effluent samples in each column experiment were analysed, sometimes the bromide concentrations were not reported by the Ion Chromatograph, indicating non-detects.

Bromide Data for Experiments 2 and 3

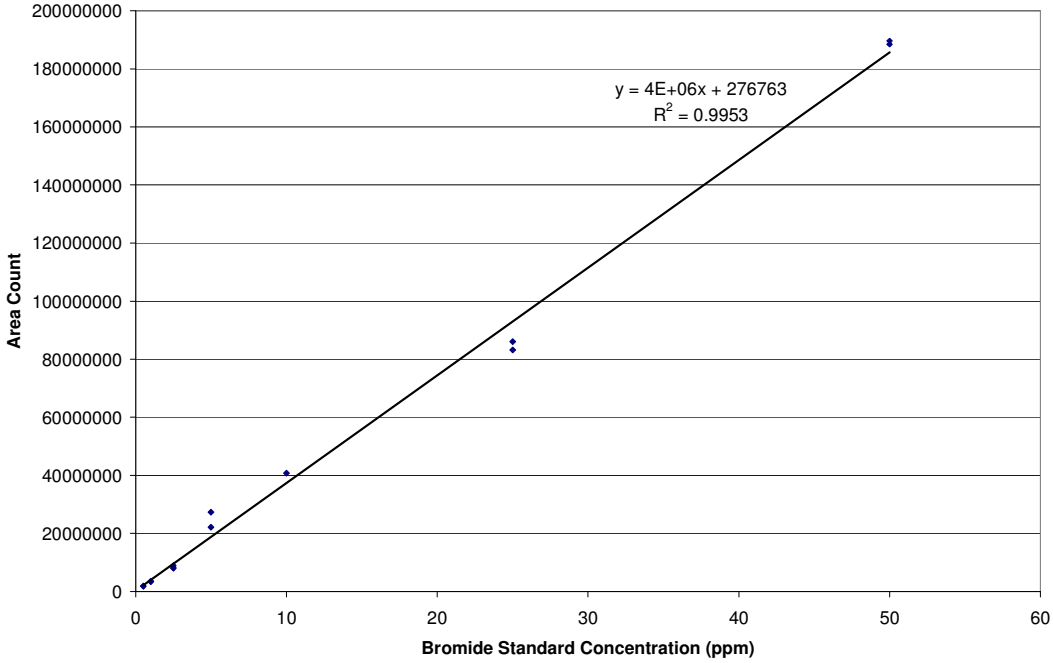

Figure C-1 – Bromide Calibration Curve for Experiments 2 and 3

Table C-1 - Calibration and Check Standard Bromide Data for Experiments 2 and 3

Standard Concentration	Area Count	Calculated Bromide Concentration (ppm)
Calibration Curve		
0.5	1878343.15	NA
0.5	1838418.71	NA
1	3425789.84	NA
1	3511631.22	NA
2.5	7967148.08	NA
2.5	9897296.21	NA
5	22156114.49	NA
5	27289540.86	NA
12.5	4734221.57	NA
12.5	3082374.85	NA
25	7235886.06	NA
25	13656549.47	NA
50	18566043.21	NA
50	12277026.89	NA
100	28480651.13	NA
100	25167212.94	NA
Check Standards		
2.5	8105939.22	1.96
2.5	8944133.82	2.17
10	40723867.31	10.11
25	83249115.53	20.74
25	86092533.46	21.45
50	188483266.7	47.05
50	189592842.4	47.33
Blanks		
0	5987013.02	1.43

Table C-2 - Bromide Data from Experiments 2 and 3, Low [MS2] Column

Sample No.	Pore Volume	IC Sample No.	Peak Area	Br ppm
1	0.56	1	4137140.06	0.97
1	0.56	1	2971132.28	0.67
3	0.80	3	149817.52	-0.03
3	0.80	3	2576053.41	0.57
4	0.86	4	1984014.34	0.43
4	0.86	4	499834.03	0.06
5	1.00	5	15404618.71	3.78
5	1.00	5	13936176.19	3.41
6	1.24	6	223778916.6	55.88
6	1.24	6	224736141.9	56.11
7	1.97	7	402795577	100.63
7	1.97	7	416178267.9	103.98
8	2.10	8	422515183.9	105.56
8	2.10	8	429828676.4	107.39
9	3.61	9	427941225.2	106.92
9	3.61	9	427009592.8	106.68
10	5.71	10	67245668.11	16.74
10	5.71	10	63458520.96	15.80
11	12.68	11	1936758.24	0.41
11	12.68	11	1667215.28	0.35
12	12.93	12	1464878.3	0.30
12	12.93	12	715056.29	0.11
13	15.29	13	1902968.06	0.41
13	15.29	13	1902306.97	0.41
14	21.48	14	2616545.56	0.58
14	21.48	14	1084659.35	0.20
15	23.29	15	2301654.7	0.51
15	23.29	15	1730338.12	0.36
16	29.96	16	3911599.84	0.91
16	29.96	16	2446134.32	0.54
17	33.32	17	1789947.15	0.38
17	33.32	17	2551843.14	0.57
18	33.32	18	512233.29	0.06
18	33.32	18	829622.54	0.14

Table C-3 - Bromide Data from Experiments 2 and 3, High [MS2] Column

Sample No.	Pore Volume	IC Sample No.	Peak Area	Br ppm
1	0.20	20	350896.89	0.02
1	0.20	20	2897776.77	0.66
2	0.32	21	3460983.56	0.80
2	0.32	21	3204412.37	0.73
3	0.60	22	2801552.25	0.63
3	0.60	22	2074551.44	0.45
4	0.84	23	2871468.52	0.65
4	0.84	23	2776788.99	0.63
5	0.90	24	1754317.59	0.37
5	0.90	24	2570971.66	0.57
6	1.04	25	81508333.8	20.31
6	1.04	25	80297334.72	20.01
7	1.27	26	351319653.5	87.76
7	1.27	26	344483944.1	86.05
8	2.14	27	434844461.3	108.64
8	2.14	27	374882617.2	93.65
9	2.38	28	424090885.8	105.95
9	2.38	28	433705807.5	108.36
10	5.78	29	7618120.21	1.84
10	5.78	29	7372120.87	1.77
11	12.97	30	1998245.52	0.43
12	13.22	31	488742.54	0.05
12	13.22	31	2282400	0.50
13	15.63	32	3282186.99	0.75
13	15.63	32	3017699.69	0.69
14	22.04	33	3796907.69	0.88
14	22.04	33	1727377.18	0.36
15	23.93	34	292551.48	0.00
15	23.93	34	2244345.03	0.49

Bromide Data for Experiments 4 through 9

The calibration curve for experiments 4 though 9 unfortunately lacked a standard point between 50 and 200 ppm bromide (normally a 100 ppm standard was included). As well, the last (200 ppm) point did not lie on a straight line with the other 6 calibration points (1-50 ppm). Therefore this last point was not used in calibrating the effluent samples due to a suspected low concentration.

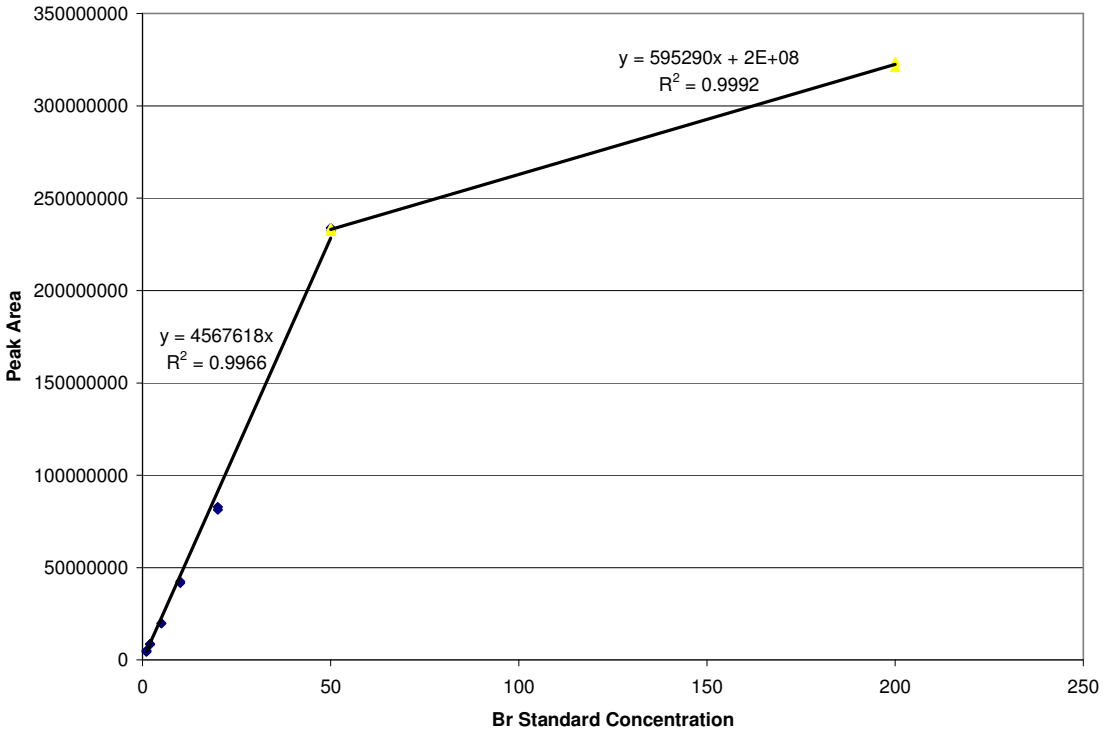

Figure C-2 – Bromide Calibration Curve for Experiments 4 through 9

Table C-4 – Calibration and Check Standard Bromide Data for Experiments 4 to 9

Standard Concentration	Area Count	Calculated Bromide Concentration (ppm)
Calibration Curve		
1	5074592.17	NA
1	4375741.21	NA
2	8615137.19	NA
2	8605989.06	NA
5	19938621.21	NA
5	19964846.42	NA
10	41642096.82	NA
10	42516893.61	NA
20	81406020.59	NA
20	82823355.7	NA
50	232242756.7	NA
50	233960804.7	NA
200	320886094.1	NA
200	323904579.1	NA
Check Standards		
10 std	23756207.37	5.20
10 std	20412860.42	4.47
10 std	21365679.79	4.68
10 std	21155639.51	4.63
10 std	20540075.69	4.50
5 std	42605371.19	9.33
5 std	41221230.43	9.02
Blanks		
blank	ND	0.00
blank	8612	0.00
blank	787375.31	0.17
blank	1779234.83	0.39
blank	2916.00	0.00
blank	2872.00	0.00
blank	53760.68	0.01
blank	864747.52	0.19
blank	44225.89	0.01
blank	1039468.16	0.23
blank	29779.86	0.01

Table C-5 – Bromide Data from Experiments 4 and 5, Low [MS2] Column

Sample No.	Pore Volume	IC Sample No.	Peak Area	Br ppm
1L	0.1	17	4104149.86	0.90
1L	0.1	17	6427820.4	1.41
2L	0.3	18	6076668.69	1.33
2L	0.3	18	3627541.06	0.79
3L	0.4	19	4614786.45	1.01
3L	0.4	19	5946964.05	1.30
4L	0.7	20	6905365.52	1.51
4L	0.7	20	4701003.08	1.03
5L	1.2	21	304894698.1	66.75
5L	1.2	21	324891865.3	71.13
6L	1.6	22	561653646.9	122.96
6L	1.6	22	554141028.4	121.32
7L	1.9	23	563604726.4	123.39
7L	1.9	23	556360808	121.81
8L	2.5	24	546129923.2	119.57
8L	2.5	24	547483564.8	119.86
9L	3.0	25	392425036.1	85.91
9L	3.0	25	392828994.4	86.00
10L	3.3	26	115709116.8	25.33
10L	3.3	26	115903569.5	25.38
11L	4.6	27	4016149.94	0.88
11L	4.6	27	4281926.21	0.94
13L	8.3	28	2826986.84	0.62
13L	8.3	28	5915004.42	1.29
14L	10.1	29	5883624.33	1.29
14L	10.1	29	4617683.36	1.01
16L	14.2	30	4983760.28	1.09
16L	14.2	30	5038895.94	1.10
R1L		31	585190797.3	128.12
R1L		31	588969432.9	128.94
R3L		89	585058814.7	128.09
R3L		89	591748004.2	129.55

Table C-6 – Bromide Data from Experiments 4 and 5, High [MS2] Column

Sample No.	Pore Volume	IC Sample No.	Peak Area	Br ppm
4H	0.7	4	5552000	1.22
4H	0.7	4	5556000	1.22
5H	1.1	5	373344604.8	81.74
5H	1.1	5	331305235.6	72.53
6H	1.5	6	529800212.6	115.99
6H	1.5	6	534901661.1	117.11
7H	1.9	7	548723940.3	120.13
7H	1.9	7	552445661.1	120.95
8H	2.4	8	539086251.7	118.02
8H	2.4	8	541629600	118.58
9H	3.0	9	311038000	68.10
9H	3.0	9	350632931.7	76.76
10H	3.3	10	81772000	17.90
10H	3.3	10	81164000	17.77
11H	4.6	11	104000	0.02
11H	4.6	11	117964	0.03
12H	6.2	12	6650801.82	1.46
12H	6.2	12	5644102.33	1.24
14H	10.1	13	5147339.01	1.13
R1H		15	562871450.3	123.23
R1H		15	565053877.7	123.71
R3H		16	557668222.3	122.09
R3H		16	564079539.5	123.50

Table C-7 – Bromide Data from Experiments 6 and 7, Low [MS2] Column

Sample No.	Pore Volume	IC Sample No.	Peak Area	Br ppm
1L	0.26	74.00	5353947.86	1.17
1L	0.26	74.00	4788478.06	1.05
2L	0.47	75.00	4675310.32	1.02
2L	0.47	75.00	6311690.74	1.38
3L	0.73	76.00	96874047.59	21.21
3L	0.73	76.00	95577941.23	20.93
4L	1.08	77.00	239831423.61	52.51
4L	1.08	77.00	240538024.82	52.66
5L	1.72	78.00	581933001.20	127.40
5L	1.72	78.00	590938278.86	129.38
6L	1.98	79	589903153.1	129.15
6L	1.98	79	597979385.4	130.92
7L	2.47	80	584733731.7	128.02
7L	2.47	80	585102206.5	128.10
8L	2.88	81.00	384502374.41	84.18
8L	2.88	81.00	363717806.66	79.63
9L	3.30	82.00	137954657.91	30.20
9L	3.30	82.00	114571265.81	25.08
10L	3.87	83.00	5417399.48	1.19
10L	3.87	83.00	6879801.15	1.51
11L	4.66	84.00	6159469.45	1.35
11L	4.66	84.00	5740394.46	1.26
12L	5.41	85.00	1261785.09	0.28
12L	5.41	85.00	1254958.16	0.27
13L	5.94	86.00	6528870.12	1.43
13L	5.94	86.00	6477001.35	1.42
R1L		87.00	605235239.08	132.51
R1L		87.00	607374872.70	132.97
R3L		88.00	592150712.70	129.64
R3L		88.00	596035419.94	130.49

Table C-8 – Bromide Data from Experiments 6 and 7, High [MS2] Column

Sample No.	Pore Volume	IC Sample No.	Peak Area	Br ppm
1H	0.26	60.00	4354605.13	0.95
1H	0.26	60.00	2626771.16	0.58
2H	0.47	61.00	4722822.16	1.03
2H	0.47	61.00	5660254.20	1.24
3H	0.73	62.00	133367925.36	29.20
3H	0.73	62.00	137059876.43	30.01
4H	1.08	63.00	284924051.86	62.38
4H	1.08	63.00	277287628.20	60.71
5H	1.74	64.00	519544569.08	113.75
5H	1.74	64.00	511955770.52	112.08
6H	2.00	65.00	589242858.86	129.00
6H	2.00	65.00	585126792.17	128.10
7H	2.48	66.00	550444357.95	120.51
7H	2.48	66.00	539043805.10	118.01
8H	2.89	67.00	319648746.72	69.98
8H	2.89	67.00	323138008.41	70.75
9H	3.31	68.00	183716672.17	40.22
9H	3.31	68.00	198989903.42	43.57
10H	3.87	69.00	39578286.04	8.66
10H	3.87	69.00	39988196.91	8.75
11H	4.67	70.00	4215270.63	0.92
11H	4.67	70.00	5386521.43	1.18
12H	5.41	71.00	3431780.67	0.75
12H	5.41	71.00	3156072.12	0.69
R1H		72.00	615015896.47	134.65
R1H		72.00	617800303.66	135.26
R3H		73.00	614657276.84	134.57
R3H		73.00	617052137.75	135.09

Table C-9 – Bromide Data from Experiments 8 and 9, Column A

Sample No.	Pore Volume	IC Sample No.	Peak Area	Br ppm
3A	0.47	34.00	18685855.82	4.09
3A	0.47	34.00	15039034.26	3.29
4A	0.94	35.00	281084799.44	61.54
4A	0.94	35.00	263536434.31	57.70
5A	1.42	36.00	465964002.53	102.01
5A	1.42	36.00	470195930.49	102.94
6A	1.86	37.00	568920383.84	124.56
6A	1.86	37.00	554469922.49	121.39
7A	2.27	38.00	604813209.33	132.41
7A	2.27	38.00	610467265.83	133.65
8A	2.73	39.00	428481352.28	93.81
8A	2.73	39.00	429701484.07	94.08
9A	3.16	40.00	252707060.09	55.33
9A	3.16	40.00	241413648.45	52.85
10A	3.72	41.00	132053404.47	28.91
10A	3.72	41.00	123709439.55	27.08
11A	4.23	42.00	92147046.50	20.17
11A	4.23	42.00	28108663.11	6.15
R1A		44.00	616094168.42	134.88
R1A		44.00	625178704.69	136.87
R2A		45.00	655122959.77	143.43
R2A		45.00	623452550.35	136.49

Table C-10 – Bromide Data from Experiments 8 and 9, Column B

Sample No.	Pore Volume	IC Sample No.	Peak Area	Br ppm
4B	0.94	49.00	206119257.2	45.13
4B	0.94	49.00	202893149.9	44.42
5B	1.42	50.00	474893349.5	103.97
5B	1.42	50.00	446755893.7	97.81
6B	1.86	51.00	567157543	124.17
6B	1.86	51.00	596097421.6	130.51
7B	2.28	52.00	604571477.3	132.36
7B	2.28	52.00	577919044.7	126.53
8B	2.74	53.00	479472373.8	104.97
8B	2.74	53.00	479539792.2	104.99
9B	3.17	54.00	221557082.7	48.51
9B	3.17	54.00	207188470.2	45.36
10B	3.73	55.00	104157306.9	22.80
10B	3.73	55.00	95876927.01	20.99
R1B		58.00	588678815.8	128.88
R1B		58.00	590805790.4	129.35
R2B		59.00	584121865.3	127.88
R2B		59.00	583958067	127.85

Bromide Data for Experiments 10 through 13

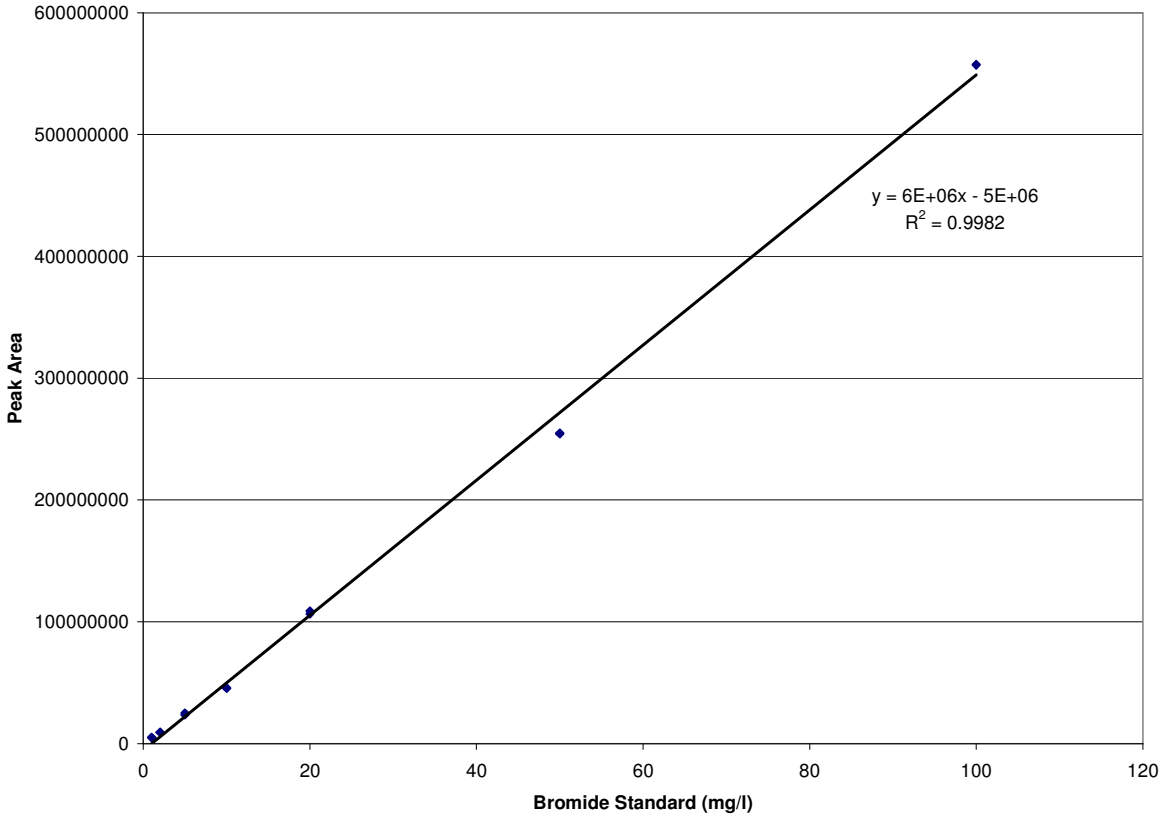

Figure C-3 – Bromide Calibration Curve for Experiments 10 through 13

Table C-11 –Calibration and Check Standard Bromide Data for Experiments 10 through 13

Standard Concentration	Area Count	Calculated Bromide Concentration (ppm)
Calibration Curve		
1	5144177.84	NA
1	4994361.41	NA
2	9290681.16	NA
2	9388581.58	NA
5	25135651.7	NA
5	23650832.51	NA
10	45746960.58	NA
10	45492168.77	NA
20	108950491	NA
20	106491398.6	NA
50	254239981.3	NA
50	255009360.9	NA
100	557016215.3	NA
100	557701872.1	NA
Check Standards		
10 std	50669613.63	9.28
10 std	45280262.82	8.38
10 std	40239933.22	7.54
10 std	37077821.63	7.01
10 std	42930472.2	7.99
10 std	36371696.6	6.90
10 std	36399788.28	6.90
10 std	35712604.83	6.79
Blanks		
blank	64935.02	0.84
blank	44779.57	0.84
blank	51650.29	0.84
blank	61732.59	0.84
blank	916330.59	0.99
blank	90668.99	0.85
blank	59960.87	0.84
blank	75309.12	0.85

Table C-12 – Bromide Data from Experiments 10 and 11, Column A

Sample No.	Pore Volume	IC Sample No.	Peak Area	Br ppm
1A	0.32	29	16529068.2	3.59
1A	0.32	29	9101174.3	2.35
2A	0.54	30	9928391.0	2.49
2A	0.54	30	16270612.0	3.55
3A	0.89	31	306991812.0	52.00
3A	0.89	31	317100998.6	53.68
4A	1.24	32	560462749.2	94.24
4A	1.24	32	563204712.8	94.70
5A	1.79	33	670399173.7	112.57
5A	1.79	33	681743821.0	114.46
6A	2.32	34	676685643.4	113.61
6A	2.32	34	673300977.0	113.05
7A	2.76	35	670568095.8	112.59
7A	2.76	35	679349105.4	114.06
8A	3.16	36	605238420.1	101.71
8A	3.16	36	602327883.2	101.22
9A	3.83	37	68407133.7	12.23
9A	3.83	37	101746440.8	17.79
10A	4.66	38	8769518.1	2.29
10A	4.66	38	8014670.6	2.17
11A	6.14	39	7338660.3	2.06
11A	6.14	39	9195748.9	2.37
12A	6.20	40	9742261.5	2.46
12A	6.20	40	9033453.8	2.34
R1A		41	687882713.1	115.48
R1A		41	692031444.6	116.17

Table C-13 –Bromide Data from Experiments 10 and 11, Column B

Sample No.	Pore Volume	IC Sample No.	Peak Area	Br ppm
1B	0.33	42	6182920.0	1.86
1B	0.33	42	7888317.2	2.15
2B	0.56	43	9419717.0	2.40
2B	0.56	43	7230574.7	2.04
3B	0.93	44	263414400.1	44.74
3B	0.93	44	260126533.6	44.19
4B	1.30	45	538809966.8	90.63
4B	1.30	45	539938280.3	90.82
5B	1.86	46	683257883.5	114.71
5B	1.86	46	632257197.7	106.21
6B	2.25	47	634097173.2	106.52
6B	2.25	47	634406904.2	106.57
7B	2.72	48	635244331.0	106.71
7B	2.72	48	629452023.2	105.74
8B	3.14	49	474438768.7	79.91
8B	3.14	49	462678187.3	77.95
9B	3.82	50	56482062.0	10.25
9B	3.82	50	26027472.5	5.17
10B	4.69	51	8386629.6	2.23
10B	4.69	51	8691837.9	2.28
11B	6.25	52	8226905.3	2.20
11B	6.25	52	7953949.5	2.16
R1B		54	618035696.0	103.84
R1B		54	605750205.8	101.79

Table C-14 – Bromide Data from Experiments 12 and 13, Column A

Sample No.	Pore Volume	IC Sample No.	Peak Area	Br ppm
1A	0.23	55	94591.1	0.85
1A	0.23	55	44955.0	0.84
3A	0.89	58	338315777.8	57.22
3A	0.89	58	371713328.4	62.79
4A	1.18	59	480658612.3	80.94
4A	1.18	59	467077999.2	78.68
5A	1.58	60	655743892.4	110.12
5A	1.58	60	629740327.8	105.79
6A	1.90	61	650180151.3	109.20
6A	1.90	61	658757210.0	110.63
7A	2.31	62	665742935.1	111.79
7A	2.31	62	662004847.8	111.17
8A	2.57	63	663197982.6	111.37
8A	2.57	63	636700377.9	106.95
9A	3.35	64	377863626.3	63.81
9A	3.35	64	377974676.1	63.83
10A	4.03	65	148844113.7	25.64
10A	4.03	65	134417411.0	23.24
11A	4.83	66	78803828.3	13.97
11A	4.83	66	73968221.7	13.16
12A	5.44	67	85945780.1	15.16
R1A		68	640692087.9	107.62
R1A		68	638522595.5	107.25

Table C-15 – Bromide Data from Experiments 12 and 13, Column B

Sample No.	Pore Volume	IC Sample No.	Peak Area	Br ppm
2B	0.39	70	51807121.5	9.47
2B	0.39	70	14327875.0	3.22
3B	0.92	71	363847003.9	61.47
3B	0.92	71	379254617.5	64.04
4B	1.22	72	484309422.3	81.55
4B	1.22	72	467684494.4	78.78
5B	1.64	73	576039287.0	96.84
5B	1.64	73	586230341.2	98.54
6B	1.98	74	626145823.0	105.19
6B	1.98	74	636731921.3	106.96
7B	2.40	75	622503532.8	104.58
7B	2.40	75	618601544.5	103.93
8B	2.67	76	645780784.4	108.46
8B	2.67	76	630950846.7	105.99
9B	3.47	77	287772313.2	48.80
9B	3.47	77	287462751.1	48.74
10B	4.18	78	139472363.4	24.08
10B	4.18	78	130510968.2	22.59
11B	5.00	79	78913983.8	13.99
11B	5.00	79	79744573.7	14.12
R1B		81	613306398.8	103.05
R1B		81	638132042.0	107.19

Bromide Data for Experiments 14 and 15

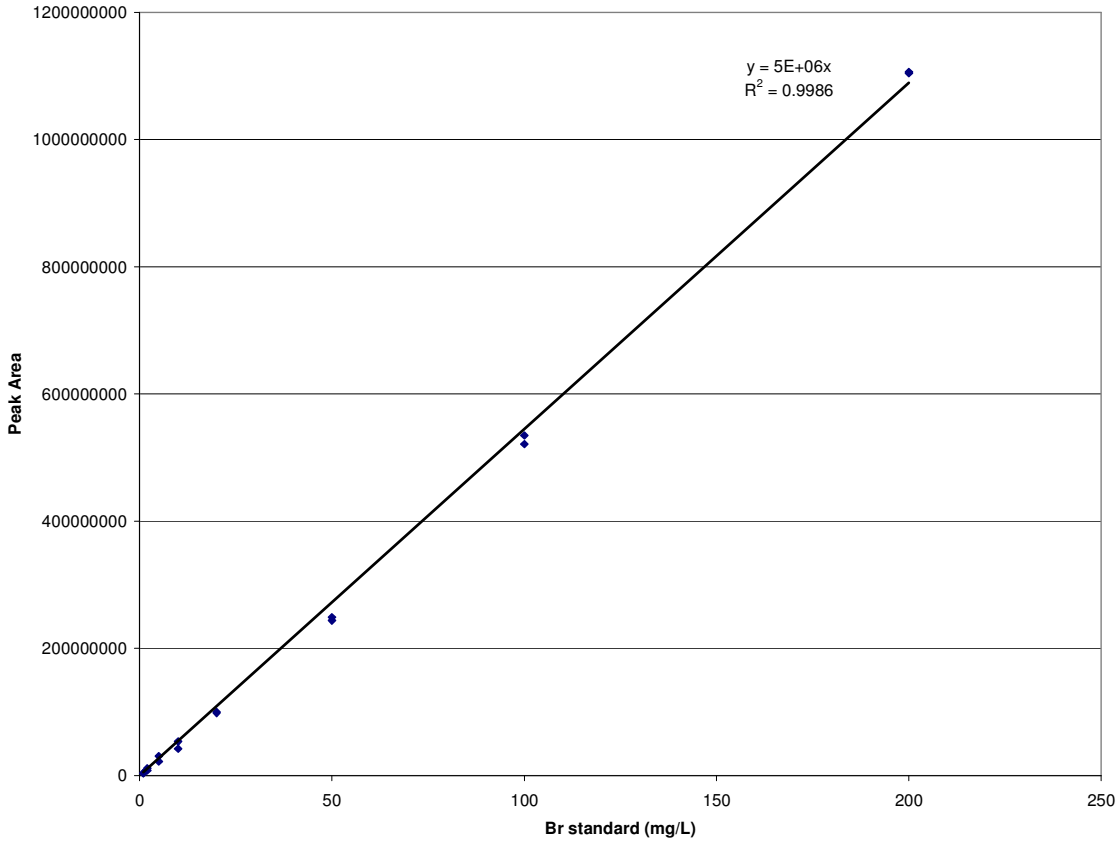

Figure C-4 - Bromide Calibration Curve for Experiments 14 and 15

Table C-16 - Calibration and Check Standard Bromide Data for Experiments 14 and 15

Standard Concentration	Area Count	Calculated Bromide Concentration (ppm)
Calibration Curve		
1	4028404.7	NA
1	3486231.4	NA
2	7718047.5	NA
2	11317758.4	NA
5	30415742.0	NA
5	22172009.9	NA
10	42080099.0	NA
10	53360399.5	NA
20	99958824.7	NA
20	98254381.1	NA
50	243779663.6	NA
50	248848493.6	NA
100	521280432.9	NA
100	534673751.1	NA
200	1104525772.3	NA
200	1106419799.3	NA
Check Standards		
10 std	42694629.4	8.54
10 std	62317383.3	12.46
Blanks		
blank	3039650.7	0.61
blank	221724.0	0.04
blank	1253081.7	0.25

Table C-17 – Bromide Data from Experiments 14 and 15, Column A

Sample No.	Pore Volume	IC Sample No.	Peak Area	Br ppm
3	0.92	3	214363816.1	42.87
3	0.92	3	284266145.4	56.85
4	1.11	4	381444198.0	76.29
4	1.11	4	364907332.3	72.98
5	1.39	5	477474124.4	95.49
5	1.39	5	480799636.4	96.16
6	1.59	6	581069189.8	116.21
6	1.59	6	591904306.1	118.38
7	2.07	7	623306472.9	124.66
7	2.07	7	632892754.3	126.58
8	2.54	8	602090270.9	120.42
8	2.54	8	599903759.0	119.98
9	2.75	9	584524836.0	116.90
9	2.75	9	584571309.3	116.91
10	2.84	10	515985162.0	103.20
10	2.84	10	524132123.8	104.83
11	3.71	11	124688135.3	24.94
11	3.71	11	129621891.2	25.92
Res 1		15	670406309.9	134.08
Res 1		15	641841666.9	128.37

Table C-18 – Bromide Data from Experiments 14 and 15, Column B

Sample No.	Pore Volume	IC Sample No.	Peak Area	Br ppm
3	0.90	18	219457192.7	43.89
3	0.90	18	183689062.7	36.74
4	1.08	19	363576650.1	72.72
4	1.08	19	361137834.1	72.23
5	1.35	20	503172177.4	100.63
5	1.35	20	529780973.3	105.96
6	1.56	21	622297065.2	124.46
6	1.56	21	592466286.0	118.49
7	2.02	22	641982493.2	128.40
7	2.02	22	611838586.4	122.37
8	2.48	23	644961401.1	128.99
8	2.48	23	579393890.2	115.88
9	2.69	24	637199383.6	127.44
9	2.69	24	640380138.0	128.08
10	2.78	25	549992701.5	110.00
10	2.78	25	585803964.0	117.16
11	3.63	26	106027652.3	21.21
11	3.63	26	157766451.2	31.55
Res 1		30	625950807.9	125.19
Res 1		30	646792147.2	129.36

D. OPERATION OF COLUMN EXPERIMENTS

Sampling Schedule and Flow Rates from Column Experiments

Table D-1 – Sampling Schedule and Flow Rate Data from Column Experiments 4 and 5, Medium Sand, Low Ionic Strength

Time from Start (hr:min:sec)											
Sample Interval				Low MS2 Reservoir				High MS2 Reservoir			
From	To	Time Centre Point	Sample #	Flow Rate (ml/hr)	Effluent Volume (ml)	Effluent Volume (Pore Vol)	Cumulative Pore Vol	Flow Rate (ml/hr)	Effluent Volume (ml)	Effluent Volume (Pore Vol)	Cumulative Pore Vol
Pre-Spike Rinsing AGW											
0:11:45	0:14:45	0:13:15		220				220			
0:15:15	0:18:15	0:16:45		190				190			
0:18:15	15:45:00	8:01:37		139				139			
15:53:30	16:02:45	15:58:08		149				149			
16:04:30	16:14:15	16:09:22		142				142			
16:16:00	16:21:30	16:18:45		218				218			
16:29:30	16:34:00	16:31:45		153				153			
Switch to MS2 Spiked Reservoirs (3 min slow)											
0:02:30	0:08:00	0:05:15	1	0				0			
0:11:00	0:15:00	0:13:00		218				218			
0:17:20	0:20:30	0:18:55		218	74	0.3	0.3	218	74	0.3	0.3
0:20:30	0:25:10	0:22:50	2				0.3				0.3
0:25:10	0:31:45	0:28:28		173	32	0.1	0.4	173	32	0.1	0.4
		0:30:00	Res 1				0.4				0.4
0:31:45	0:37:15	0:34:30	3				0.4				0.4
1:00:00	1:05:30	1:02:45	4				0.4				0.4
1:05:30	1:39:15	1:22:23		167	188	0.7	1.1	164	185	0.7	1.1
1:39:20	1:46:05	1:42:42	5				1.1				1.1
1:46:10	2:19:45	2:02:58		165	93	0.3	1.4	163	91	0.3	1.4
2:19:45	2:25:30	2:22:37	6				1.4				1.4
2:55:45	3:01:00	2:58:22	7			0.0	1.4	0		0.0	1.4
3:01:00	3:07:45	3:04:23		169	135	0.5	1.9	0		0.0	1.4
3:01:00	3:09:15	3:05:08		0		0.0	1.9	167	138.0	0.5	1.9
Colloid-free AGW			***Spike Total***		***523***	***1.9***	1.8		***521***	***1.9***	1.8
3:44:15	3:53:00	3:48:38	8	0		0.0	1.8	0		0.0	1.8
3:53:45	4:05:30	3:59:38		169	162	0.6	2.4	169	162.2	0.6	2.4
4:39:50	4:45:15	4:42:32	9	0		0.0	2.4	0		0.0	2.4
4:45:35	5:13:50	4:59:43		164	186	0.7	3.1	164	186.3	0.7	3.1
5:13:50	5:20:40	5:17:15	10			0.0	3.1	0		0.0	3.1
7:17:30	7:24:00	7:20:45	11	0		0.0	3.1	0		0.0	3.1
9:50:30	9:55:30	9:53:00	12	0		0.0	3.1	0		0.0	3.1
9:55:30	10:03:15	9:59:23		170	822	3.0	6.1	170	822	3.0	6.1
13:11:15	13:17:10	13:14:12	13	0		0.0	6.1	0		0.0	6.1
16:03:00	16:08:15	16:05:37	14	0		0.0	6.1	0		0.0	6.1
16:08:15	16:13:00	16:10:37		171	1051	3.9	10.0	171	1051	3.9	10.0
22:51:50	22:58:00	22:54:55	15	0		0.0	10.0	0		0.0	10.0
		22:57:00	Res 2			0.0	10.0			0.0	10.0
22:58:15	23:08:30	23:03:23		164	1135	4.2	14.2	164	1135	4.2	14.2
26:41:00	26:46:30	26:43:45	16	0		0.0	14.2	0		0.0	14.2
26:47:05	26:53:30	26:50:18		168	631	2.3	16.5	168	631	2.3	16.5
34:15:30	34:21:00	34:18:15	17	0		0.0	16.5	0		0.0	16.5
34:21:00	34:26:15	34:23:38		171	1294	4.8	21.2	171	1294	4.8	21.2
		34:24:00	Res 3			0.0	21.2			0.0	21.2
47:37:40	47:43:00	47:40:20	18	0		0.0	21.2	0		0.0	21.2
47:43:00	47:53:00	47:48:00		165	2219	8.2	29.4	165	2219	8.2	29.4
		47:48:00	Res 4			0.0	29.4			0.0	29.4
		Cumulative Total			***6326***	***29.47***			***6323***	***29.47***	

Table D-2 - Sampling Schedule and Flow Rate from Column Experiments 6 and 7, Medium Sand, Low Ionic Strength

Time from Start (hr:min:sec) Sampled				High MS2 Reservoir				Low MS2 Reservoir			
From	To	Time Centre Point	Sample #	Flow Rate (ml/hr)	Effluent Volume (ml)	Effluent Volume (Pore Vol)	Cumulative Pore Vol	Flow Rate (ml/hr)	Effluent Volume (ml)	Effluent Volume (Pore Vol)	Cumulative Pore Vol
Pre-Spike Rinsing AGW											
0:00:00	0:02:00	0:01:00		660				660			
0:05:10	0:07:10	0:06:10		1680				1680			
0:54:00	0:58:00	0:56:00		1373				1410			
1:10:30	1:20:30	1:15:30		183				186			
1:32:45	1:41:50	1:37:17		185				185			
Switch to MS2 Spiked Reservoirs											
0:01:00	0:11:00	0:06:00		147	27	0.1	0.1	147	27	0.1	0.1
0:14:15	0:19:00	0:16:38		202			0.1	202		0.0	0.1
0:19:00	0:24:10	0:21:35	1		44	0.2	0.3	0	44	0.2	0.3
0:24:10	0:29:00	0:26:35		186	15	0.1	0.3	186	15	0.1	0.3
0:37:00	0:42:30	0:39:45	2	0	42	0.2	0.5	0	42	0.2	0.5
0:52:35	1:01:30	0:57:02		178	56	0.2	0.7	178	56	0.2	0.7
1:01:30	1:06:30	1:04:00	3	0	15	0.1	0.7	0	15	0.1	0.7
1:32:00	1:38:12	1:35:06	4	0	94	0.3	1.1	0	94	0.3	1.1
1:38:30	1:46:20	1:42:25		176	24	0.1	1.2	176	24	0.1	1.2
2:22:00	2:32:30	2:27:15		174		0.0	1.2	180		0.0	1.2
2:32:30	2:38:00	2:35:15	5	0	150	0.6	1.7	0	155	0.6	1.7
2:48:30	2:56:00	2:52:15		180	54	0.2	1.9	184	55	0.2	1.9
Switch to bacteriophage-free AGW					***522***				***528***		
2:56:40	3:01:50	2:59:15	6	0	17	0.1	2.0	0	18	0.1	2.0
3:32:10	3:40:00	3:36:05		184	117	0.4	2.4	180	115	0.4	2.4
3:40:00	3:45:00	3:42:30	7	0	15	0.1	2.5	0	15	0.1	2.5
4:16:50	4:22:00	4:19:25	8	0	113	0.4	2.9	0	111	0.4	2.9
4:22:00	4:30:00	4:26:00		180	0	0.0	2.9	180	0	0.0	2.9
5:03:00	5:08:00	5:05:30	9	0	114	0.4	3.3	0	114	0.4	3.3
5:08:00	5:13:00	5:10:30		180		0.0	3.3	180		0.0	3.3
5:53:45	5:59:05	5:56:25	10	0	153	0.6	3.9	0	153	0.6	3.9
5:59:05	6:05:30	6:02:17		182		0.0	3.9	182		0.0	3.9
6:58:35	7:05:00	7:01:47		182		0.0	3.9	182		0.0	3.9
7:05:00	7:10:30	7:07:45	11	0	217	0.8	4.7	0	217	0.8	4.7
8:15:20	8:17:15	8:16:18	12	0	203	0.7	5.4	0	203	0.7	5.4
8:17:15	8:25:45	8:21:30		173		0.0	5.4	176		0.0	5.4
8:52:05	9:01:20	8:56:42		175		0.0	5.4	178		0.0	5.4
9:01:20	9:06:30	9:03:55	13	0	144	0.5	5.9	0	146	0.5	6.0
12:23:00	12:28:55	12:25:57	14	0	591	2.2	8.1	0	602	2.2	8.2
15:30:15	15:35:45	15:33:00	15	0	545	2.0	10.1	0	555	2.0	10.2
15:35:45	15:51:50	15:43:48		160		0.0	10.1	162		0.0	10.2
18:09:00	18:11:45	18:10:22	16	0	417	1.5	11.6	0	422	1.6	11.8
26:49:00	26:54:30	26:51:45	17	0	1398	5.1	16.8	0	1414	5.2	16.9
26:54:30	27:02:00	26:58:15		172		0.0	16.8	172		0.0	16.9
33:44:50	33:50:30	33:47:40	18	0	1193	4.4	21.2	0	1193	4.4	21.3
33:50:30	33:54:00	33:52:15		189		0.0	21.2	189		0.0	21.3
45:50:20	45:56:30	45:53:25	19		2282	8.4	29.5		2282	8.4	29.7
		45:52:00	Res 2			0.0	29.5			0.0	29.7
45:56:35	46:07:30	46:02:03		168		0.0	29.5	170		0.0	29.7
52:43:45	52:49:00	52:46:23	20		1152	4.2	33.8		1171.4	4.3	34.0
52:49:00	52:57:10	52:53:05		165		0.0	33.8	169		0.0	34.0
			Total (ml)		***9715***				***9786***		

Table D-3 - Sampling Schedule and Flow Rates from Column Experiments 8 and 9, Medium Sand, High Ionic Strength

Time from Start (hr:min:sec) Sampled				Column A				Column B			
From	To	Time Centre Point	Sample #	Flow Rate (ml/hr)	Effluent Volume (ml)	Effluent Volume (Pore Vol)	Cumulative Pore Vol	Flow Rate (ml/hr)	Effluent Volume (ml)	Effluent Volume (Pore Vol)	Cumulative Pore Vol
Pre-Spike Rinsing AGW											
about 6 L of Water or about 10 pore volumes overnight flush											
Switch to MS2 Spiked Reservoirs											
0:03:00	0:11:10	0:07:05		169	31	0.1	0.1	169	31	0.1	0.1
0:11:10	0:17:00	0:14:05	1	0	16	0.1	0.2	0	16	0.1	0.2
0:25:00	0:30:30	0:27:45	2	0	38	0.1	0.3	0	38	0.1	0.3
0:31:00	0:40:00	0:35:30		173	27	0.1	0.4	173	27	0.1	0.4
0:40:00	0:45:30	0:42:45	3	0	16	0.1	0.5	0	16	0.1	0.5
1:24:00	1:29:30	1:26:45	4	0	127	0.5	0.9	0	127	0.5	0.9
1:29:30	1:37:00	1:33:15		172	22	0.1	1.0	172	22	0.1	1.0
2:09:45	2:15:15	2:12:30	5	0	110	0.4	1.4	0	110	0.4	1.4
		2:15:00	Res 1								
2:37:40	2:46:00	2:41:50		173	89	0.3	1.7	173	89	0.3	1.7
2:50:40	2:56:30	2:53:35	6	0	30	0.1	1.9	0	30	0.1	1.9
2:56:30	3:03:30	3:00:00		171	20	0.1	1.9	176	21	0.1	1.9
Switch to bacteriophage-free AGW											
3:29:45	3:35:15	3:32:30	7	0	91	0.3	2.3	0	93	0.3	2.3
3:35:15	3:52:30	3:43:52		169	49	0.2	2.4	169	49	0.2	2.5
4:14:30	4:20:30	4:17:30	8	0	79	0.3	2.7	0	79	0.3	2.7
4:30:30	4:56:00	4:43:15		169	100	0.4	3.1	169	100	0.4	3.1
4:56:00	5:01:45	4:58:53	9	0	16	0.1	3.2	0	16	0.1	3.2
5:50:15	5:55:30	5:52:53	10	0	152	0.6	3.7	0	152	0.6	3.7
6:20:10	6:34:30	6:27:20		170	110	0.4	4.1	170	110	0.4	4.1
6:39:15	6:44:30	6:41:52	11	0	28	0.1	4.2	0	28	0.1	4.2
9:24:15	9:30:00	9:27:07	12	0	468	1.7	5.9	0	468	1.7	6.0
12:10:30	12:16:05	12:13:18	13	0	480	1.8	7.7	0	504	1.9	7.8
12:16:05	12:23:00	12:19:32		173	20	0.1	7.8	182	21	0.1	7.9
16:37:30	16:43:00	16:40:15	14	0	752	2.8	10.5	0	789	2.9	10.8
19:55:30	20:01:00	19:58:15	15	0	578	2.1	12.7	0	561	2.1	12.8
20:01:30	20:07:30	20:04:30		175	19	0.1	12.7	170	18	0.1	12.9
23:49:10	23:55:10	23:52:10	16	0	664	2.4	15.2	0	645	2.4	15.3
23:55:10	24:01:00	23:58:05	17	0	17	0.1	15.2	0	17	0.1	15.3
		23:59:00	Res 2			0.0	15.2			0.0	15.3
24:01:00	24:11:10	24:06:05		165	28	0.1	15.3	165	28	0.1	15.4
25:50:00	25:55:30	25:52:45	18	0	287	1.1	16.4	0	287	1.1	16.5
27:15:15	27:21:00	27:18:08	19	0	243	0.9	17.3	0	243	0.9	17.4
29:13:30	29:23:00	29:18:15		171	347	1.3	18.6	171	347	1.3	18.7
29:23:00	29:29:30	29:26:15	20	0	18	0.1	18.6	0	18	0.1	18.7
30:18:30	30:27:30	30:23:00	21	0	165	0.6	19.2	0	165	0.6	19.3
31:03:00	31:19:00	31:11:00		0	146	0.5	19.8	165	146	0.5	19.9
31:19:00	31:25:00	31:22:00	22	0	17	0.1	19.8	0	17	0.1	19.9
		Cumulative Total			***5400***				***5429***		

Table D-4 - Sampling Schedule and Flow Rates from Column Experiments 10 and 11, Fine Sand, Low Ionic Strength

Time from Start (hr:min:sec) Sampled				Column A				Column B			
From	To	Time Centre Point	Sample #	Flow Rate (ml/hr)	Effluent Volume (ml)	Effluent Volume (Pore Vol)	Cumulative Pore Vol	Flow Rate (ml/hr)	Effluent Volume (ml)	Effluent Volume (Pore Vol)	Cumulative Pore Vol
Pre-Spike Rinsing AGW											
about 4.5 L of Water											
Switch to MS2 Spiked Reservoirs											
0:01:00	0:07:00	0:04:00		190	22	0.1	0.1	195	23	0.1	0.1
0:09:45	0:19:45	0:14:45		159	34	0.1	0.2	165	35	0.1	0.2
0:19:45	0:23:10	0:21:27	Br1	0	13	0.0	0.3	0	14	0.1	0.3
0:23:20	0:28:00	0:25:40	1	0	18	0.1	0.3	0	19	0.1	0.3
0:28:00	0:30:30	0:29:15		228	10	0.0	0.4	240	10	0.0	0.4
0:30:30	0:33:45	0:32:07	Br2		12	0.0	0.4		12	0.0	0.4
0:33:45	0:39:45	0:36:45		215	22	0.1	0.5	225	23	0.1	0.5
0:39:45	0:45:00	0:42:22	2		17	0.1	0.5		18	0.1	0.6
0:45:00	0:51:10	0:48:05		195	20	0.1	0.6	204	21	0.1	0.6
0:51:10	1:02:00	0:56:35	Br3	0	30	0.1	0.7	0	32	0.1	0.8
1:02:00	1:11:15	2:15:00		169	26	0.1	0.8	175	27	0.1	0.9
1:11:15	1:16:30	1:13:52	3	0	18	0.1	0.9	0	19	0.1	0.9
1:16:30	1:26:45	1:21:37		211	36	0.1	1.0	220	38	0.1	1.1
1:26:45	1:32:40	1:29:42	Br4	0	21	0.1	1.1	0	22	0.1	1.1
1:32:40	1:37:40	1:35:10		216	18	0.1	1.2	222	19	0.1	1.2
1:37:45	1:43:40	1:40:42	4	0	22	0.1	1.2	0	22	0.1	1.3
2:19:35	2:24:35	2:22:05	5	0	148	0.5	1.8	0	153	0.6	1.9
2:24:35	2:32:45	2:28:40		217	30	0.1	1.9	224	31	0.1	2.0
2:32:45	2:41:00	2:36:53	Br5	0	29	0.1	2.0	0	30	0.1	2.1
2:41:10	2:53:30	2:47:20		212	44	0.2	2.2	221	46	0.2	2.2
2:59:20	3:05:10	3:02:15	6	0	41	0.2	2.3	0	43		2.2
3:05:45	3:11:45	3:08:45	Br6	0	23	0.1	2.4	0	24	0.1	2.3
switch B to bacteriophage-free water											
3:19:25	3:34:45	3:27:05		209	80	0.3	2.7	221	85	0.3	2.7
switch A to bacteriophage-free water											
3:34:45	3:39:50	3:37:18	7	0	18	0.1	2.8	0	19	0.1	2.7
3:39:50	3:58:00	3:48:55	Br7	0	65	0.2	3.0	0	67	0.2	3.0
3:59:15	4:06:00	4:02:37		213	28	0.1	3.1	222	30	0.1	3.1
	4:03:00	4:03:00	Res 1			0.0	3.1	0		0.0	3.1
4:06:00	4:10:30	4:08:15	8	0	16	0.1	3.2	0	17	0.1	3.1
4:56:30	5:01:10	4:58:50	9	0	182	0.7	3.8	0	186	0.7	3.8
5:01:10	5:07:10	5:04:10		215	22	0.1	3.9	220	22	0.1	3.9
5:07:10	5:11:00	5:09:05	Br8	0	14	0.1	4.0	0	14	0.1	4.0
5:59:21	6:03:51	6:01:36	10	0	192	0.7	4.7	0	200	0.7	4.7
6:03:51	6:09:55	6:06:53		218	22	0.1	4.7	227	23	0.1	4.8
7:48:25	7:52:40	7:50:33	11	0	380	1.4	6.1	0	402	1.5	6.2
7:52:40	7:57:24	7:55:02		222	18	0.1	6.2	235	19	0.1	6.3
9:21:20	9:25:43	9:23:32	12	0	0	0.0	6.2	0	0	0.0	6.3
9:25:43	9:32:18	9:29:01		210	23	0.1	6.3	219	24	0.1	6.4
11:10:30	11:16:00	11:13:15	13	0	367	1.4	7.6	0	380	1.4	7.8
11:16:05	11:28:30	11:22:17		213	44	0.2	7.8	220	46	0.2	8.0
13:13:20	13:17:45	13:15:32	14	0	383	1.4	9.2	0	399	1.5	9.4
13:17:45	13:28:10	13:22:57		210	37	0.1	9.3	219	38	0.1	9.6
14:53:40	14:58:30	14:56:05	15	0	317	1.2	10.5	0	330	1.2	10.8
16:16:20	16:20:50	16:18:35	16	0	288	1.1	11.6	0	300	1.1	11.9
17:00:50	17:05:15	17:03:02	17	0	156	0.6	12.1	0	162	0.6	12.5
18:39:10	18:43:50	18:41:30	18	0	367	1.3	13.5	0	383	1.4	13.9
22:38:20	22:42:40	22:40:30	19	0	888	3.3	16.7	0	928	3.4	17.3
22:42:40	22:48:35	22:45:37		223	22	0.1	16.8	233	23	0.1	17.4
24:50:01	24:54:12	24:52:07	20	0	431	1.6	18.4	0	454	1.7	19.1
24:54:12	25:02:30	24:58:21		206	29	0.1	18.5	217	30	0.1	19.2
27:00:57	27:05:30	27:03:14	21	0	422	1.6	20.1	0	445	1.6	20.8
		Cumulative Total			***5462***				***5704***		

Table D-5 - Sampling Schedule and Flow Rates from Column Experiments 12 and 13, Fine Sand, High Ionic Strength

Time from Start (min) Sampled				Column A				Column B			
From	To	Time Centre Point	Sample #	Flow Rate (ml/hr)	Effluent Volume (ml)	Effluent Volume (Pore Vol)	Cumulative Pore Vol	Flow Rate (ml/hr)	Effluent Volume (ml)	Effluent Volume (Pore Vol)	Cumulative Pore Vol
Pre-Spike Rinsing AGW											
about 4 L of Water in 16 hrs											
Switch to MS2 Spiked Reservoirs											
0:00:15	0:06:15	0:03:15		200	21	0.1	0.1	210	22	0.1	0.1
0:07:05	0:13:10	0:10:07		217	25	0.1	0.2	232	27	0.1	0.2
0:13:10	0:18:00	0:15:35	1	0	18	0.1	0.2	0	18	0.1	0.2
0:18:00	0:24:00	0:21:00		220	22	0.1	0.3	225	23	0.1	0.3
0:24:00	0:28:20	0:26:10	2	0	16	0.1	0.4	0	16	0.1	0.4
1:02:15	1:06:45	1:04:30	3	0	141	0.5	0.9	0	144	0.5	0.9
1:24:30	1:29:00	1:26:45	4	0	79	0.3	1.2	0	83	0.3	1.2
1:29:00	1:41:00	1:35:00		213	43	0.2	1.3	223	45	0.2	1.4
1:55:00	2:00:00	1:57:30	5	0	67	0.2	1.6	0	70	0.3	1.6
2:00:05	2:20:05	2:10:05		210	70	0.3	1.8	222	74	0.3	1.9
2:25:00	2:25:00	2:25:00	6		17	0.1	1.9		18	0.1	2.0
2:43:45	2:48:45	2:46:15		222	88	0.3	2.2	228	90	0.3	2.3
2:48:45	2:54:40	2:51:42	7	0	22	0.1	2.3	0	22	0.1	2.4
switch A to bacteriophage-free water											
switch B to bacteriophage-free water											
3:01:50	3:09:20	3:05:35		216	53	0.2	2.5	228	56	0.2	2.6
3:09:30	3:14:30	3:12:00	8	0	19	0.1	2.6	0	20	0.1	2.7
	3:14:00	3:14:00	Res 1	0		0.0	2.6	0		0.0	2.7
4:09:27	4:13:49	4:11:38	9	0	212	0.8	3.3	0	217	0.8	3.5
4:13:49	4:25:06	4:19:28		213	40	0.1	3.5	218	41	0.2	3.6
5:02:20	5:06:45	5:04:33	10	0	146	0.5	4.0	0	151	0.6	4.2
5:06:45	5:35:53	5:21:19		210	102	0.4	4.4	217	106	0.4	4.6
6:03:10	6:09:00	6:06:05	11	0	116	0.4	4.8	0	120	0.4	5.0
6:49:45	6:56:20	6:53:02	12	0	166	0.6	5.4	0	171	0.6	5.6
9:16:05	9:20:35	9:18:20	13	0	513	1.9	7.3	0	534	2.0	7.6
10:06:40	10:11:00	10:08:50	14	0	179	0.7	8.0	0	187	0.7	8.3
10:11:00	10:24:30	10:17:45		213	48	0.2	8.2	222	50	0.2	8.5
11:22:15	11:30:30	11:26:22	15	0	226	0.8	9.0	0	237	0.9	9.3
11:30:30	11:43:20	11:36:55		206	44	0.2	9.2	215	46	0.2	9.5
12:41:25	12:46:00	12:43:42	16	0	215	0.8	9.9	0	225	0.8	10.3
13:41:00	13:48:15	13:44:37	17	0	213	0.8	10.7	0	223	0.8	11.2
14:46:00	14:50:40	14:48:20	18	0	226	0.8	11.6	0	233	0.9	12.0
14:50:40	14:59:30	14:55:05		217	32	0.1	11.7	224	33	0.1	12.1
15:19:10	15:23:30	15:21:20	19	0	87	0.3	12.0	0	90	0.3	12.5
20:16:45	20:21:15	20:19:00	20	0	1068	3.9	15.9	0	1129	4.1	16.6
20:21:15	20:28:30	20:24:53		215	26	0.1	16.0	228	28	0.1	16.7
22:42:15	22:46:39	22:44:27	21	0	495	1.8	17.8	0	524	1.9	18.6
25:25:35	25:29:46	25:27:41	22	0	585	2.1	20.0	0	619	2.3	20.9
27:41:30	27:45:27	27:43:29	23	0	487	1.8	21.8	0	515	1.9	22.8
			Cumulative Total		***5926***				***6205***		

Table D-6 - Sampling Schedule and Flow Rates from Column Experiments 14 and 15, Medium Sand, High Ionic Strength

Time from Start (min) Sampled				Column A				Column B			
From	To	Time Centre Point	Sample #	Flow Rate (ml/hr)	Effluent Volume (ml)	Discrete Effluent Volume (Pore Vol)	Cumulative Pore Vol	Flow Rate (ml/hr)	Effluent Volume (ml)	Discrete Effluent Volume (Pore Vol)	Cumulative Pore Vol
Pre-Spike Rinsing AGW											
about 3.5 L of Water in 16 hrs											
Switch to MS2 Spiked Reservoirs											
0:00:00	0:02:30	0:01:15		264	11	0.0	0.0	264	11	0.0	0.0
0:06:00	0:20:20	0:13:10		188	56	0.2	0.2	184	55	0.2	0.2
0:20:30	0:25:25	0:22:57	1		16	0.1	0.3		16	0.1	0.3
0:41:00	0:47:15	0:44:08	2		69	0.3	0.6		67	0.2	0.5
1:13:25	1:18:35	1:16:00	3		98	0.4	0.9		96	0.4	0.9
1:18:35	1:29:30	1:24:03		192	35	0.1	1.0	187	34	0.1	1.0
1:29:30	1:34:45	1:32:08	4		17	0.1	1.1		16	0.1	1.1
1:34:45	1:49:15	1:42:00		190	46	0.2	1.3	186	45	0.2	1.2
1:49:15	1:58:30	1:53:52	5	0	29	0.1	1.4	0	29	0.1	1.4
2:11:00	2:16:15	2:13:37	6	0	56	0.2	1.6	0	55	0.2	1.6
2:51:30	2:57:00	2:54:15	7	0	129	0.5	2.1	0	126	0.5	2.0
Switch to B-free water											
3:33:45	3:36:05	3:34:55	8	0	128	0.5	2.5	0	125	0.5	2.5
3:38:10	3:45:30	3:41:50		196	31	0.1	2.7	192	30	0.1	2.6
3:47:50	3:53:30	3:50:40	9	0	26	0.1	2.7	0	26	0.1	2.7
3:56:20	4:01:05	3:58:43	10	0	25	0.1	2.8	0	24	0.1	2.8
5:08:30	5:13:40	5:11:05	11	0	238	0.9	3.7	0	233	0.9	3.6
6:16:00	6:21:00	6:18:30	12	0	213	0.8	4.5	0	213	0.8	4.4
7:38:15	7:51:15	7:44:45	13	0	286	1.0	5.5	0	286	1.0	5.5
7:51:15	7:57:45	7:54:30	14	0	21	0.1	5.6	0	21	0.1	5.5
8:00:45	8:08:20	8:04:32		190	33	0.1	5.7	190	33	0.1	5.7
8:33:50	8:39:00	8:36:25	15	0	97	0.4	6.1	0	97	0.4	6.0
11:35:45	11:41:30	11:38:37	17 i	0	578	2.1	8.2	0	578	2.1	8.1
11:41:30	11:47:00	11:44:15	17 ii	0	17	0.1	8.3	0	17	0.1	8.2
15:04:00	15:09:00	15:06:30	18 i	0	639	2.3	10.6	0	639	2.3	10.6
15:09:00	15:15:00	15:12:00	18 ii	0	19	0.1	10.7	0	18	0.1	10.6
23:42:03	23:47:05	23:44:34	19	0	1591	5.8	16.5	0	1567	5.8	16.4
27:42:50	27:48:01	27:45:25	20	0	749	2.8	19.3	0	737	2.7	19.1
29:23:40	29:29:00	29:26:20	21	0	314	1.2	20.5	0	309	1.1	20.2
29:36:15	29:57:10	29:46:43		186	88	0.3	20.8	184	86	0.3	20.5
32:22:45	32:27:50	32:25:18	22	0	468	1.7	22.5	0	461	1.7	22.2
			Cumulative Total		***6122***				***6051***		

Table D-7 – Flow Rates from Column Experiments 2 and 3

	Low [MS2] Column			High [MS2] Column		
Central Sampling Time	Flow Rate (ml/hr)	Discrete Flow Volume (ml)	Cumulative Pore Volumes	Flow Rate (ml/hr)	Discrete Flow Volume (ml)	Cumulative Pore Volumes
0:00:00	849	25	0.09	814	24	0.09
0:01:45	849	159	0.68	814	153	0.65
0:13:00	849	0	0.68	814	0	0.65
0:13:00	710	62	0.90	690	60	0.87
0:18:15	710	0	0.90	690	0	0.87
0:18:15	484	93	1.24	484	93	1.21
0:29:45	484	0	1.24	484	0	1.21
0:29:45	360	281	2.27	350	273	2.21
1:16:30	360	0	2.27	350	0	2.21
1:16:30	212	79	2.56	203	75	2.49
1:38:45	212	0	2.56	203	0	2.49
1:38:45	1155	34	2.69	1080	31	2.60
1:40:30	1155	510	4.56	1080	477	4.36
2:07:00	1155	0	4.56	1080	0	4.36
Switched to Spiked Reservoirs after Rinsing						
2:07:00	129	35	4.69	129	35	4.49
2:23:30	129	0	4.69	129	0	4.49
2:25:46	0	0	4.69	129	18	4.55
2:34:00	0	0	4.69	129	0	4.55
3:22:00	0	0	4.69	129	30	4.66
3:36:00	0	0	4.69	129	13	4.71
3:42:00	137	63	4.93	131	61	4.93
4:09:45	137	64	5.16	131	61	5.16
4:37:53	130	51	5.35	130	51	5.35
5:01:25	171	62	5.57	171	62	5.57
5:23:03	170	190	6.27	170	190	6.27
6:30:15	166	33	6.39	171	33	6.40
6:42:00	166	45	6.56	171	46	6.57
Switched High [MS2] column to colloid-free AGW						
6:58:17	167	17	6.62	171	18	6.63
Switched Low [MS2] column to colloid-free AGW						
7:04:30	167	331	7.84	171	338	7.87
9:03:15	168	544	9.84	168	544	9.87
12:17:30	168	1810	16.49	173	1864	16.72
23:04:05	172	676	18.97	176	692	19.26
27:00:00	168	1606	24.87	174	1664	25.38
36:33:40	165	2202	32.96	171	2282	33.76
49:54:15	172	871	36.16	176	891	37.03

Flow During Column Experiments 2 and 3

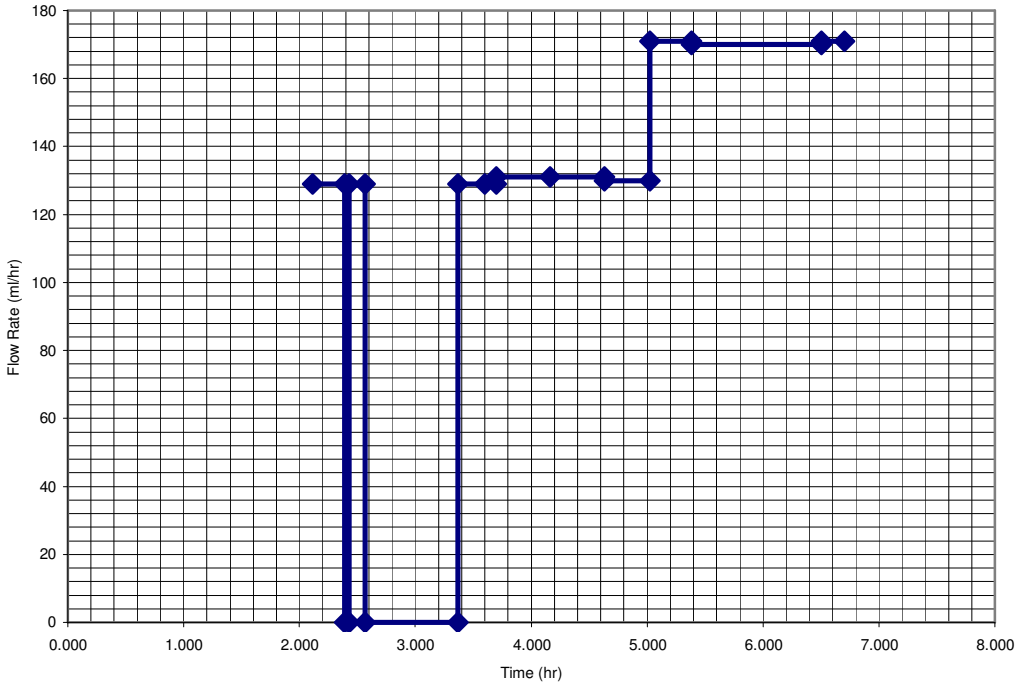

Figure D-1 - Column Runs 2 & 3 High Concentration Flow Rate Graph

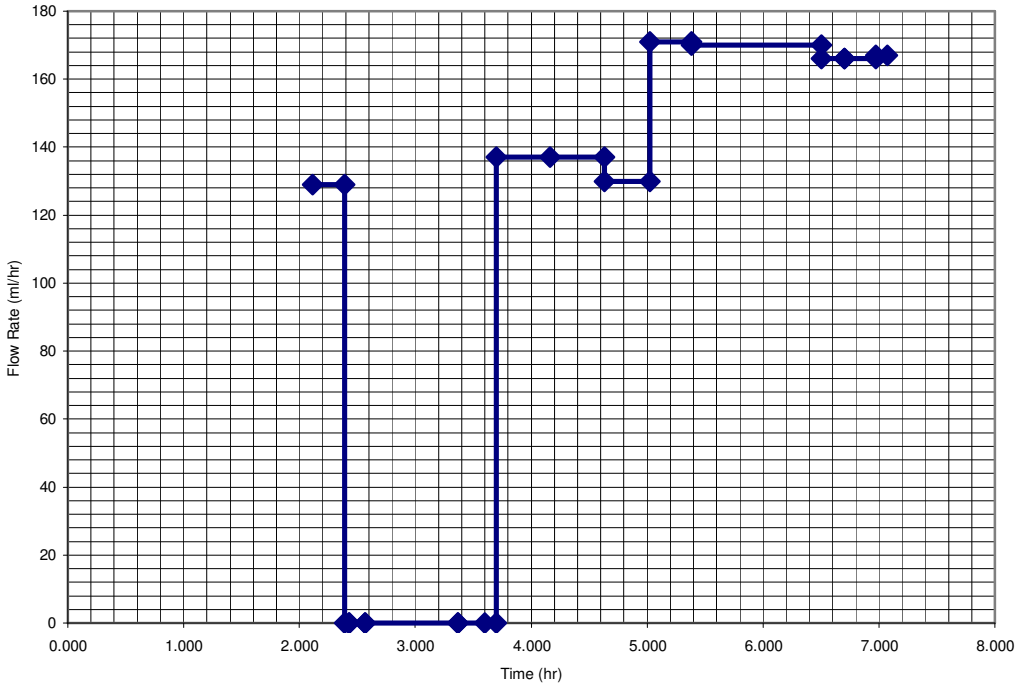

Figure D-2 - Column Runs 2 & 3 Low Concentration Flow Rate Graph

First Prototype Column Run

Figure D-3 indicates MS2 and bromide breakthrough during the first trial column experiment utilizing a 10 cm, horizontally oriented column. This figure indicates a rapid rise of both MS2 and bromide during the first hour of column operation. MS2 and bromide concentrations during the first column experiment effluent plateau and then decline rapidly after 5 hours at which point the column influent is only AGW. During this experiment MS2 reached a maximum breakthrough concentration of 50 % of the influent concentration after 3 hours and 30 minutes of column operation. Although the column effluent was sampled for 72 hours after the introduction of MS2 no MS2 was detected in the column effluent after 13 hours operation.

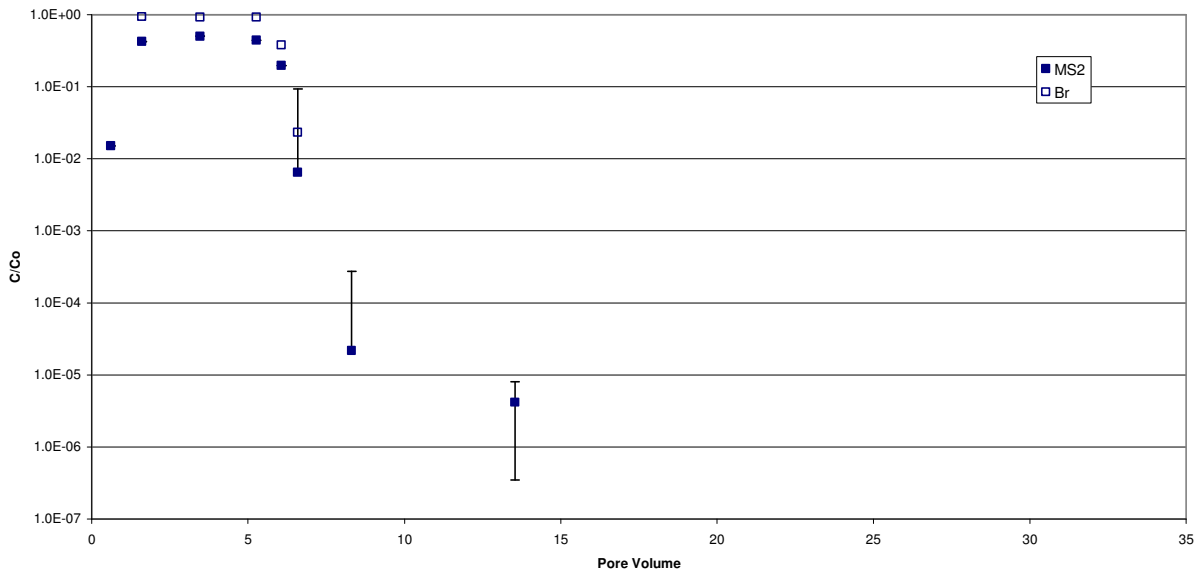

Figure D-3 - Column Run 1, Normalised MS2 Breakthrough in 10 cm column, Medium Sand, Very High Ionic Strength